Spatial Profiles of Sediment Denitrification at the Ground Water – Surface Water Interface in Cobb Mill Creek on the Eastern Shore of Virginia

Holly Sue Galavotti
Charlottesville, Virginia

B.S., James Madison University, 1998

A Thesis Presented to the Graduate
Faculty of the University of Virginia
In Candidacy for the Degree of
Master of Science

Department of Environmental Sciences

University of Virginia
May, 2004

_____

_____

_____

_____

ABSTRACT

Intensive use of nitrogenous fertilizers on agricultural fields has contaminated the shallow, unconfined Columbia aquifer on the Eastern Shore of Virginia, which contains high NO_3^- levels at 10-20 mg N L^{-1}, which are above USEPA drinking water limits of 10 mg N L^{-1}. In a small, low-relief stream in one watershed, Cobb Mill Creek (CMC), on the Eastern Shore, which is fed almost exclusively from the surrounding sandy aquifer, the stream NO_3^- concentrations of 1-2 mg N L^{-1} are considerably lower under base flow conditions. Synthesis of hydrological and biogeochemical ground water and stream data collected at the experimental hillslope draining to Cobb Mill Creek indicated that high concentrations of NO_3^- were maintained along deep, oxidized ground water flow paths approximately greater than two meters deep and discharge vertically into the stream. The NO_3^- was not removed until the pore water reached the ground water- surface water interface approximately 20 cm below the streambed. The objectives of this research were to determine the contribution of, and controls on denitrification in removing NO_3^- at the ground water/ surface water interface. Vertical and lateral profiles of NO_3^- levels, total organic carbon, redox potential (platinum electrode potential), and denitrification potential rates (acetylene block method) were measured in intact cores collected from the streambed. Vertical profiles showed a decrease of 8.27 mg NO_3^--N L^{-1} or 84.24% between the open channel and 60 cm below the stream sediment surface in cores taken on July 11, August 4, August 26, and October 26, 2003. The greatest decrease in NO_3^- occurred in the top 20 cm of the stream sediments. In these shallow sediments, conditions of high organic matter content, low redox potential, and available NO_3^- promoted high

denitrification rates. Organic matter content was significantly positively correlated to potential denitrification rates for all four sampling events. The results of this research indicate that denitrification is responsible for NO_3^- removal from the discharging ground water, and reducing conditions stimulated by surface-derived organic matter drive the reaction. Along lateral profiles, increased total organic matter and increased potential denitrification at depths greater than 20 cm below the stream sediment surface were found only along the right bank facing downstream in all sampling dates. Due to the curvature of the stream at the sampling reach, organic matter deposited into the stream from the surrounding riparian forest may be consolidated and buried specifically along the right bank of the stream.

The average denitrification potential rates were 661, 567, and 16.8μmol N m^{-2} h^{-1} in the stream sediments on July 11, August 4, and October 26, 2003, respectively. The lowest denitrification rate was observed in October due to lower temperatures. The rates observed this study are similar to denitrification rates observed in other studies in the literature. While denitrification rates in Cobb Mill Creek sediments were spatially and temporally variable, denitrification was a significant NO_3^- sink at the ground water-surface water interface. Riparian buffers surrounding streams supply an important input of organic matter that fuels denitrification. The maintenance of riparian buffers with organic-rich soils is essential for natural remediation of NO_3^- concentrations in streams sediments, to prevent nutrient enrichment of downstream environments.

TABLE OF CONTENTS

LIST OF FIGURES

LIST OF TABLES

INTRODUCTION

Nitrate Contamination on the Eastern Shore of Virginia

Intensive use of nitrogenous fertilizers on agricultural land has led to extensive contamination of water supplies throughout the United States (Winter, 1998). Agricultural fields on upland soils fill the drainage waters with fertilizers flowing to streams. Nitrate contamination of ground water and surface water is widespread because, as an anion, nitrate is very mobile in the environment. High concentrations of nitrate in surface waters can lead to eutrophication, which contributes to the extensive growth of aquatic plants, depletion of oxygen, fish kills, and degradation of aquatic environments (Winter, 1998). There are also potential health hazards for humans and some animals if nitrate is consumed in sufficient quantities, such as fatal levels of anoxia in the blood stream called methemaglobinemia. In addition, the presence of nitrate and nitrite in food materials could increase the likelihood of the formation of carcinogenic nitrosamines (Delwiche, 1976). It has also been proposed that the flux of N_2O gas due to reduction of nitrate from agricultural and adjacent land by denitrification is one of the major contributors to atmospheric N_2O on a global scale. Since N_2O is a chemically unreactive gas, it can reach the stratosphere by transport and diffusion and may affect the destruction of the stratospheric ozone layer. Fertilizer use and an increase in the amount of grassland and cultivated land make up about 90% of the anthropogenic N_2O source. N_2O accounts for 4% of the greenhouse warming effect (Wagner-Riddle, 1996).

Nitrate contamination of ground water is a major concern for the agricultural regions of the Eastern Shore of Virginia. All drinking water on the Eastern Shore is

derived from a high yielding multiaquifer system since there are no large surface water supplies available. Total ground water use, including drinking water and withdrawal for industry and irrigation, is estimated by the U.S. Geological Survey to be 5 Mgal/day. About 25% of the population derives its water from the shallow, unconfined Columbia aquifer, while the remainder draws water from the deeper Eastover-Yorktown confined aquifer. Due to the presence of salts at depth, the Columbia and Yorktown-Eastover aquifers constitute the entire freshwater system on the Eastern Shore of Virginia (U.S. EPA, 1997).

Agriculture dominates the small peninsula of the Eastern Shore of Virginia, as it accounts for approximately 50% of the land use (Reay, 2001). Typical crops planted are soybeans, corn, and wheat or rye. In addition, tomatoes, cotton, and cucumbers are regionally grown. The hydrogeology of the Eastern Shore facilitates the infiltration of the nitrate from upgradient agricultural farms into the shallow ground water. The shallow unconfined Columbia aquifer contains NO_3^- levels (10-20mg N L^{-1}) (Chauhan and Mills, 2002) above USEPA drinking water limits (10 mg N L^{-1}). The flat land surface, dominated by well drained fine-sandy to sandy loam soils, facilitates ground water contamination and the subsequent transport of nutrients to the streams, which ultimately contributes to nutrient enrichment of the Chesapeake Bay and seaside lagoons. A small, low relief stream, Cobb Mill Creek, on the seaside of the Eastern Shore is fed exclusively from the surrounding sandy aquifer under base flow conditions. The NO_3^--N concentrations of the stream are considerably lower (1-2 mg N L^{-1}) than the contributing ground water (Chauhan and Mills, 2002; Mills et al., 2002). This discrepancy between high nitrate concentration in the discharging ground water and low nitrate concentrations

in stream water has prompted the examination of NO_3^- removal in the stream sediments before the pore water discharges into Cobb Mill Creek.

Near-stream saturated zones are active sites of nitrogen cycling. Natural attenuation of nitrate flowing from upland hillslopes through the ground water/ stream water interface is determined by the interaction of the hydrologic flow-paths and the biogeochemical characteristics of the sediment along that flow-path. This integrated relationship is relatively unstudied with respect to nitrate transformations in riparian zones (Cirmo & McDonnell, 1997). The research reported here contributes to determining the controls of nitrate removal in the near-stream zone by investigating both biogeochemical and hydrologic functioning. Removal of nitrate from the ground water before it discharges into the stream is important to downstream estuaries.

Nitrate Transformations

Nitrate and ammonium are major components of fertilizer and manure. Ammonium is readily transformed to nitrate under aerobic conditions by nitrifying microbes (Winter, 1998). Nitrate is soluble in water and because of its solubility and anionic form, it can easily leach through the soil and reach the water table, where it can persist in shallow ground water for decades (Nolan, 1999). Nitrate does not form coordination complexes with metals or sorb on inorganic or organic surfaces. Transformations of nitrate are mostly biochemically mediated and its fate is dependent upon reducing conditions and the amount of dissolved organic carbon present (Winter, 1998). In shallow, oxidized ground water in highly permeable sediment, nitrates can

travel long distances and can feed streams and flow downstream with little or no retardation (Freeze & Cherry, 1979).

Stream riparian zones are areas of direct interaction between terrestrial and aquatic systems involving exchanges of energy and matter (Hill, 1996). The riparian ecotone can serve as a nutrient filter, removing up to 90% of nitrate from shallow ground waters along its flow path across the riparian zone (Lowrance et al. 1984, Peterjohn & Correll, 1984, Jacobs & Gilliam, 1985). Attenuation of NO_3^- concentrations occurs in riparian zones through dilution, plant uptake, and microbial processes, particularly denitrification. Dilution includes precipitation seeping though forest soils to the ground water that contains less nitrate than seepage below an agricultural field. The amount of recharge to an aquifer can influence nitrate concentrations on a seasonal basis. Dilution of nitrate in discharging ground water can also occur when nitrate-poor stream water mixes with nitrate rich ground water (Lowrance, 1992). Nitrogen is essential to life and will be taken up for growth by plants, fauna, and microbes. Plant uptake can be very effective in removing nitrate from the ground water, but its contribution depends upon season (dormancy during the winter), vegetation type, and vegetation age (Hill, 1996). Plant-root uptake of nitrate is maximal when the height of the water table is within reach of the root zone during the growing season (Simmons, 1992). Vegetation uptake requires the presence of a substantial fine root biomass at depth as the water table declines in the summer. Information describing the vertical distribution and the seasonal dynamics of fine root biomass in relation to water table fluctuations is lacking (Hill, 1996). Plants can also immobilize nitrate by drawing nitrate through the roots by capillary action when the water table is below the root zone. Microbial uptake of nitrate usually occurs in the

absence of inhibitory concentrations of NH_4^+ (Hill, 1996). Plant uptake and microbial immobilization at the ground water- surface water interface is considered less significant on long term nitrate uptake since nitrogen pools become saturated over time and immobilized nitrogen is deposited back to the system by mineralization (Hedin, 1998). Dissimilatory reduction of NO_3^- to NH_4^+ is carried out by bacteria that can be either obligate or facultative anaerobes, which can co-occur with denitrifiers (Hill, 1996). Dissimilatory reduction of nitrate is minor in riparian areas where seasonally variable ground water flows with high nitrate concentrations are in contact with sediments that are not highly anaerobic because they are not permanently saturated (Hill, 1996). In addition, loss of nitrate in riparian zones has not been associated with increased concentrations of NH_4^+ in the ground water (Hill, 1996). Under anaerobic conditions, microbial denitrification is generally considered the most important mechanism in removing nitrate along the flow path to streams.

Denitrification is a microbial process in which heterotrophic, generally facultative anaerobic bacteria, e.g. *Paracoccus denitrificans*, use nitrate (NO_3^-) and nitrite (NO_2^-) as electron acceptors in the oxidation of organic matter. Under hypoxic conditions, the reaction follows the path: $NO_3^- \rightarrow NO_2^- \rightarrow N_2O \rightarrow N_2$. When all dissolved oxygen in ground water is consumed, denitrifiers oxidize organic matter and reduce nitrate according to the following equation (Freeze & Cherry, 1979):

$$CH_2O + 4/5\ NO_3^- \rightarrow 2/5\ N_2(g) + HCO_3^- + 1/5H^+ + 2/5H_2O \qquad (1)$$

Nitrous oxide (N_2O) is a byproduct of the denitrification process that is released through incomplete reduction of the NO_3^- to N_2. N_2O and N_2 exist as dissolved gases in the ground water. If the water moves into the unsaturated zone, some of the N_2O and N_2 will

be lost to off-gassing (Lamontagne, 1995). Measurements of denitrification rates have generally been accomplished by measuring its products: N_2O and N_2 gases. An alternative method of measuring denitrification by N_2 production is necessary due to the high background concentration of atmospheric and aqueous N_2, which makes detecting small increases of the gas due to denitrification difficult. Consequently, methods have been developed in which acetylene (C_2H_2) is added to sediments, which inhibits the enzymatic reduction of N_2O to N_2. Denitrification potential rates are determined based on the production of N_2O is measured instead of measuring direct N_2 flux.

Sediment conditions influencing the uptake of nitrate by heterotrophic denitrification include 1) hypoxic conditions, 2) the amount of organic matter available in a consumable form, 3) pH, 4) the presence of nitrate, and 5) temperature. Dissolved oxygen is thermodynamically preferred as a terminal electron acceptor over nitrate by microbes, in that nitrate reduction is not expected to occur when dissolved oxygen (DO) is present (Tesoriero et al., 2000). Denitrification ideally occurs in water with a decline in redox potential (approximately Eh= +250 mV) at pH 7 and 25^{o}C. At this redox potential, the water contains no dissolved oxygen, and nitrate is used as the electron acceptor (Freeze & Cherry, 1979) by those organisms capable of doing so. Organic carbon is the most common electron donor, although reduced inorganic species may also act as electron donors for denitrification for a small subset of autotrophs. Sulfur and less commonly, ferrous iron (Fe^{2+}) from pyrite (FeS_2) oxidation can also be possible electron donors for denitrification (Tesoriero et al., 2000) by the following mechanisms:

$$5FeS_2 \text{ (pyrite)} + 14\ NO_3^- + 4H^+ \rightarrow 5\ Fe^{2+} + 7N_2 + 10SO_4^{2-} + 2H_2O \quad (2)$$

$$5Fe^{2+} + NO_3^- + 7H_2O \rightarrow 5FeOOH \text{ (goethite)} + 1/2N_2 + 9H^+ \quad (3)$$

The importance of organic carbon in controlling the occurrence of denitrification in riparian zones is well documented (Starr & Gillham, 1993). The amount and type of organic matter can affect denitrification, in that higher rates of denitrification have been found to occur with more labile forms of organic matter (Pfenning & McMahon, 1996). The availability of labile organic matter is also important for microbial respiration, which consumes oxygen creating hypoxic conditions that allows denitrification to occur. In areas adjacent to agricultural fields where there is a ready source of nitrate to the ground water flow path, it is often organic matter content and redox conditions that limit denitrification rates (Hedin, 1998). Finally, denitrification rates usually peak during the spring, when there is a concurrence of high temperature and nitrate availability. Despite high temperatures during the summer, nitrate concentration usually decreases due to lower run off and increased macrophytic uptake (Pattinson et al., 1998).

Spatial gradients of biogeochemical regulators such as NO_3^-, O_2, and organic matter have shown to be steep in riparian zones, and processes such as denitrification can be concentrated very close to the ground water/ stream water interface (Hedin, 1998). The pattern of ground water redox zones near discharge areas is poorly known, but has a major effect on the transformation of nitrate near the stream channel (Bohlke et al., 2002).

Characteristics of the Ground Water- Surface Water Interface

In agricultural areas, such as the Cobb Mill Creek watershed, high levels of nitrate occur along a shallow ground water hydrological flow path from the hillslope to the stream, ultimately passing through the ground water- surface water interface. The

hyporheic zone is defined as the component of the ground water- surface water interface surrounding a stream that contains water originating both from the neighboring aquifer and stream water (at least 10%) (Hinkle, 2001; Triska, 1989). Based on previous conservative tracer studies, Cobb Mill Creek is not thought to have a distinct hyporheic zone (data not shown). The present study examines the ground water- surface water interface extending beyond the hyporheic zone.

The ground water- surface water interface can display disproportionately high rates of biogeochemical activity and serve as a control point within the riparian area by affecting the amount and form of nutrients that are transported along the paths of nutrient flux (Hedin, 1998). The ability to predict the extent to which the ground water/ stream water interface will affect the nitrate flux depends on an understanding of how biogeochemical processes are linked to hydrologic processes (Hedin, 1998). The interaction of thermodynamic constraints on microbial communities and the input of supplies of electron donors (oxidizable dissolved organic carbon) and electron acceptors (NO_3^-) through subsurface flow paths control the transformation of nitrate (Hedin, 1998). The terrestrial-aquatic interface is considered a "hot spot" of biogeochemical activity attributed to its location where hydrological flow paths converge and consequently mix essential substrates producing high reaction rates (McClain et al., 2003). Saturated sediments beneath and beside streams, where there is a movement of upwelling deep ground water carrying NO_3^-into shallow, organic-rich, reducing substrate are ideal sites for high rates of denitrification (McClain et al., 2003).

Nitrogen transformations and retention ideally occur under reducing conditions where the hydraulic residence time is great and where saturated conditions persist (Cirmo

& McDonnell, 1997). At the near-stream area, the water table is typically at, or near, the surface for much of the year, and sediments are often saturated (Cirmo & McDonnell, 1997). Water movement through the ground water- surface water interface is slowed by fine textured muds near the sediment surface. This resistance lends to increased residence time for the discharging ground water (Mills et al., 2002).

From the direction of the open channel, there is a frequent input of readily assimilated organic carbon by deposition and burial of particulate organic carbon in reworked sediment, or by advection of dissolved organic carbon in the stream that flows through the hyporheic zone (Hinkle, 2001). Near-stream zones that mix with surface water organic carbon sources that are labile have been shown to support higher denitrification rates than deeper streambed sediments (Pfenning & McMahon, 1996).

Variability at the Ground Water- Surface Water Interface

There can be great differences among the characteristics of the ground water-surface water interface in different streams. The interaction between ground water and surface water is dynamic in both time and space, and varies with spatially heterogenous aquifer properties, stream-bed topography, and hydraulic gradients between the two zones (Hinkle, 2001). There are also great differences between denitrification rates within streams in which the chemistry of subsurface waters and ground water, microbial processes, and hydrological flow paths can change over short distances of less than a meter (Hedin, 1996). From a channel perspective, the depth and lateral extent of advective exchange in the hyporheic zone are determined by geomorphological features of the surface channel such as roughness, permeability, and pool-riffle sequence (Triska,

1993). The extent of hyporheic change can be determined by conservative tracer experiments. High variation in tracer travel times can indicate heterogeneity of the permeability of the sediments in the hyporheic zone (Triska, 1993).

Knowledge of the complexities of the biogeochemical interaction between ground water and surface water in the hyporheic zone has evolved over the last two decades (Hinkle, 2001). Along a stream reach, most of the water and dissolved nutrients usually represents the upstream environment (Triska, 1993). But, there is also an incremental input of ground water to the stream by two dominant flow paths of ground water. There can be great variability along the hyporheic zone where there is a rapid upwelling of deeper ground water in areas near the stream and a less rapid transport of shallow soil water from inland environments toward the stream (Hedin, 1998). Ground water and stream water can exchange both vertically in the subchannel and laterally at the banks under the riparian zone. During hyporheic exchange, dissolved nutrients become available to terrestrial biota and then to the stream channel community. Solutes can also be transiently stored by physical geomorphology of the channel. Retention can span from long term, as in the case of burial of particulates for years, or short term, as in the storage of solutes in slow moving water (Triska, 1993).

Spatial Profiles of Solutes at the Ground Water- Surface Water Interface

Despite great heterogeneity, there are general physical, chemical, and biological gradients between oxidized and reduced near-stream environments. Hedin (1996) adopted a thermodynamic approach to evaluate the biogeochemical variability of the ground water- surface water interface of a riparian wetland. Low oxygen conditions are

found in sediment layers with high organic matter content. Organic matter fuels respiration, which consumes oxygen and creates hypoxic conditions. There is an expected trend of decreasing dissolved organic carbon (DOC) under increasing oxidized conditions due to its rapid consumption by aerobic respiration. Nitrate is typically higher in aerobic interstitial water than either channel or ground water in that under low oxygen conditions it is reduced by denitrification (Triska, 1993). With the discharge of aerobic, nitrate-rich ground water to streams, vertical concentrations of nitrate can increase as a function of depth within the stream-sediment environment, with much of the nitrate reduced close to the ground water- stream water interface (Hedin, 1998). Ammonium concentrations also typically increase in aerobic interstitial water. Under oxic conditions, nitrification converts ammonium to nitrate. This process can act as a sink for oxygen, and as DO is depleted, facultative anaerobes, like denitrifiers, can switch to nitrate as the terminal electron acceptor in the oxidation of organic carbon (Triska, 1993). Heterogeneity in DO can be caused by microbial metabolism in pockets of organic matter stored in stream sediments, forming patches of an oxygen-depleted habitat surrounded by oxygenated environment (Triska, 1993). High rates of denitrification activity have been found to occur in localized "hot spots" that display a patchy distribution in soils and sediments (Hill, 1996). Because the biogeochemical reactions are intimately linked to hydrological flow paths within the ground water- surface water interface, understanding hydraulic head and solute concentration distributions at a high resolution are important in determining nutrient fluxes that control denitrification rates over these short distances (Duff et al., 1998).

Preliminary Assessment at Cobb Mill Creek

The discrepancy between high nitrate concentrations in the stream sediments (10-20 mg N L^{-1}) and low nitrate concentrations in stream water (1-2 mg NO_3^--N L^{-1}) prompted the examination of NO_3^- removal in the stream sediments before the ground water discharges into Cobb Mill Creek (Chauhan and Mills, 2002; Mills et al., 2002). Along the experimental hillslope, fertilizer- derived nitrate is transported along ground water flow paths from an upland agricultural field, through the riparian hillslope to the ground water- surface water interface, and, thus, into Cobb Mill Creek. Stream and ground water samples were collected from five stream-bank piezometer nests located immediately adjacent to Cobb Mill Creek (N1-N6) and one in-stream piezometer nest (S1) in October 2000 (Figure 1). All stream-bank piezometer nests were set back approximately 0.5 m from the edge of the stream except for N3 and N4 which were about 1 m upslope along the bank. The distribution of NO_3-N in the riparian zone near the stream indicated that most of the nitrogen removal occurred in the last meter of stream sediment before the ground water discharges to the stream. There was a substantial decrease of NO_3^--N with elevation in the piezometer nests. Since the nitrate transported in the ground water from the hillslope remained at high concentrations close to its discharge point, it is suggested that the ground water remained oxic along its flow path. The thin ground water- surface water ecotone seemed to be effective in the removal of nitrate. Biological removal of nitrate at this interface requires hypoxic, organic rich sediments; however, these sediments were surrounded by oxic stream and ground water.

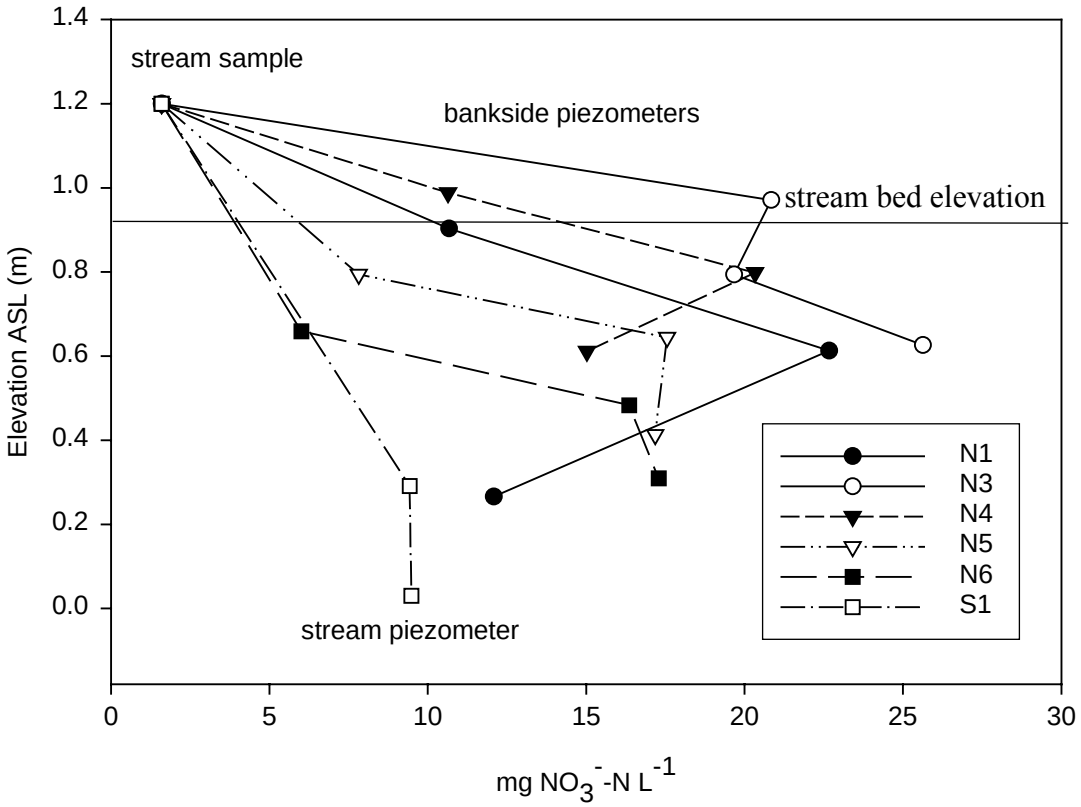

Figure 1. Ground water and stream NO_3^--N concentration collected in October 2000 from the stream bank immediately adjacent to Cobb Mill Creek.

Research Objectives

The objectives of this research were to determine the contribution of, and controls on denitrification in removing nitrate at the ground water- surface water interface before it reached the open channel of Cobb Mill Creek under base flow conditions. The major hypothesis tested was that denitrification is the biogeochemical pathway that removes the majority of ground water nitrate in the near stream environment. To address this hypothesis, I investigated the following questions: 1) In the near stream zone, what are the vertical and horizontal profiles of denitrification potentials? 2) Are the denitrification potential profiles correlated to the concentration profiles of their biogeochemical controllers such as NO_3^-, O_2, and organic carbon in the near-stream environment?

METHODS

Field Site Description

The study site is located along a non-tidal portion of Cobb Mill Creek, a small sandy-cobble first order stream in Northhampton County, on the Eastern Shore of Virginia (Figure 2). The watershed is approximately 496 hectares, and it drains to seaside lagoons. Agriculture is substantial within the watershed accounting for approximately 34.2% of the land cover while 62.3% is forested (Chauhan, unpublished). Downstream of the creek, land cover includes marshes that lead to the Sand Shoal Channel. Cobb Mill Creek is surrounded by an oak - maple - pine riparian forest. Surface relief is generally low, with slopes ranging from 0-2% over most of the watershed, with greater slopes along regions immediately adjacent to the streams. Upland soils are dominated by Bojac sandy loam, which is a well-drained soil with high permeability in the subsoil and in the substratum. Molena loamy sand dominates along Cobb Mill Creek (Soil Survey of Northhampton County, Virginia, 1989). These permeable soils are underlain by the shallow, unconfined Columbia aquifer, which consists of an eastward thickening wedge of unconsolidated sand and gravel (U.S. EPA, 1997). The sediments were deposited on a crystalline bedrock platform, which has subsided since early Cretaceous time. The Columbia aquifer is underlain by the Yorktown- Eastover confined aquifer at a depth ranging from 8-20 meters below ground elevation (Richardson, 1992). The deeper confined aquifer is recharged by water from the surficial aquifer. The sediments of the Yorktown-Eastover aquifer generally consist of shelly sands while the

confining units are silts and clays. The total recharge to the Columbia aquifer (including Accomack and Northhampton counties) is estimated to be 257 Mgal/day. Although most of this recharge is discharged into either the Atlantic Ocean or the Chesapeake Bay, an estimated 11 Mgal/day leaks through the first confining unit and into the upper portion of the Yorktown-Eastover aquifer (U.S. EPA, 1997). This generally occurs along the narrow

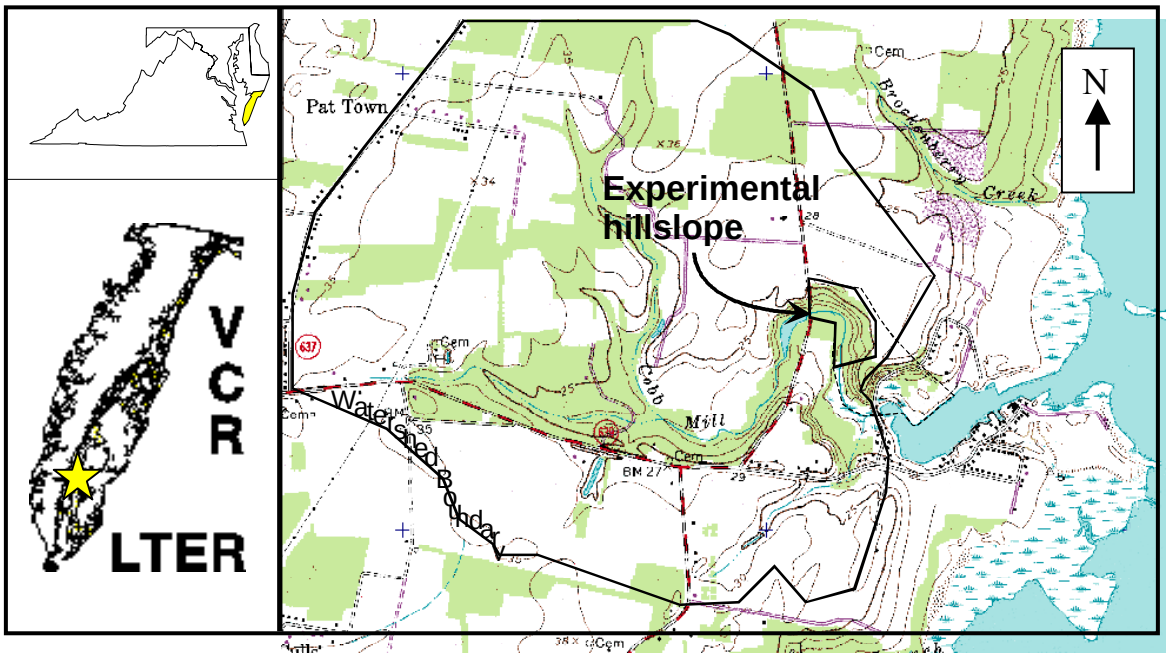

Figure 2. Map showing location of the experimental field site at Cobb Mill Creek on the Eastern Shore of Virginia near Oyster, VA.

zone called the "spine" in the center of the peninsula. The shallow, sandy unconsolidated sediments of the Columbia aquifer allow for possible contaminants originating from surrounding agricultural fields to leak to the Yorktown Eastover aquifers, especially along the "spine" of the Delmarva Peninsula (Reay, 2001).

Determination of the Hydrological Gradient

During the summer of 2001, a series of shallow wells and piezometers were installed in order to sample within and through the anaerobic portions of the riparian zone along Cobb Mill Creek (Figure 3). Piezometers consist of 1-inch well casing with ports in the sides near the capped bottom. Eleven piezometers nests were placed along and near the stream bank and in the center of the streambed. Each nest contains one ground water well screened across the water table, and, in most cases, three piezometers that open at discrete points between 0.2 to 0.8 m below the water table. The clusters were placed in a transect parallel to the stream and in two short transects up the hillslope perpendicular to the stream. The nested design of the piezometers allows for determination of both the horizontal and vertical components of the subsurface flow near the stream. These piezometers were used to directly measure vertical head gradients and as sampling ports to draw water from several depths for chemical analysis. The vertical head gradient was determined for each piezometer nest. The gradient was determined by dividing the difference in elevation above sea level (m) of the water level between individual piezometers in the nest that were open at different depths (dh) by difference in elevation above sea level (m) of the hole between the piezometers (dz). Negative vertical head gradient (when the water level in the deeper piezometer is higher (close to 0masl) than the water level in the shallower piezometer) indicated an upward flow of ground water. The longitudinal gradient between two stream piezometers was also determined. The gradient was determined by dividing the difference in elevation above sea level (m) of the water level between the two piezometers that were open at approximately the same depth (dh) by the longitudinal distance between the piezometers (dz). The ground water

wells were used to track changes of the water table elevation through time. The latitude, longitude, and elevation of the piezometer nests and the streambed were located using a total station referenced to permanent monuments located with Global Positioning System (GPS). The general hydrological flow paths from the hillslope to the stream were determined from the vertical head gradients and the water table elevation.

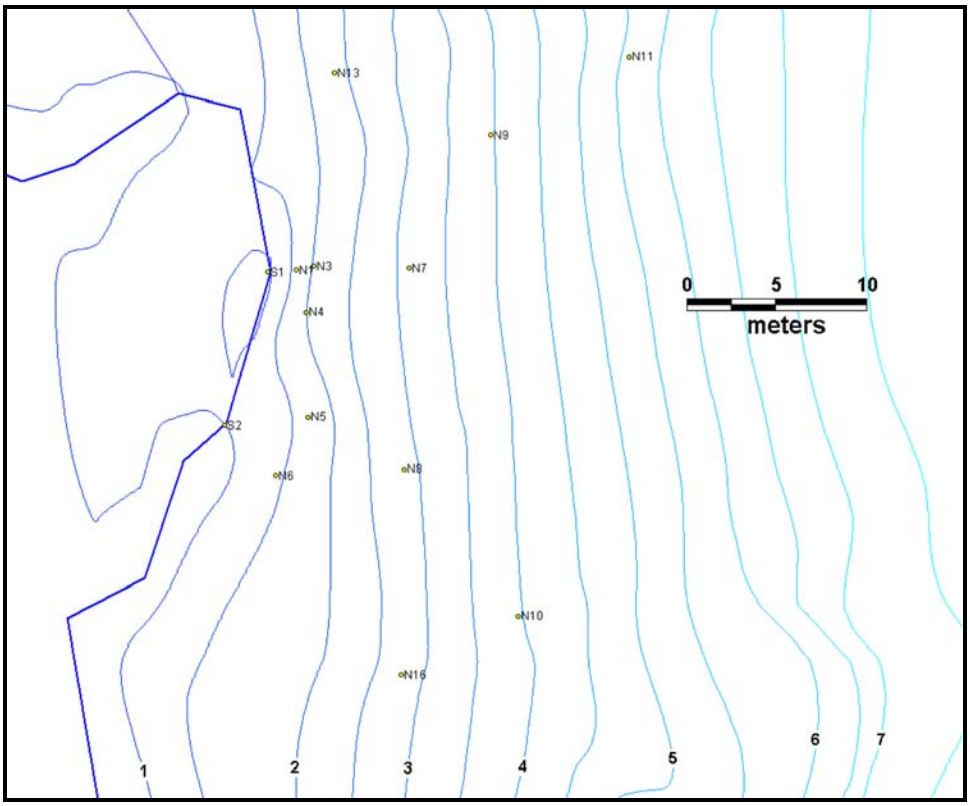

Figure 3. Location of piezometer and well nest along the hillslope and in Cobb Mill Creek. Contour line elevations depict elevation above sea level (m).

Experimental Design to Determine Spatial Profiles in the Stream Sediments

Vertical and horizontal distributions of water quality and denitrification potential were measured along three cross sections in the stream sediments stretching across the stream channel and down to approximately 60 centimeters below the sediment surface.

The three cross sections were positioned across the stream in line with the bank-side piezometers, N1, N4, and N5 (Figure 4). Pore water samples used to determine vertical and horizontal solute profiles were collected first near the sediment surface at approximately 2 cm deep and then at 10-cm increments down to approximately 60 cm below the sediment surface from intact sediment cores. Cores were spaced approximately 0.5 m apart. The cores were collected using PVC cylinders (5.1 cm inner diameter, 120 cm length) driven into the sediment. The cylinders were filled with stream water above the intact sediment, sealed with a rubber stopper, and carefully removed from the streambed. The bottom of each core was then sealed with an additional rubber stopper. To prevent water leakage during transport, the stopper and the tube were sealed with a thick bead of waterproof caulking (Plumber's Goop®), which was held in place by a tight wrapping of duct tape while it cured. In the laboratory, evenly spaced, ¾ inch ports were drilled at 10-cm intervals along the length of each core tube. The ports allowed for sampling of pore water and for determination of potential denitrification rates along a vertical gradient. The solute concentrations and denitrification potential rates were measured during four intensive sampling dates: July 11, August 3, August 28, and October 23, 2003.

Mini Drive Point Piezometer

Spatial profiles of water quality in the streambed from the surface to a depth of approximately 20 cm were determined at a 2.5-cm resolution using a mini drive point sampler (Duff et al., 1998). Measurement of the spatial distributions of the solutes of interest in highly permeable stream sediments requires close interval sampling without

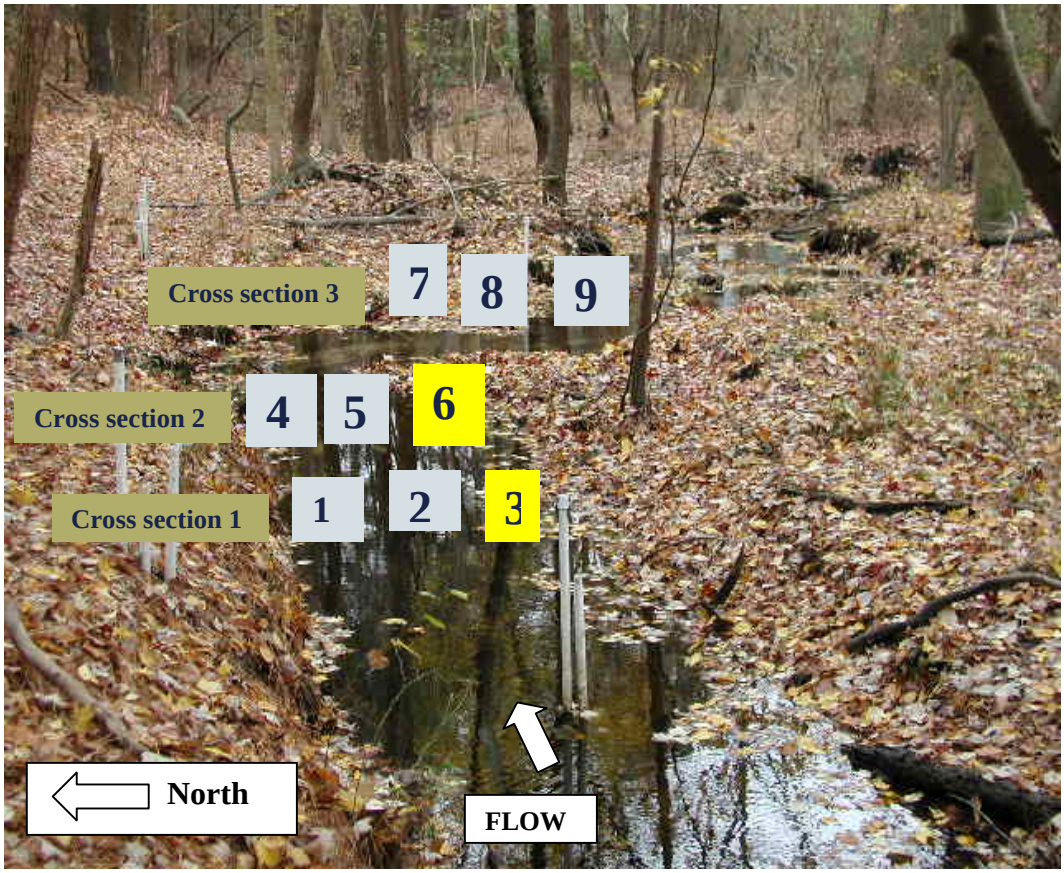

Figure 4. Experimental Design: Intact sediment cores taken in three cross sections across Cobb Mill Creek, Oyster, VA.

disturbing natural mixing processes (Duff et al., 1998). Historically, diffusion equilibrators and cores have been used to measure solutes in pore water. Diffusion equilibrators are effective for evaluating pore water transported at low velocities, primarily by diffusion (Duff et al., 1998). However, in permeable sediments, velocities can be high. Cores can disturb natural gradients and redistribute pore water during insertion and removal. Duff et al. (1998) devised a new method for collecting pore water samples that was less destructive. The mini drive-point piezometer (MDPP) technique collects pore water from streambed sediments at a 2.5-cm vertical resolution to a depth of approximately 20 cm (depending on stream sediments) simultaneously without disturbing

the surrounding pore water. The sampler has six small diameter (1/8 inch) steel drive points arranged in a 10-cm diameter circular array on a tripod. Steep vertical gradients at a fine resolution have been measured with the MDPP in the top 20 cm of the streambed. Below 20 cm, the vertical solute gradients seem to be more uniform in the streams examined with the device (Duff et al., 1998).

Sampling and Analysis of Solutes

Ground water samples for dissolved inorganic constituents were collected with a peristaltic pump from the wells and piezometers through silicone vinyl tubing to 25-mL centrifuge tubes after purging for at least 3 well volumes. In the laboratory, samples were filtered with a Gelman Sciences® 0.45 μm membrane filter using a vacuum pump. For samples collected before May 2003, nitrate plus nitrite-nitrogen was determined by a cadmium-reduction colorimetric method. A sample of 25 mL of the ground water was shaken with approximately 0.2 mg of powdered cadmium for 5 minutes in 50-mL centrifuge tubes to reduce nitrate to nitrite (Jones, 1984). The nitrite concentration was determined by treating 10 mL of the reduced sample with 2.5 mL sulfanilic acid solution (27.2 g of $KHSO_4$ and 3.46 g of sulfanilic acid in 1L deionized water) for 10 minutes. Next, the solution was coupled with 2.5 mL of N-(1-naphthyl) ethylenediamine (0.04%) for 20 minutes to produce a highly colored azo dye. The final solution was measured by a spectrophotometer at a wavelength of 550 nm (Montgomery & Dymock, 1961). A series of standards, in which NO_3^- -N concentration was 0.1, 0.5, 1.0, 1.5, 3.0, and 6.0 mg L^{-1}, were run along with every set of samples. Results obtained from the standards were used to determine ion concentrations in the samples.

Ground water samples collected after May 2003, were analyzed for nitrate, chloride, and sulfate on a Dionex® Ion Chromatograph using a Gilson® 234 Autoinjector and a Dionex IonPac AS4A® 4 x 250 mm Analytical Column. Samples were first filtered with 0.45 μm disposable syringe filters. The eluent solution consisted of 1.44 mM Na_2CO_3 and 1.36 mM $NaHCO_3$ and was pumped at a flow rate of 2 mL min^{-1}. The regenerant solution used was 0.028 N H_2SO_4. The eluent and regenerant were pressurized with helium gas with the valve pressure at approximately 70 psi. A series of standards in which each ion concentration was 1.0, 5.0, and 10.0 mg L^{-1} were run along with every set of samples. Results obtained from the standards were used to determine ion concentrations in the samples.

Pore water samples were collected from intact sediment cores from each sampling port using a 3-cm^3 syringe and a 20-gauge needle. Pore water from both the intact cores and the mini drive point piezometer were filtered with 0.45 μm disposable syringe filters and analyzed for NO_3^-, and Cl^-, and SO_4^{2-} (by ion chromotography). Standards were used to determine ion concentrations as described above. To determine sediment water content, a portion of the sediment collected from the subsamples was dried overnight at 500^oC and weighed. Total organic carbon in the bulk sediment was determined by weight loss on combustion of the dried samples at 500^oC for at least 5 hours. Separate intact sediment cores were also collected to determine *in situ* redox potential measured by platinum electrode potential (PtEP). An Accumet® Calomel reference electrode was held in the surface water in the top of the core and a platinum wire was inserted into the sediment through side ports at various depths. The reference electrode consisted of a

mercury/mercury (I) chloride reference element surrounded by gelled saturated KCl solution and tipped with a porous polymer junction.

Sediment color can be very informative about the conditions at different depth layers in the streambed. Most sediment colors are derived from the colors of iron oxides (yellow, orange, and red) and organic matter (dark black or brown) that coat the surfaces of soil particles (Brady and Weil, 1999). The sediment color pattern was investigated in four cores taken to a depth of approximately 40 cm below the stream surface. The cores were cut lengthwise and photographed. Because color changes when iron-containing minerals in the sediment undergo oxidation and reduction reactions, sediment color can indicate the oxygen conditions of the upwelling pore water. Under oxic conditions, iron coatings are oxided and are typically high-chroma colors (red or brown), but prolonged anaerobic conditions can cause the iron oxide coatings to become chemically reduced, changing high-chroma colors to low-chroma (gray) colors.

Denitrification Potential

Potential denitrification rates were determined from N_2O accumulation in laboratory incubations of streambed sediments amended with acetylene (Tiedje, 1982). The sediment samples were vertically distributed (2 cm below sediment surface and then at 10 cm increments) along the length of the sediment cores and were collected using a 10-cm^3 syringe. The sediments samples were placed in 60-mL serum bottles with 15 mL of artificial ground water and capped with a septum and crimped shut with a metal cap. Artificial ground water was made to consist of the following salts dissolved in 1 L of deionized water: 60 mg $MgSO_4 \cdot 7H_2O$, 36 mg $NaHCO_3$, 36 mg $CaCl_2$, 25 mg

$CaSO_4 \cdot 2H_2O$. Nitrate was not added to the sediment slurries. *In situ* pore water in the sample was the only source of nitrate. The sediment slurry was made anaerobic by bubbling with N_2 gas through a 22-gauge spinal needle for 5 minutes. Five percent acetylene was injected into the sediment suspension with a 20-gauge needle. The bottles were shaken on a rotary shaker and periodic samples of the headspace were withdrawn for analysis. N_2O production was determined on a Varian CP-3800® Gas Chromatograph using a ^{63}Ni electron capture detector and a HP- Plot Q silica capillary column (30 m in length, 0.53 mm ID, 40 μm film thickness). The specific settings of the GC method include:

Front Injector (type 1079) Oven: 50°C
Flow/Pressure Setting: Front EFC 10.8 psi at constant flow
Column Oven: 30°C
ECD Detector Oven: 300°C

The dry weight of the sediment was determined after the assay was completed. The volume of sediment added to each serum bottle was also recorded. A control sample was tested that included artificial ground water only, with no added sediment.

A standard curve was created for the determination of the mass of N_2O produced by denitrifying bacteria from measured peaks on the gas chromatograph (Figure 5). Pure nitrous oxide was diluted with N_2 gas to create three different concentrations (v/v): 1%, 1000 ppm, and 100 ppm. The peaks of five consecutive volumes (0.1 mL to 0.5 mL) of the diluted standards, 100 ppm and 1000 ppm, were measured on the GC and used to create the range of mass for the standard curve below. The area of the nitrous oxide peak from the GC (mVolts*sec) was converted to mass of N_2O in nmol using the ideal gas law, where 1 mole = 22.4 liters or 1 mL = 0.0446 mmole = 44.6 μmol = 44600 nmole.

The minimal detectable mass was approximately 5 nmoles (1 mL of 100ppm standard). This standard curve was used for all four sampling dates.

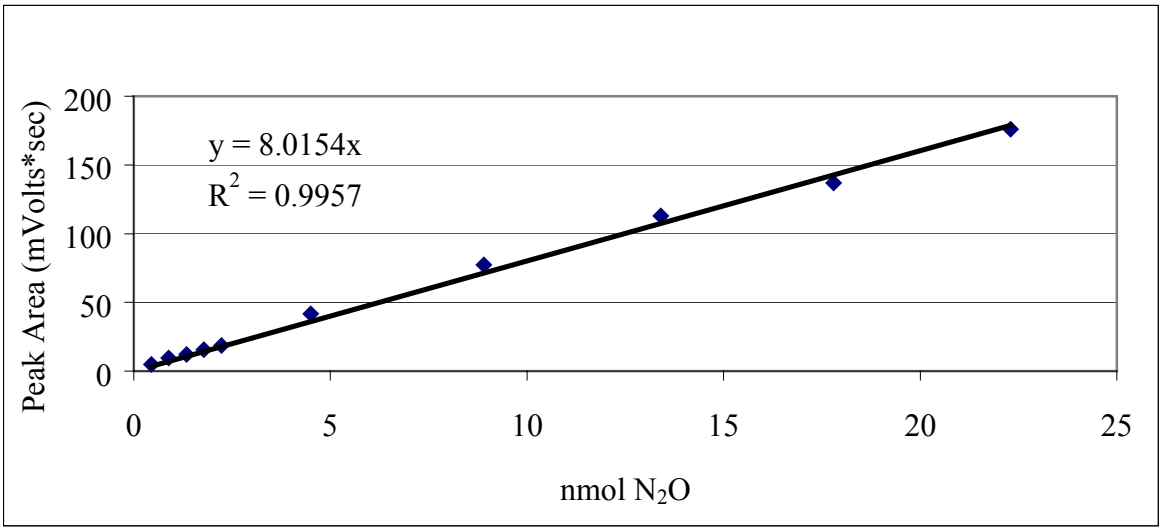

Figure 5. Standard curve to determine mass of nitrous oxide (nmol) from peak area collected from the gas chromatograph.

Once the mass of the injection sample was determined, the concentration of the injection sample was determined by dividing the mass (nmol) by the injection volume (usually 0.5mL). The injection concentration was then used to determine the total N_2O production in the headspace and dissolved N_2O in the liquid phase. Based on Tiedje (1982), total N_2O mass (M) can be calculated using the Bunsen absorption coefficient according to the equation:

$$M = C_g (V_g + V_l \ \alpha) \qquad (4)$$

where M is the total mass of N_2O in the water plus gas phases (nmol), C_g is the concentration of N_2O in the gas phase (nmol/mL), V_g is the volume of gas phase (mL), V_l is the volume of liquid phase (mL), and α is the Bunsen absorption coefficient. In the present case, α =0.544 at 25 ^oC was used (Tiedje, 1982).

The potential denitrification rate was determined by dividing the total mass of N_2O produced in the serum bottles by the incubation time and the sample volume, in which the rate was expressed in units of nmol N_2O mL sediment^{-1} hr^{-1}. In addition, the dry weight of the sediment was determined to compare denitrification rates found in this study to other studies in the literature (nmol N_2O g DW^{-1} hr^{-1}). Also, the denitrification potential expressed as nmol N_2O mL sediment^{-1} hr^{-1} was converted to μmol N m^{-2} h^{-1} to compare the observed rates to those in other studies that express their rates in those units. The conversion was done by multiplying the N_2O production rate in the subsample collected in each depth segment by the total area for that segment in the core ($\pi r^2 h$), which resulted in the N_2O production for the total volume of the sediment for each depth segment. The N_2O production for each depth segment was summed to determine the N_2O production along the entire length of the core. Finally, the units were converted to μmol N m^{-2} h^{-1}.

$$\sum \frac{\text{nmol } N_20}{\text{mL sediment} * \text{hr}} * \prod * (2.25cm) \; * h(cm) * \frac{2\text{mol N}}{\text{mol } N_2O} * \frac{1\,\mu\text{molN}}{10^3\,\text{nmolN}} * \frac{10^4\,\text{cm}^2}{\text{m}^2} = \frac{\mu molN}{m^2 * hr} \quad (5)$$

Mass Balance between the Potential Nitrate Removal Rate by Denitrification and the Observed Nitrate Loss Rate

First, the potential nitrate removal rate was determined based on the production of N_2O by denitrification in the sediment slurries in the acetylene block assay. The rate of N_2O production was converted to the rate of NO_3^- removal based on the assumption that denitrification in the sediments was complete, such that all N_2O would be converted to N_2. It was also assumed that the acetylene assay completely blocked N_2 formation in the

denitrification process. Based on these assumptions, the N_2 production in equation 1 can be replaced by N_2O production. Using the coefficients in equation 1, 2 mol of nitrate are removed for every mol of N_2O produced. Next, the volume of saturated sediment was converted to a volume of pore water by multiplying the bulk volume by an average porosity value of 0.35. The equation below (6) converts the rate of N_2O production to the potential rate of nitrate removal.

$$\frac{\text{nmol } N_2O}{\text{ml sediment} * \text{hr}} * \frac{1\text{mol}}{10^9\text{nmol}} * \frac{2\text{mol N}}{\text{mol } N_2O} * \frac{14\text{g N}}{\text{mol}} * \frac{1000\text{mg}}{\text{g}} * \frac{1\text{ml sediment}}{0.35\text{ml porewater}} * \frac{1000\text{ml}}{\text{L}} =$$

$$\frac{\text{mg}NO_3^-}{\text{L} * \text{hr}} \qquad (6)$$

This potential nitrate removal rate was calculated for each depth segment and then summed for all segments in the core.

Next, the observed decrease in nitrate concentration was converted to a loss rate using the advection dispersion equation; however, dc/dt was replaced by R, which represents a nitrate loss rate:

$$\frac{dc}{dt} = -u * \frac{\partial c}{\partial x} + D * \frac{\partial^2 c}{\partial x^2}, \qquad R = -u * \frac{\partial c}{\partial x} + D * \frac{\partial^2 c}{\partial x^2} \qquad (7)$$

In this equation, u is the average linear velocity (3×10^{-4} cm sec^{-1}) determined by dividing the Darcy velocity (1.04×10^{-4} cm sec^{-1}) by the porosity (0.35). The Darcy velocity was determined by a laboratory biological simulation experiment in which the flow rate was altered until the difference in output and input nitrate concentration matched that of field conditions (Gu, unpublished data). Dispersion ($D*(\partial c^2/\partial x^2)$) in the sediment was assumed to be negligible compared to the advective flow of discharging

ground water. To determine the observed nitrate loss rate along the length of the entire core ($\partial c/\partial x$), the equation was rearranged. The advection equation was multiplied by dx (8). Then, the equation was integrated (9), followed by taking the derivative and solved for the nitrate concentration (c), which resulted in the line equation (10):

$$R * \partial x = -u * \partial c \tag{8}$$

$$x * R = u * c + A \tag{9}$$

$$c = \frac{R}{u} x + B, \tag{10}$$

where B is a constant. The concentration of nitrate at each depth segment in the cores was graphed, and a linear regression line was fit to the data. The slope of the line ($R \cdot u^{-1}$) was multiplied by the average linear velocity (u), which resulted in the observed nitrate loss rate (R). Subsequently, the potential nitrate removal rate based on N_2O production was compared to the observed nitrate loss rate in the sediment cores.

RESULTS

Ground Water Flow Paths to Cobb Mill Creek

Sampling of the water table elevation, hydraulic head and nitrate concentrations in the ground water well and piezometer nests along the hillslope and the stream began in April 2001 and continued to October 2003. The slope of the water table elevation followed the ground water surface contours along a lateral transect from the hillslope (well N9) to the stream, except at bankside wells N3 and N1 (Figure 6). The water table was generally level in the wells at the bank of the stream although these wells were on a slope. The depths of the mean water table below ground level at hillslope positions N9, N7, N3, and N1 were 1.80, 1.34, 0.93, and 0.56 meters, respectively.

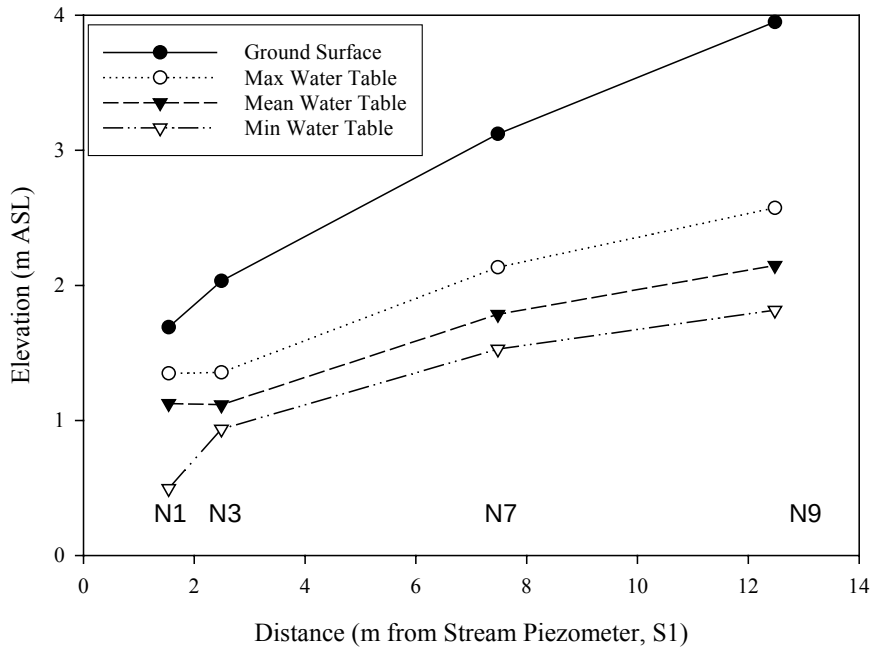

Figure 6. Water table gradients and the ground surface contour along a transect up the hillslope. The maximum, mean, and minimum water table depth from April 2000 to October 2003 is shown.

Vertical hydraulic head gradients were determined in the nested piezometers along the hillslope and in the stream (Table 1). These gradients describe only shallow ground-water flow (less than one meter). The stream piezometer nests, S1 and S2, showed an upward hydrologic flow path from the ground water to the stream indicated by a negative vertical head gradient. The bankside piezometer nests, N1 and N3, also showed an upward flow of ground water for the majority of the sampling dates. Alternately, vertical head gradients in the bankside piezometer nests, N4, N5, and N6 showed a less consistent pattern but indicated that more downward flow occurred in these locations compared to N1 and N3, despite their close proximity. Vertical head gradients at N7, located near the top of the hillslope, indicated that strong downward flow occurred at this location. The negative head gradients in the stream piezometers indicated there was a deeper flow path that discharged vertically into the stream. The data are consistent with the classical conceptual model of subsurface flow discharging to a stream from a hillslope (Hubbert, 1940). Longitudinal gradients were also determined between two stream piezometers, S1A and S2B, which were placed at similar depths underground, 60 and 62 cm, respectively (Table 2). The piezometers were 8.4 meters apart. The vertical head gradients were approximately a magnitude greater than the longitudinal head gradients indicating that the upward advective flow of the discharging groundwater was stronger than the downstream or longitudinal subsurface flow.

Table 1. Vertical head gradients for various sampling dates for nested piezometers at three depths in most cases (A: shallowest, B: mid C: deepest depth) along the hillslope (N1- N7) and in the stream (S1 and S2). For piezometer depths see Table A-2 in Appendix.

Piezometer	Date							
	5/31/01	6/15/01	7/3/01	8/17/01	5/13/02	6/5/02	6/7/02	8/22/02
S1 A:B	N/A	-0.034	-0.073	-0.073	-0.050	-0.054	-0.038	-0.042
S2 A:B	N/A	N/A	N/A	0.000	-0.071	-0.059	-0.065	-0.076
N1 A:B	-0.003	-0.038	-0.038	-0.003	0.041	-0.228	-0.141	-0.038
N1 B:C	-0.040	-0.012	-0.012	-0.040	-0.052	-0.061	-0.055	-0.055
N3 A:B	-1.288	-1.401	-1.458	0.915	-0.017	-0.373	-0.260	-0.638
N3 B:C	-0.131	-0.131	-0.101	-0.071	-0.042	-0.071	-0.024	-0.101
N4 A:B	0.579	0.579	0.711	-0.053	-0.053	-0.011	0.084	-0.053
N4 B:C	-0.604	-0.658	-0.738	0.198	0.059	0.016	0.021	0.037
N5 A:B	-0.767	-0.700	-0.700	-0.300	-0.020	-0.100	-0.073	0.167
N5 B:C	-0.017	0.069	0.069	0.156	0.065	0.039	0.030	-0.017
N6 A:B	0.006	-0.108	-0.136	0.006	-0.011	0.040	-0.278	0.062
N6 B:C	0.023	0.023	0.023	0.138	0.121	0.023	0.339	-0.006
N7 A:B	N/A	1.000	1.000	3.143	2.000	1.571	1.857	1.571
S1 A:B	-0.057	-0.149	N/A	-0.023	0.023	-0.073	-0.073	-0.103
S2 A:B	-0.076	-0.059	N/A	-0.088	-0.059	-0.088	-0.059	-0.059
N1 A:B	-0.279	-0.203	-0.138	-0.186	-0.290	-0.021	-0.228	-0.193
N1 B:C	0.795	-0.046	-0.055	-0.040	-0.104	-0.069	-0.127	-0.127
N3 A:B	-0.282	-0.328	-0.011	-0.096	-0.130	0.266	-0.311	-0.073
N3 B:C	-0.089	-0.077	-0.089	-0.107	-0.161	0.524	-0.089	-0.042
N4 A:B	-0.542	-0.032	-0.021	-0.047	-0.079	0.605	-0.105	0.105
N4 B:C	0.519	0.422	0.422	0.016	0.011	0.037	0.037	0.037
N5 A:B	-0.100	-0.133	-0.107	-0.113	-0.167	-0.033	-0.167	-0.127
N5 B:C	0.091	0.043	0.048	0.074	0.048	0.026	0.048	0.039
N6 A:B	0.011	0.017	0.023	-0.006	-0.006	0.062	0.034	0.006
N6 B:C	0.046	0.000	-0.006	0.017	0.006	0.080	0.052	0.069
N7 A:B	1.000	1.429	1.000	1.286	1.000	1.000	1.714	2.000

Table 2. Longitudinal head gradients between two stream piezometers, S1A & S2B, at similar depths below the stream surface (60 and 62 cm, respectively) for various sampling dates. The piezometers are 8.4 m apart.

Piezometer	8/17/01	5/13/02	6/5/02	6/7/02	8/22/02	9/17/02
S1A: S2B	-0.008	-0.005	-0.006	-0.005	-0.005	-0.005

Piezometer	10/28/02	12/19/02	2/3/03	7/8/03	9/28/03	10/26/03
S1A: S2B	-0.008	-0.004	-0.003	-0.005	-0.005	-0.007

Ground Water and Stream Nitrate Concentrations

The measured nitrate concentrations in the stream piezometers were generally lower in the Fall 2002 than samples collected in the Summer -Winter of 2003 (Table 3). The general pattern of increasing nitrate concentration with depth (decreasing elevation) was illustrated in every sampling month. The exception to this trend was one piezometer nest along the stream bank, N4. Nitrate concentrations were lower with depth in this case, although the piezometers were placed at the same depth below ground as the adjacent bank side piezometer nests. The general pattern was shown especially in the stream sediments in which the nitrate concentration of the upwelling ground water that was collected from stream piezometers was on average greater (9.01 mg NO_3^--N L^-1) than the open channel nitrate concentrations (2.77 mg NO_3^--N L^{-1}).

Ground water sampling on October 26, 2003, illustrated the general pattern of increasing nitrate with depth, again with the exception of nest 4 (Figure 7). The trend was especially evident when comparing the deeper upwelling ground water collected from the stream piezometers nests, S1 and S2, and the stream nitrate concentrations. The ground water collected from the two piezometers at station S1 (40 and 62 cm below the stream

Table 3. Nitrate Concentration (mg NO3--N L-1) of Groundwater collected from CMC Piezometer Nests for all Sampling Dates. Error is reported as standard error of the mean (SEM). Depth below ground surface is generally shown by piezometer letter: A: Shallowest B: Mid C: Deepest Depth. For piezometer depths see Table A-2 in Appendix A.

Method:	Cadmium		Cadmium		Cadmium		Cadmium		ION CHRM		ION CHRM		ION CHRM		ION CHRM	
Piezometer	9/17/02	SEM-9/17/02	10/28/02	SEM-10/28/02	11/20/02	SEM-11/20/02	12/19/02	SEM-12/19/02	7/11/03	SEM-7/11/03	10/26/03	SEM-10/26/03	11/30/03	SEM-11/30/03	12/19/03	SEM-12/19/03
N1A	2.22	0.00	1.34	0.00	1.07	0.15	0.21	0.21	n/a	n/a	3.11	0.07	4.81	0	2.40	0.35
N1B	5.54	0.14	1.53	0.10	4.28	0.05	2.67	0.48	n/a	n/a	7.49	1.25	9.98	0	10.97	0.49
N1C	7.07	2.00	1.97	0.11	6.47	1.89	4.61	0.62	n/a	n/a	10.69	0.33	11.92	0	13.05	0.13
N3A	6.93	0.00	1.76	0.33	1.25	0.08	6.33	0.00	n/a	n/a	6.98	0.00	n/a	n/a	6.56	0
N3B	7.02	0.92	1.88	0.13	1.51	0.25	1.99	0.60	n/a	n/a	5.71	0.79	8.71	0.1	11.58	0
N3C	7.70	0.59	2.46	0.35	3.20	0.24	5.18	1.09	n/a	n/a	9.47	0.59	11.91	0	13.93	0.1
N4A	6.31	0.00	n/a	n/a	1.63	0.17	1.55	0.43	n/a	n/a	2.26	1.27	1.34	0	4.25	0.5
N4B	3.46	0.00	2.99	0.28	0.71	0.19	0.13	0.07	n/a	n/a	0.69	0.02	0.81	0	1.60	0.1
N4C	2.55	0.22	1.68	0.18	0.59	0.05	0.00	0.00	n/a	n/a	0.37	0.13	0.14	0	0.41	0.1
N5A	4.16	0.00	1.32	0.17	2.86	0.83	1.03	0.12	n/a	n/a	0.64	0.07	1.76	0	1.63	0
N5B	4.86	0.36	2.25	0.39	4.73	1.06	1.62	0.22	n/a	n/a	0.75	0.02	2.94	0	7.68	0.1
N5C	4.11	0.00	3.14	0.46	3.14	0.12	1.80	0.77	n/a	n/a	4.12	0.53	9.68	0.1	9.56	0
N6A	7.24	0.00	2.20	0.35	4.40	0.82	1.48	0.22	0.58	0.05	1.00	0.16	4.76	0	9.67	0.2
N6B	8.93	0.50	3.07	0.12	4.44	0.84	2.02	0.07	3.20	0.19	3.02	0.45	6.36	0	9.55	0
N6C	9.26	2.18	4.18	0.94	4.02	0.42	2.48	0.26	3.36	0.16	3.37	0.45	8.88	0.1	12.72	0.3
N7A	2.24	0.25	2.70	0.39	1.61	0.03	0.40	0.31	0.95	0.49	8.59	0.59	10.68	0.1	13.37	0.1
N7B	3.57	0.05	5.98	0.57	4.89	0.70	3.39	1.04	7.20	0.19	10.31	0.53	11.48	0	13.09	0
N10A	n/a	n/a	2.02	0.03	1.36	0.34	0.90	0.01	2.34	0.14	4.72	1.67	6.21	0	2.77	0.1
S1A	5.99	2.22	4.72	0.48	4.67	0.14	6.22	0.48	12.55	0.11	11.48	0.04	11.29	0	11.72	0.2
S1B	4.03	0.59	7.05	0.29	5.42	0.19	6.56	0.76	13.29	0.16	11.65	0.08	11.26	0	12.32	0
S2A	7.00	0.90	6.89	0.61	5.41	0.60	8.63	0.57	13.13	0.09	9.27	0.26	11.22	0	11.83	0.1
S2B	5.09	1.21	9.60	1.08	6.34	0.58	7.45	0.41	13.35	0.05	9.36	0.02	11.31	0	12.17	0
Stream at Hillslope	2.74	0.03	2.67	0.41	5.46	0.24	5.36	0.14	1.91	0.00	1.37	0.02	2.20	0	2.50	0
Stream at Culvert	n/a	n/a	n/a	n/a	2.50	0.21	3.62	0.13	n/a	n/a	1.02	0.23	n/a	n/a	n/a	n/a

Note: In addition, Stream at Exp Hillslope for August 4th, 2003 (1.72 mg NO_3^--N L^{-1} (SEM= 0.18)) and August 26th, 2003 (1.65 mg NO_3^--N L^{-1} (SEM: 0.13)).

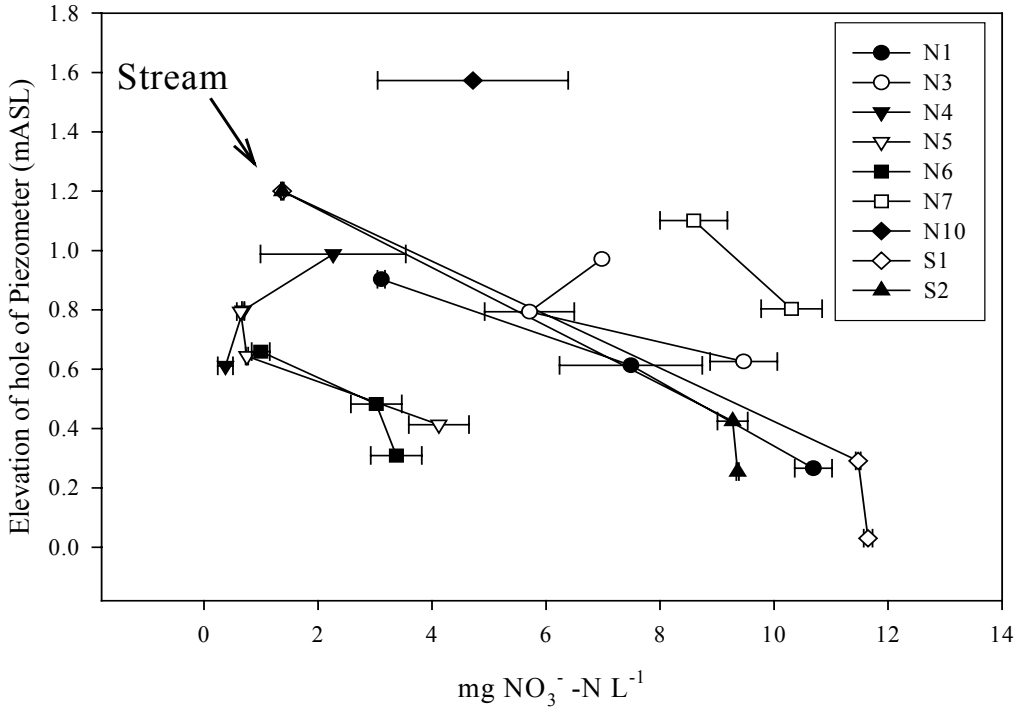

Figure 7. Nitrate concentration in ground water collected from piezometer nests on October 26, 2003

sediment surface) had nitrate concentrations of 11.48 and 11.65 mg NO_3^--N L^{-1}, respectively. The ground water collected from the two piezometers at station S2 (60 and 88 cm below the stream sediment surface) had nitrate concentrations of 9.27 and 9.36 mg NO_3^--N L^{-1}, respectively. The stream nitrate concentration was 1.37 NO_3^--N L^{-1}. On this sampling event, there was an average decrease of 9.14 mg NO_3^--N L^{-1} between the upwelling pore water, which was collected from four points in the streambed approximately 60 cm deep, and the stream.

The nitrate concentrations in the stream piezometers were generally greater than the adjacent hillslope piezometers (Figure 8A). The nitrate concentrations of the shallow

bankside piezometers ranged from 1- 3 mg NO_3^--N L^{-1} on October 26, 2003. Farther up the hillslope, the piezometers at a similar depth below ground also had low nitrate concentrations at stations N10 (2- 5 mg NO_3^--N L^{-1}), but higher nitrate concentrations at station N7 (8.5-10 mg NO_3^--N L^{-1}). The nitrate concentration of the stream was 1.37 mg NO_3^--N L^{-1}. The nitrate concentration of the stream piezometers ranged from 9-12 mg NO_3^--N L^{-1}. These nitrate concentrations at different positions along the hillslope were used to determine the flow path of ground water that feeds the stream. The increased nitrate concentrations along with the negative vertical head gradients of the stream piezometers indicated that a deeper flow path led to the stream that may have traveled beneath the agricultural field. This deeper flow path contained higher nitrate concentrations than the shallow flow path that followed the ground contours.

The four piezometer nests that line up the hillslope formed a cross-sectional transect that was perpendicular to the stream (Figure 8B). In this transect, the nitrate concentration of the stream piezometer, S1, was four times larger than that of the open channel. In the piezometers near the bank of the stream (N1&3), the nitrate concentration increased with depth. The nitrate concentration of piezometer N7 was similar to the stream piezometers and may originate from the agricultural field. The evidence suggested two distinct ground water flow paths along the experimental hillslope.

Chemical Analysis of the Pore Water from Stream Sediments

The stream piezometers, S1 & S2, showed that the nitrate concentration of the inflowing ground water ranged from 9-12 mg NO_3^--N L^{-1} at approximately 60-80 cm beneath the stream bed, whereas the nitrate concentration in the stream was much lower, and ranged

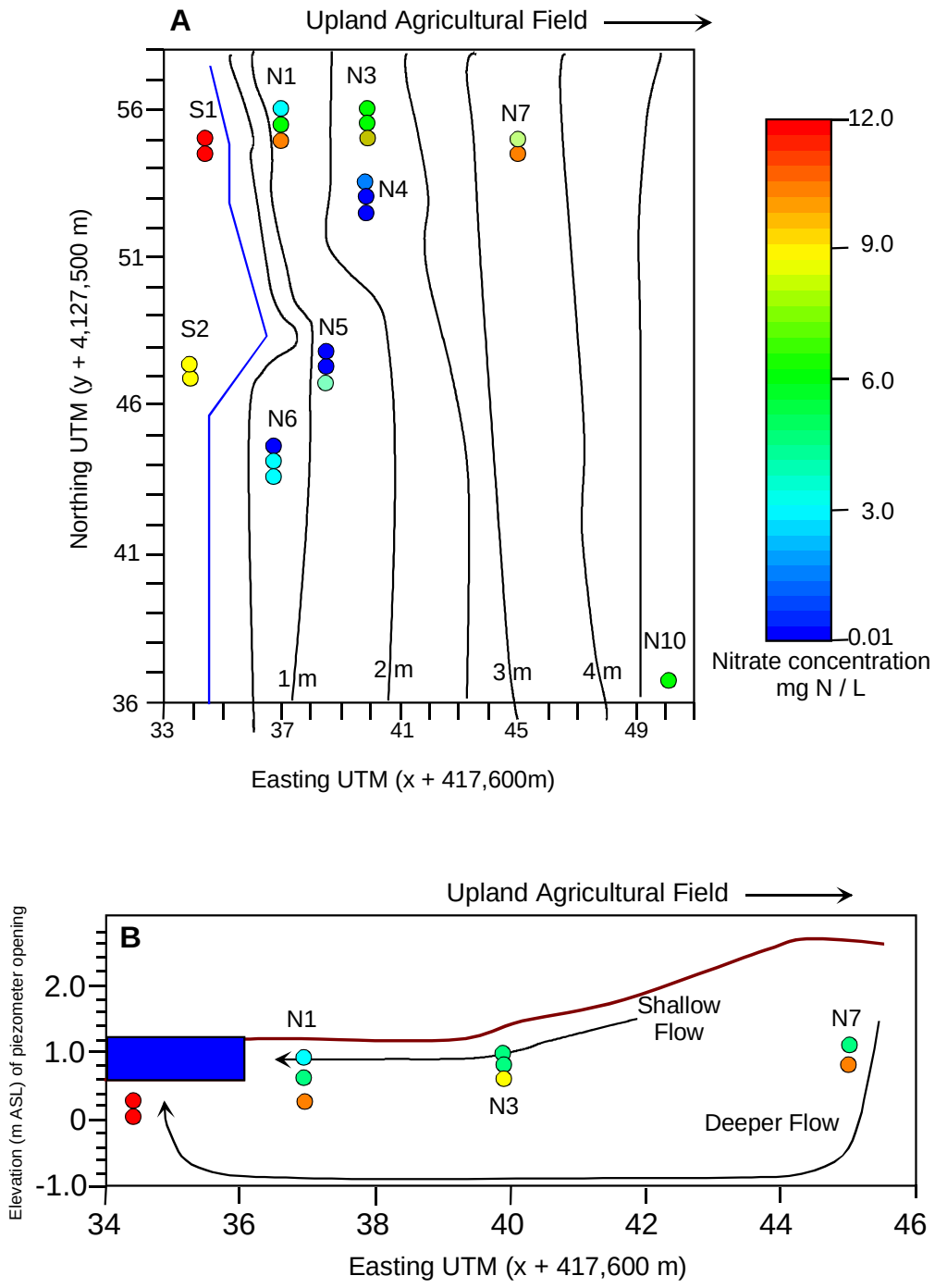

Figure 8: **A:** Mapview of nitrate concentrations of samples collected October 26, 2003, from piezometers in the stream and along the hillslope at Cobb Mill Creek. Piezometers are represented by circles and stacked according to depth below ground. The top circle is the shallowest. Elevation lines in meters above sea level are approximate. **B:** Cross-sectional view of hillslope including suggested ground water flow paths based on observed nitrate concentrations.

from 1- 2 mg NO_3^--N L^{-1}. This is a loss of approximately 90% of the upwelling nitrate. The intact sediment cores taken in the stream sediments (approximately 60cm below the stream bed) showed a similar pattern, with higher NO_3^--N concentrations in the deeper sediments of the core and low nitrate concentration in shallow sediments less than 10 cm deep (Figure 9). On July 11, 2003, there was a decrease of 10.03 mg NO_3^--N L^{-1},

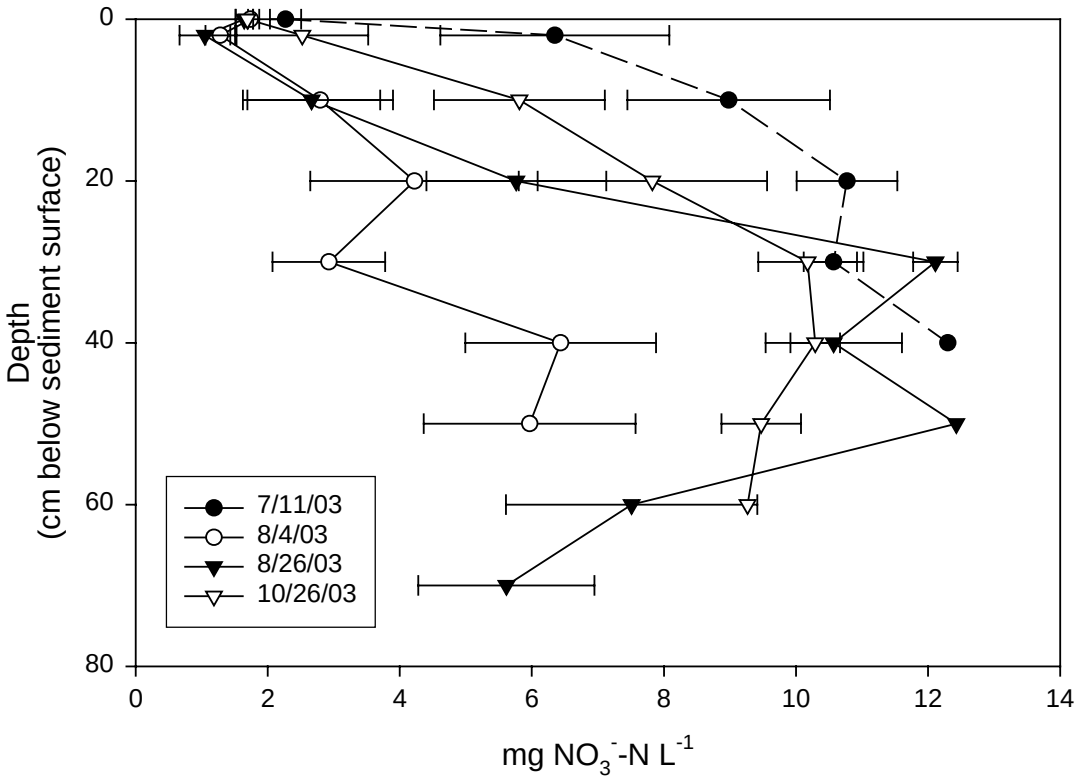

Fig. 9. Depth profiles of NO_3^--N concentration in cores from Cobb Mill Creek taken on the dates indicated. Error bars represent 1 SEM (n=3 cores). Stream water values are represented as the concentration at 0-cm depth.

representing an 81.53% loss of NO_3^- as the ground water discharged toward the stream. In subsequent samples, there were similar NO_3^- losses of 80.3%, 91.6%, and 83.5% in the top 40-60 cm of the sediments on August 4, August 26, and October 26, 2003,

respectively. On average, there was a loss of 84.24% of the NO_3^- over 55 cm in the intact sediment cores. This result corresponds to the estimate of 90% nitrate loss when comparing the nitrate concentrations in the stream piezometers and the open channel.

Whereas, the nitrate concentrations in the sediment pore water increased substantially with depth in the cores, the chloride and sulfate concentrations decreased with depth in all cores (Table 4). The greatest incremental difference was seen between the stream concentrations and the first sediment depth analyzed. The chloride and sulfate concentrations were generally stable beneath the shallow sediments (below 10 cm). The chloride concentration in the stream channel ranged from 14.07- 31.99 mg $Cl^- L^{-1}$ and the stream sulfate concentration ranged from 38.55- 58.97 mg $SO_4^{2-} L^{-1}$ (as SO_4^{2-}) over all the sampling dates.

Changes in the nitrate concentration in comparison to the chloride concentration are indicative of the relative effects of biological transformations and uptake processes as opposed to dilution of the discharge water (Lowrance, 1992). There was not a corresponding decrease in chloride concentration in locations where there were steep declines in nitrate, therefore the nitrate loss is assumed to be due to biological activity (Figure 10).

Pore water samples were collected using the mini drive point piezometer (MDPP) in the center of the stream channel on the same sampling dates as the intact sediment cores (Table 5). Three profiles were collected on July 11 and August 4, 2003, and two profiles were collected on October 26, 2003. Maximum sampling depths were 40 cm, 20cm, and 12 cm for the three dates, respectively. The solute profiles collected with the MDPP were compared both to the profiles collected with the individual core taken in the same

Table 4: Concentration of dissolved inorganic anions (mg L^{-1}) in pore water collected in sediment cores. Values are the mean of n cores. Error is reported as standard error of the mean (SEM).

Depth (cm)	NO_3^--N	NO_3^--N-SEM	Cl^-	Cl^- SEM	SO_4^{2-}	SO_4^{2-} SEM
7/11/03 (n=3 cores)						
0	2.27	0.24	14.07	0.32	58.97	2.46
2	6.35	1.73	9.62	0.73	35.59	4.55
10	8.98	1.53	8.54	0.24	31.75	1.45
20	10.77	0.76	7.96	0.14	28.37	0.45
30	10.57	0.45	8.59	0.16	33.34	4.27
40	12.30	0	8.50	0	28.82	0
8/4/03 (n=9 cores)						
0	1.74	0.04	19.48	0.14	38.55	0.34
2	1.26	0.29	19.13	0.70	38.14	3.11
10	2.59	1.03	22.41	2.25	41.89	5.26
20	4.22	1.58	17.29	0.66	36.12	4.67
30	2.93	0.85	16.53	1.27	41.51	4.17
40	6.44	1.44	17.19	1.26	44.42	9.83
50	5.97	1.60	20.88	3.21	30.74	0
80	6.40	0	14.35	0	31.64	0
8/26/03 (n=9 cores)						
0	1.65	0.13	21.51	0.32	51.22	3.25
2	1.05	0.38	18.42	1.53	40.36	5.90
10	2.66	1.04	14.63	1.05	32.52	3.27
20	5.76	1.36	11.22	1.25	40.25	5.01
30	12.11	0.34	13.57	0.26	35.21	1.47
40	10.57	1.03	13.76	0.78	32.89	1.28
50	12.43	0	13.01	0	27.40	0
60	7.51	1.90	12.72	1.76	37.31	2.02
70	5.61	1.33	11.63	3.58	36.80	7.24
10/26/03 (n=8 cores)						
0	1.69	0.18	31.99	2.00	49.70	1.06
2	2.52	1.00	20.81	3.50	36.05	5.00
10	5.81	1.29	19.37	2.45	26.73	3.65
20	7.83	1.74	17.03	1.94	25.28	2.00
30	10.18	0.75	19.74	3.17	25.20	1.68
40	10.29	0.37	16.68	1.23	23.54	0.81
50	9.47	0.60	18.37	1.27	26.02	1.52
60	9.27	1.48	20.82	1.42	26.90	4.29

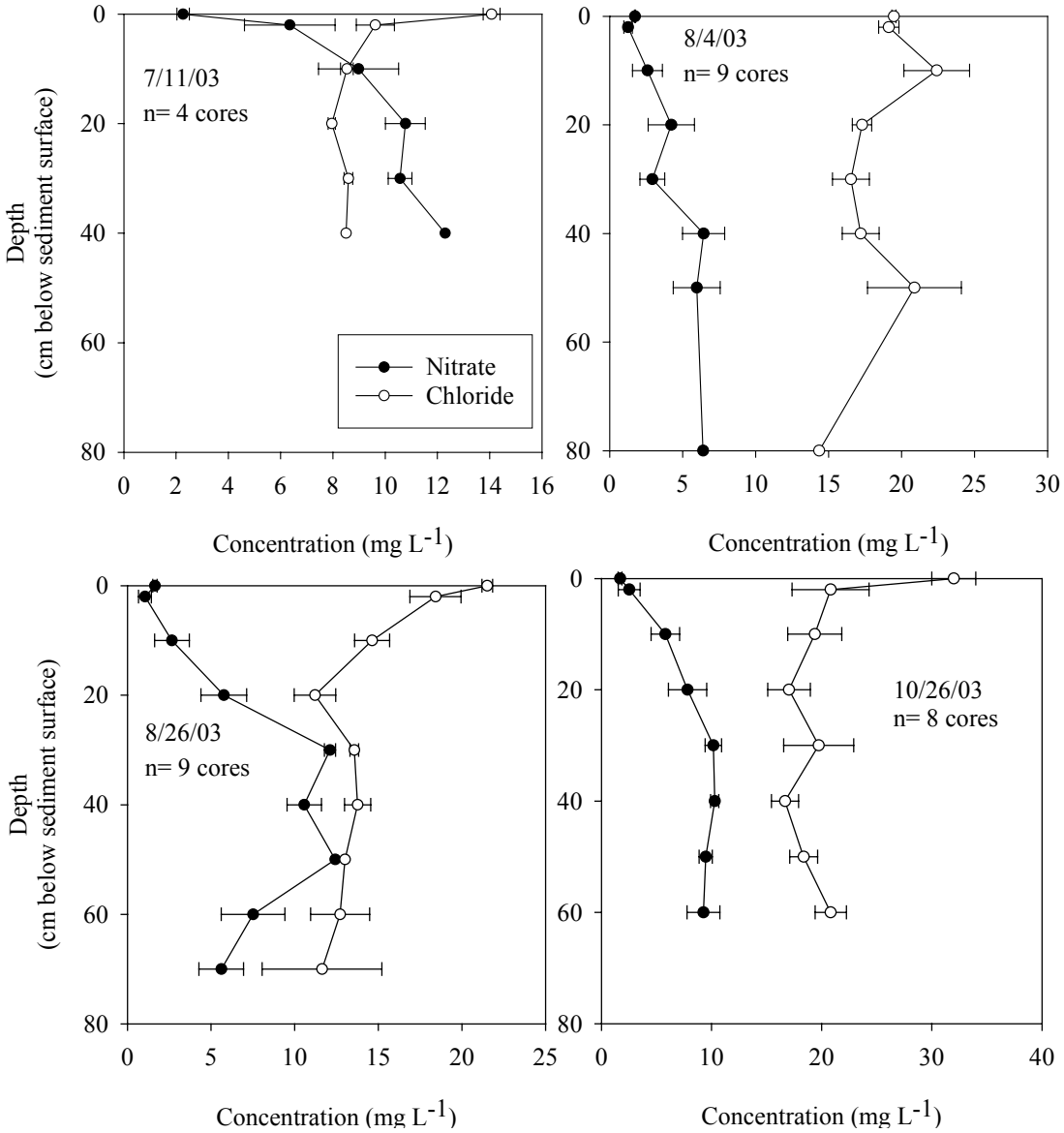

Figure 10: Profiles of average pore water nitrate and chloride concentrations in stream sediments collected with intact sediment cores on four sampling dates. Error bars are SEM. Lack of SEM bars indicate that only one sample was collected.

location as the MDPP sample (in the center of the stream) and to the average of the intact cores collected in all cross sections in the stream (Figure 11). In general, there was good agreement between the nitrate concentrations in the pore water collected from the MDPP

and the intact cores. Chloride and sulfate concentration profiles were similar to the intact core samples, showing generally decreasing concentrations with depth.

Table 5: Concentration of pore water anions collected with the mini drive point piezometer in CMC sediments. Error is reported as standard error of the mean (SEM).

Depth	Cl^-	Cl^- SEM	NO_3^--N	NO_3^--N-SEM	SO_4^{2-}	SO_4^{2-}-SEM
7/11/2003	(n = 3 samples)					
0	15.42	0.45	4.50	2.37	43.87	9.79
5	9.01	0.48	8.06	1.44	25.51	2.11
10	8.07	0.24	7.56	2.15	24.00	1.09
12.5	8.41	0.29	7.96	1.19	27.31	1.83
15	8.25	0	9.49	0	22.95	0
17.5	8.77	0	11.38	0	24.30	0
20	8.98	0.96	9.06	1.83	31.23	6.60
30	8.41	0	9.94	0	24.30	0
33	9.73	0	9.86	0	30.63	0
40	10.22	0	8.44	0	33.34	0
8/4/2003	(n = 3 samples)					
0	16.47	1.97	1.72	0.18	28.05	2.26
2.5	14.88	0.71	1.93	0.81	26.86	2.16
5	14.53	0.67	1.88	1.16	24.17	1.82
7.5	12.58	0.11	1.50	0.91	17.59	5.21
10	12.97	0	3.00	2.75	14.60	10.76
15	13.10	0.36	2.23	1.14	24.17	0.79
20	13.07	0.49	1.62	1.53	30.30	8.52
10/26/2003	(n = 2 samples)					
0	30.10	0	1.44	0	45.46	0
2.5	15.72	2.72	0.48	0.04	24.30	10.68
5	13.13	0.49	0.31	0	19.25	15.73
7.5	12.95	0.31	0.74	0.30	16.73	11.27
10	13.53	0.53	0.37	0	10.71	8.35
12.5	15.85	0	1.04	0	5.46	0

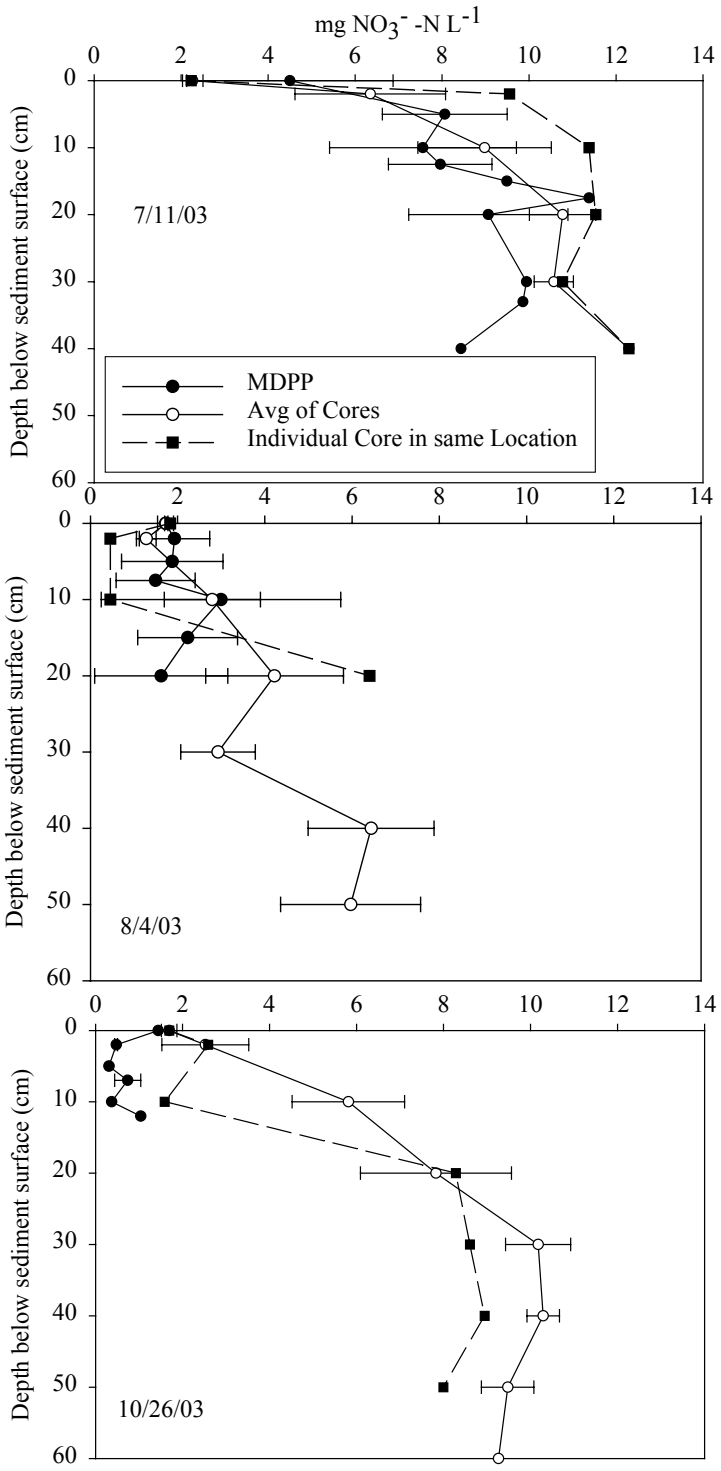

Figure 11: Profiles of NO_3^--N concentration determined with the mini drive point piezometer (MDPP), individual core collected in the same location as the MDPP, and average of cores collected in all locations in the stream. Error bars are standard error of the mean (SEM). Lack of SEM bars indicate that only one sample was collected.

Total Organic Matter Content

Concentrations of total organic matter (determined by ignition) were highest in the top 20 cm of the creek sediment and decreased with depth (Figure 12). The maximum values (for all cores collected at all times) ranged from about 2% to 5.2% at 10 cm. Below 20 cm, the organic matter concentration decreased substantially to about 0.18% below 60 cm. The zone of maximum concentration of organic matter coincided with the zone of observed maximum decreases in NO_3^--N concentration (Figure 8).

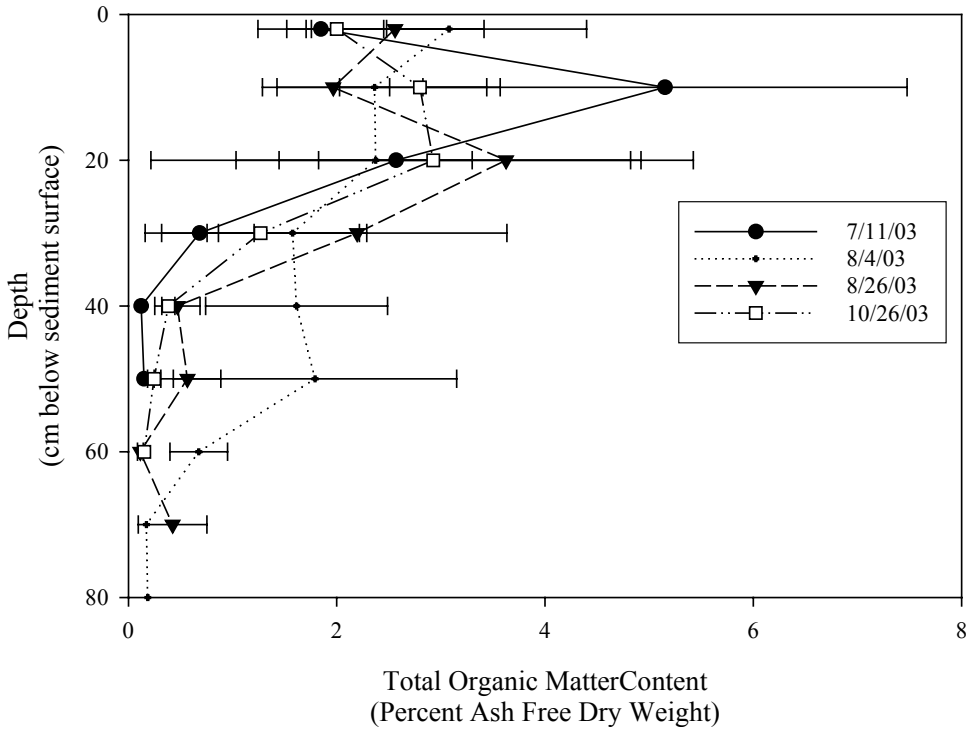

Fig. 12. Depth profiles of total organic matter content in intact cores taken on the dates indicated. Error bars represent 1 SEM (n=3, 9, 9, and 8 cores for sampling dates July, August 4, August 26, and October 26, 2003, respectively).

Platinum Electrode Potential

Redox status was estimated by measuring platinum electrode potential on August 26 and October 26, 2003 (Figure 13). The average of five cores is reported for samples taken on August 26. In both sampling events, there was a distinct change in platinum electrode potential at approximately 10 – 20 cm below the sediment surface with the voltages reflecting a more oxidized environment below that point. The zone of low redox potential corresponded to the zone of high organic matter content and low nitrate concentrations. Dips in platinum electrode potential at various depths below 20 cm in the three profiles were also found.

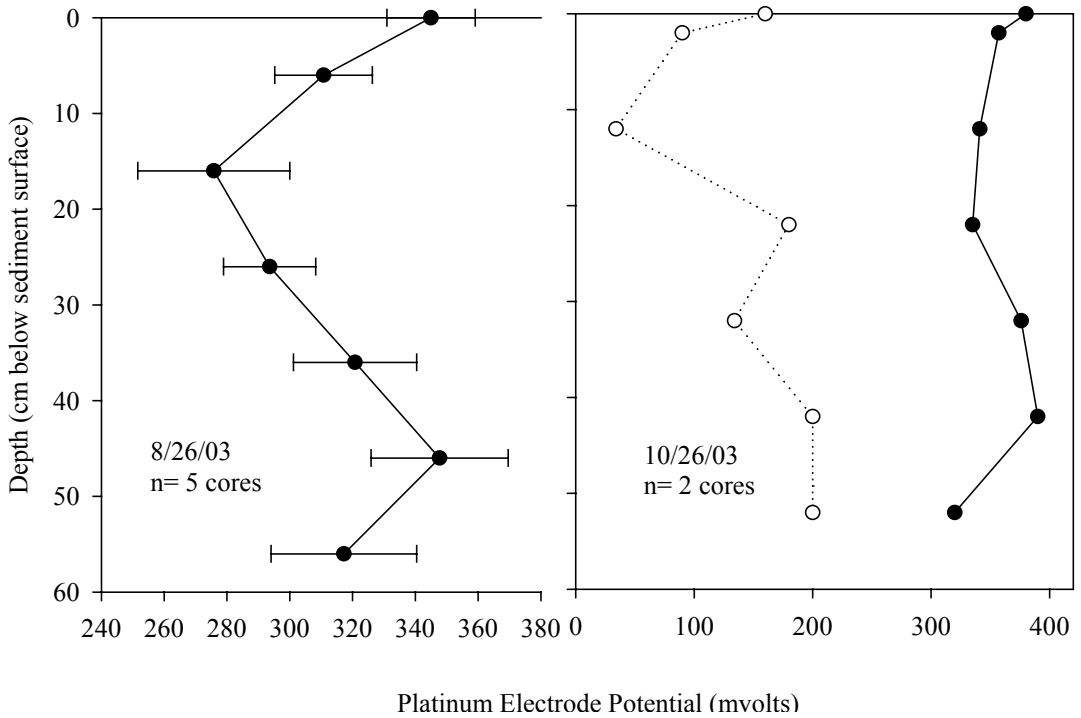

Fig. 13. Depth profiles of platinum electrode potential in cores from Cobb Mill Creek. Cores were taken on the dates indicated. Error bars represent 1 SEM.

Photographs of the sediment cores also showed thick black layers concentrated near the stream-bed surface, 10- 20 cm deep (Figure 14). Based on the organic matter

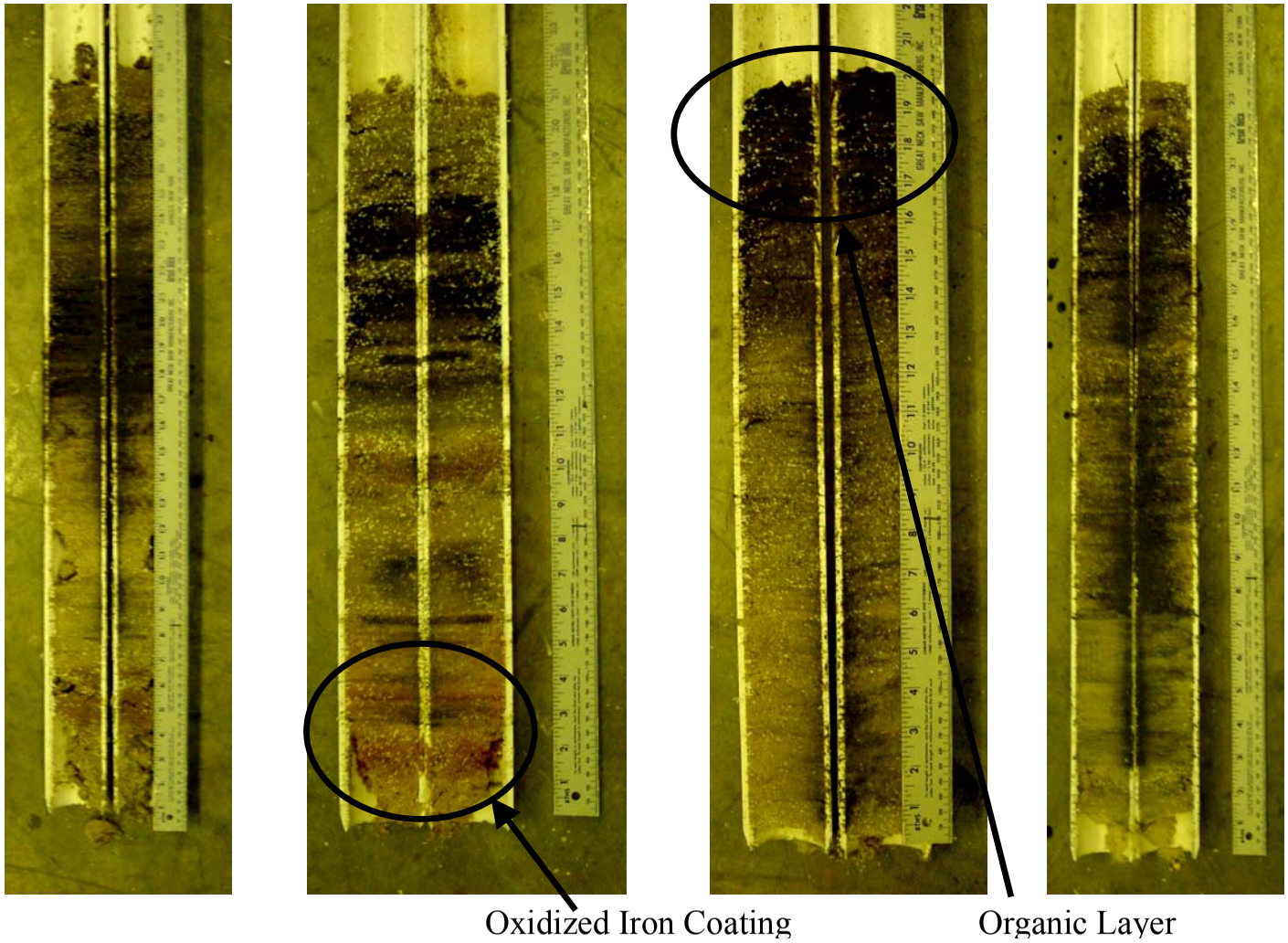

Figure 14: Stream sediment cores from CMC collected October 26th, 2003, that have been cut in half to display the organic matter and iron layers along the depth profile.

content sediment profiles, the thick black layers most likely represent organic matter and not reduced iron or sulfide coatings. Black ribbon-like pockets were also seen below this depth and may represent buried organic matter. These buried pockets may support hot spots of denitrification at depth if conditions are reducing in microsites. In two of the cores collected, pockets of red sediment were evident below 30 cm, and may represent oxidized iron coatings on the sediment. This oxidized iron state signifies aerobic pore water conditions. This supports the suggestion that at depth, upwelling ground water was aerobic, and reducing conditions were not reached until the pore water was closer to the stream sediment surface. The fact that the red oxidized coatings were only seen in some of the cores points to the great heterogeneity in the stream sediments.

Potential Denitrification Rate

The potential denitrification rate was determined by measuring N_2O production over time using the acetylene block method (Tiedje, 1982). Preliminary results indicated that the N_2O production was linear with time until the reactants were exhausted and then production was constant with time. N_2O increased linearly up to 4-5 hours. Then after a 24 hour period, N_2O was still produced but at a slower rate, and following this period a saturation level was reached. In order to determine maximum N_2O production, headspace samples were collected during the 4-5 hour window of linear maximum production.

On all four sampling dates, a pattern was evident in which the highest denitrification potential corresponded to depths of greatest change in nitrate concentration and high organic matter content (Figure 15). The zone of high denitrification rates generally occurred at shallow depths less than 10 cm below the sediment surface. On July

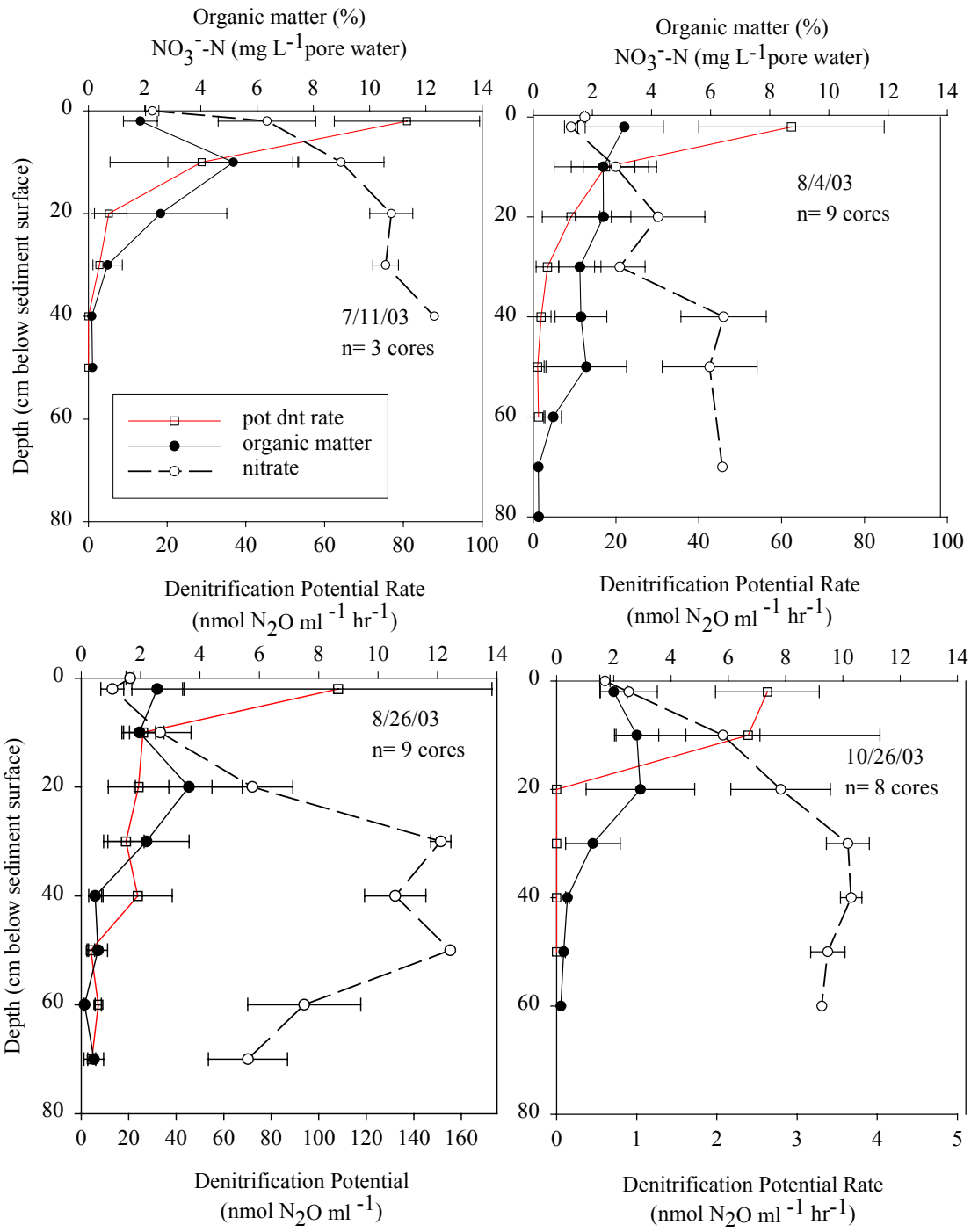

Fig. 15. Depth profiles of organic matter, nitrate, and denitrification potential rate in cores from Cobb Mill Creek. Cores were taken on the dates indicated. Error bars represent standard error of the mean (SEM). Denitrification potential is expressed as a rate (nmol N_20 ml^{-1} hr^{-1}) for all sampling dates except for August 26th in which only maximum N_2O production was possible.

11 and August 4, the highest denitrification potential rate results were similar (80.93 and 62.39 nmol N_2O mL sediment^{-1} hr^{-1}, respectively) and occurred at a depth of 2 cm below the stream sediment surface; and the second highest potential denitrification rates (28 and 26.14 nmol N_2O mL sediment^{-1} hr^{-1}, respectively) occurred at a depth of 10 cm below the stream sediment surface. On August 26, denitrification potential was reported as the maximum potential denitrification (N_2O production) as opposed to a potential denitrification *rate* due to technical difficulties with the gas chromatograph. Hourly rate data could not be recorded. The highest potential denitrification (108.16 nmol N_2O mL sediment^{-1}) occurred at a depth of 2 cm below the stream sediment surface, and the second highest potential denitrification rate (26 nmol N_2O mL sediment^{-1}) occurred at a depth of 10 cm below the stream sediment surface. On October 26, the potential denitrification rates were much lower and occurred slightly deeper in the sediments. The highest rate (2.63 nmol N_2O mL sediment^{-1} hr^{-1}) occurred at a depth of 10 cm below the stream sediment surface, and the second highest potential denitrification rate (2.39 nmol N_2O mL sediment^{-1} hr^{-1}) occurred at a depth of 20 cm below the stream sediment surface.

During all sampling dates, the greatest denitrification potential was found at shallower depths (2-20 cm) beneath the stream sediment surface. The zone of high denitrification potential was located with areas of high amounts of total organic matter, low NO_3^- concentrations, and low platinum electrode potential determined with the Spearman Test, which is nonparametric correlation analysis (Table 6). The significance level (α) was adjusted for multiple correlations using the sequential bonferroni method (Rice, 1989). There was a significant positive correlation between denitrification potential and total organic matter in all sampling dates. The negative correlation between

Table 6: Correlation matrix of denitrification potential, organic matter content, platinum electrode potential (PtEP), and nitrate concentrations for all sampling dates. Correlation Spearman Test with sequential bonferroni correction.

	Den. Pot-Organic Matter	Den. Pot-PtEP	Den. Pot-NO3-	Organic Matter-NO3-
July 11	r = 0.62* P = 0.0075 n =17	n/d	r = -0.79* P = 0.0014 n =13	r = -0.59* P = 0.0277 n =14
August 4	r = 0.44* P = 0.0007 n =55	n/d	r = -0.12 P = 0.5363 n =28	r = 0.08 P = 0.6947 n =27
August 26	r = 0.48* P = 0.0001 n =59	r = -0.06 P = 0.7446 n =30	r = 0.06 P = 0.7573 n =34	r = -0.42* P = 0.0156 n =32
October 26	r = 0.46* P = 0.0010 n =49	n/d	r = -0.53* P = 0.0003 n =41	r = -0.66* P < 0.0001 n =41

* significant at $\alpha = 0.05$ (after sequential bonferroni correction); n/d: not determined

denitrification potential and PtEP found on August 26 was not found to be significant. Correlation analysis between denitrification potential and PtEP for October 26 was not performed since only two cores were collected. Denitrification potential was negatively correlated with pore water nitrate concentration in two of the sampling dates, July 11 and October 26. Total organic matter of the streambed sediments was negatively correlated to both pore water nitrate concentrations and platinum electrode potential, except on August 4 (data not shown).

Lateral Profiles across the Streambed

Lateral profiles of pore water nitrate concentration, total organic matter, and potential denitrification were examined in cross sections in the streambed to examine areal variability of nitrate removal by denitrification and its controllers (Figures 16-19).

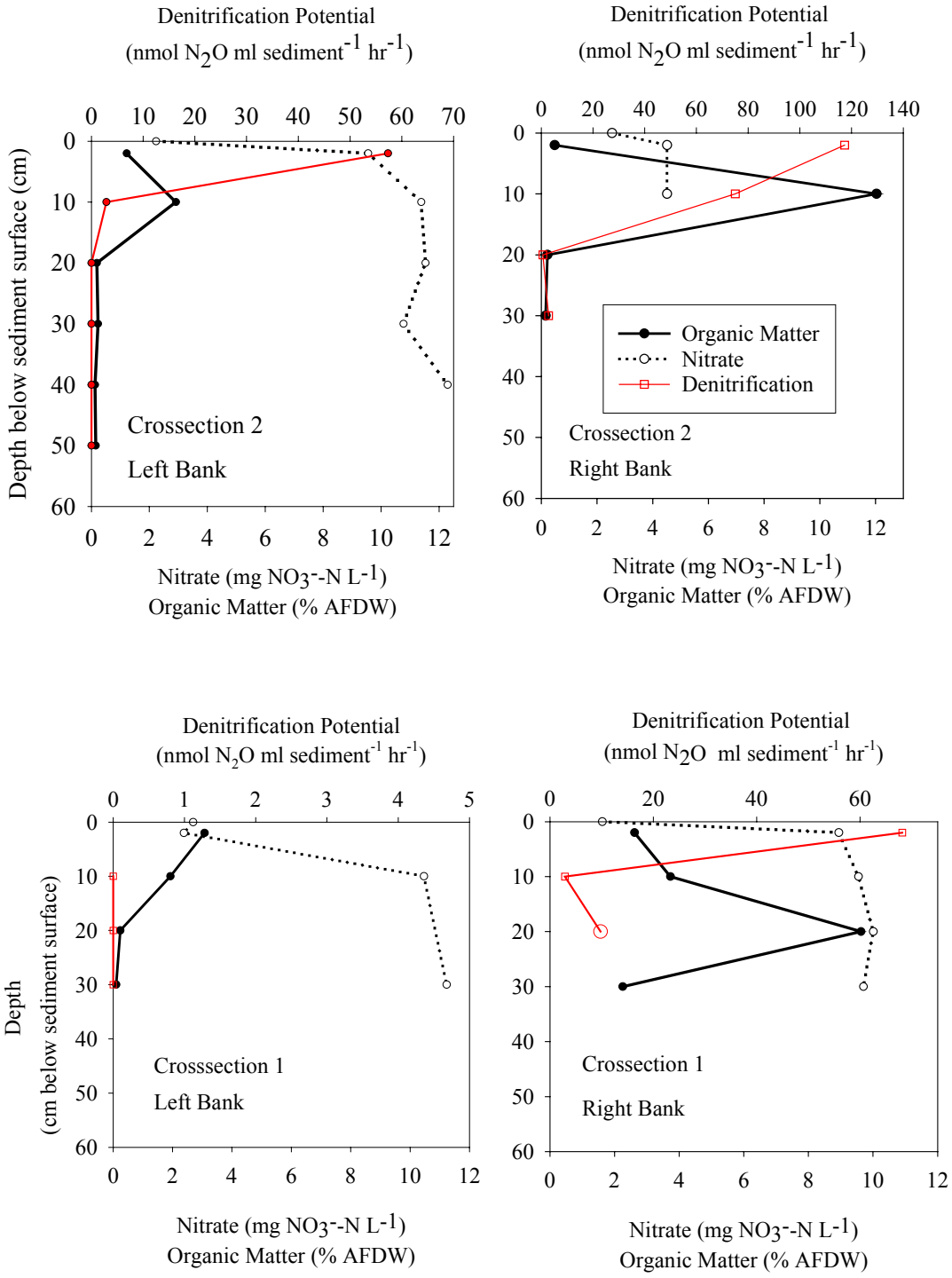

Figure 16: Profiles of denitrification potential, nitrate concentration, and organic matter content of cores collected in CMC on July 11, 2003. Graphs are placed on the page to correspond to sampling locations of cores in the stream (see Figure 3). The graphs on the left show cores collected along the left bank and the graphs on the right show cores on the right bank.

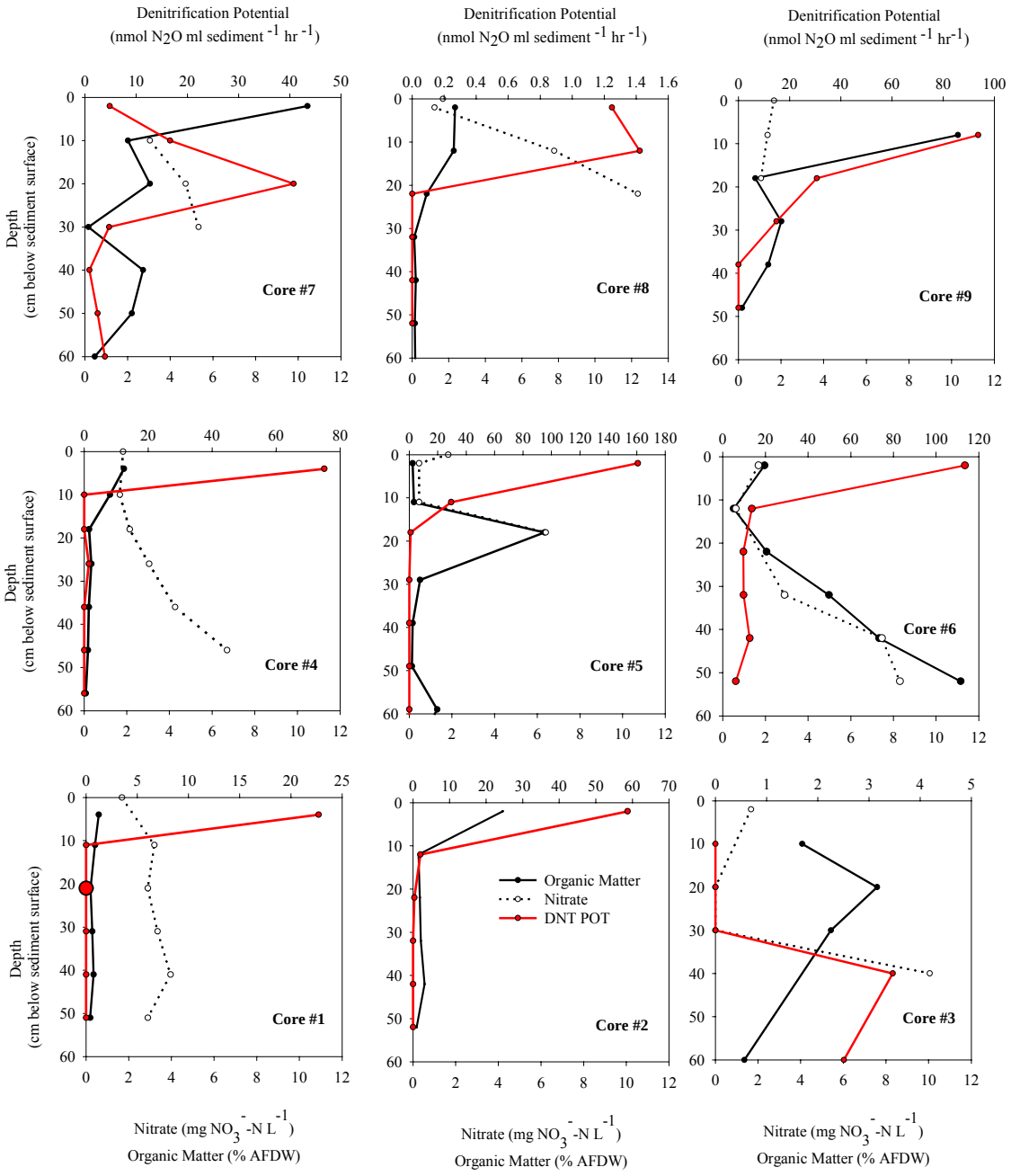

Figure 17: Profiles of denitrification potential, nitrate concentration, organic matter content, and of cores collected in CMC on August 4, 2003. Graphs are placed on the page to correspond to sampling locations of cores in the stream (see Figure 3. The graphs on the left show cores collected along the left bank and the graphs on the right show cores on the right bank.

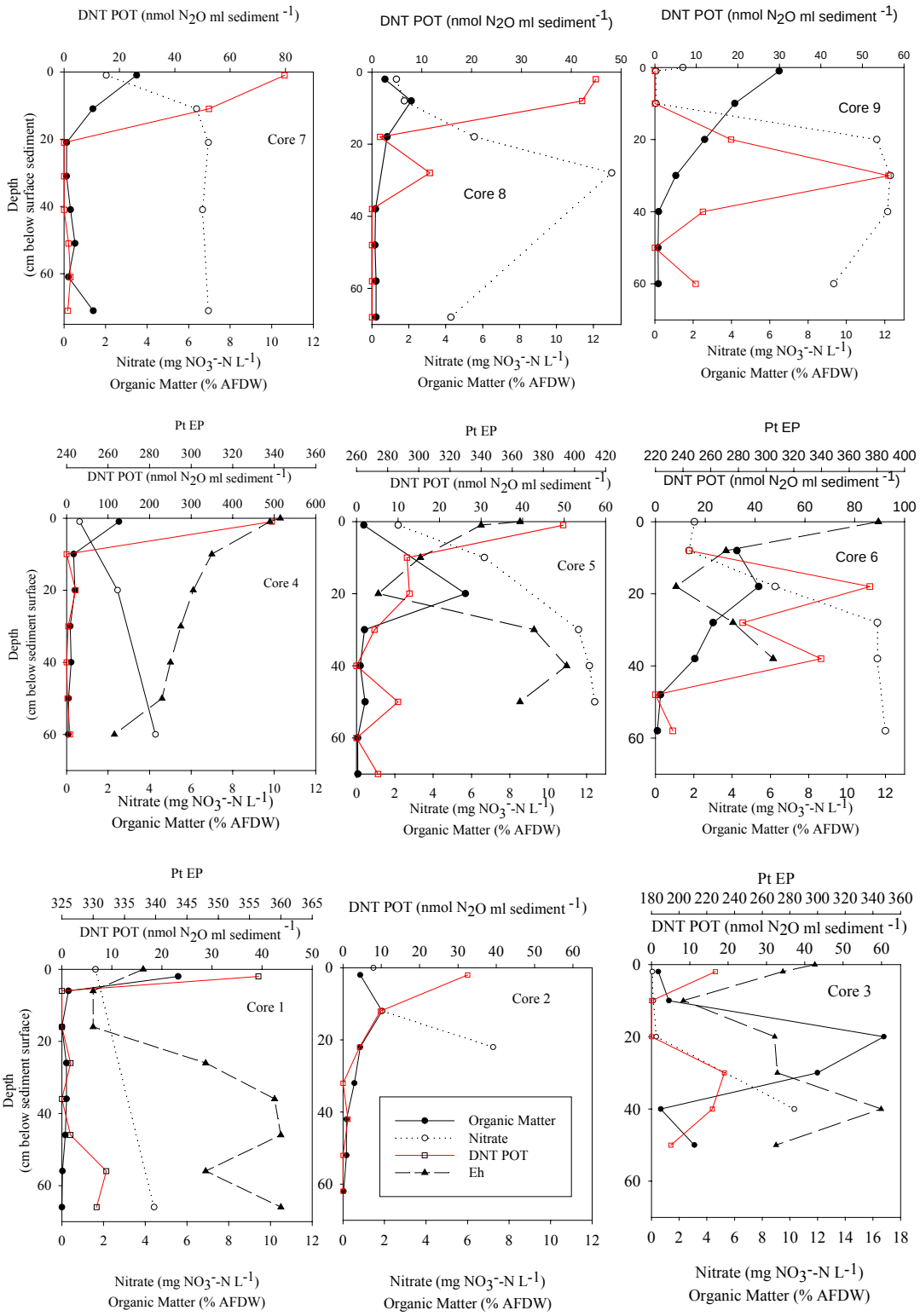

Figure 18: Profiles of denitrification potential, nitrate concentration, organic matter content, and PtEP of cores collected on August 26, 2003. Graphs are situated to correspond to sampling locations (Fig 3).

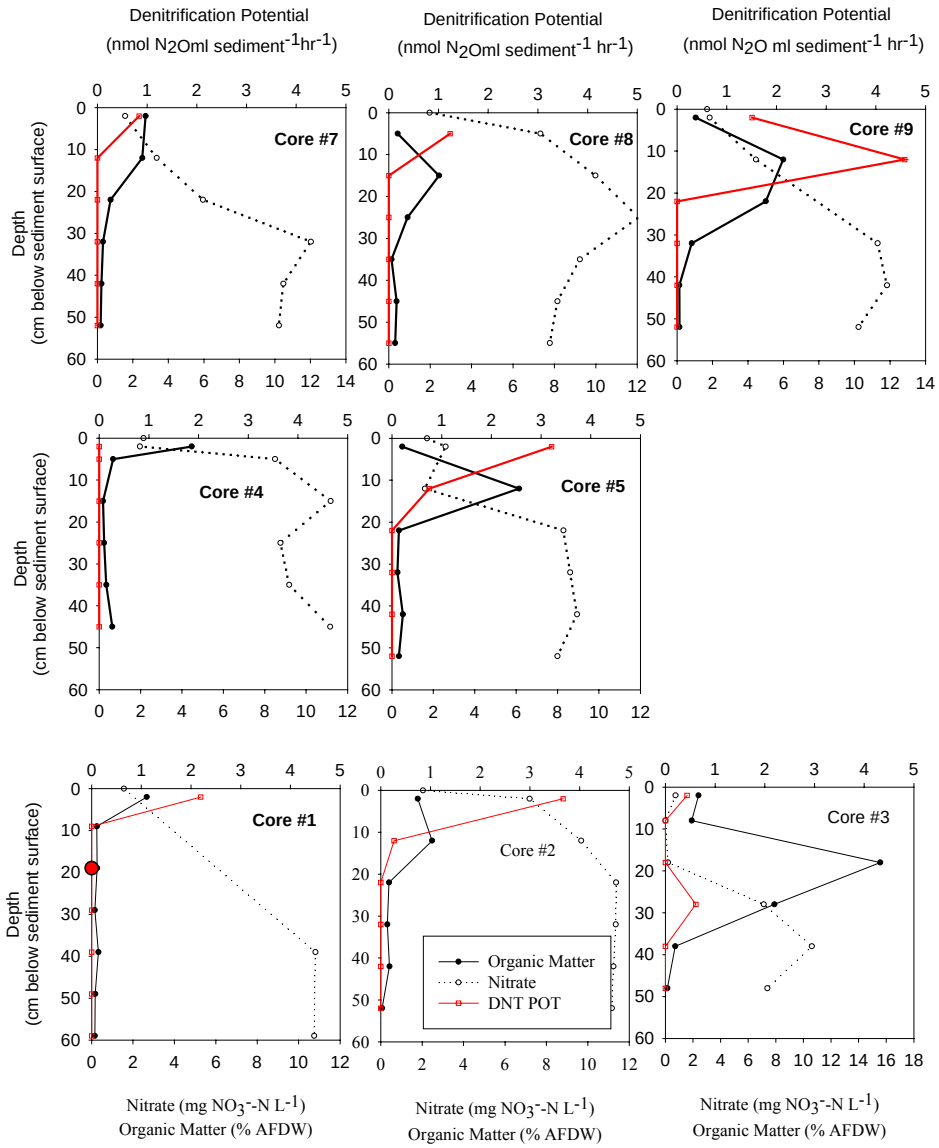

Figure 19: Profiles of denitrification potential, nitrate concentration, and organic matter content of cores collected in CMC on October 26, 2003. Graphs are placed on the page to correspond to sampling locations of cores in the stream (see Figure 3). The graphs on the left show cores collected along the left bank and the graphs on the right show cores on the right bank.

In general, increased total organic matter and increased potential denitrification were found at depths greater than 20 cm below the stream sediment surface only in cores 3, 6, & 9, which were taken along the right bank (facing downstream). Among all four sampling events, core #3 (taken along the right bank in cross section one) had up to 17% total organic matter at 20 cm (Figures 18 & 19) and up to 12% total organic matter at 30 cm below the sediment surface (Figure 18). In core #6 (taken along the right bank in cross section two) there were also high amounts of organic matter found at depths greater than 20 cm (Figures 17 & 18). On August 4, organic matter increased with depth to 11% at 50 cm below the sediment surface in core #6, although denitrification potential was greatest at 2 cm in this core (Figure 17). In core #9 (taken along the right bank in cross section three) there were considerable amounts of organic matter also found at deeper depths, up to 5% at 25 cm on October 26, and considerable potential denitrification was found at 30 cm (Figure 19). Among all the sampling dates, the percent organic matter in core #5 (taken in the center of the stream in cross section two) peaked at 6% at approximately 20 cm (Figure 17-19). At all other sampling locations, total organic content was less than 2% at depths greater than 20 cm, the location where the least amount of potential denitrification occurred.

Mass Balance

The average potential NO_3^- removal rate (based on N_2O production) was compared to the average observed NO_3^- loss rate (based on calculations made with the advection-dispersion equation) along the length of each core. In order to convert the observed decreases in nitrate concentration into a nitrate loss rate, a linear trend line was

fit to the change in nitrate concentration along the length of the core. The slope of the line ($R\ u^{-1}$) was 0.15, 0.10, 0.16, and 0.13 for sampling dates July 11, August 4, August 26, and October 26, 2003, respectively. Each slope was multiplied by the average linear velocity ($3.1*10^{-4}$ cm sec^{-1}), which resulted in the observed nitrate loss rate (R) for each sampling date. The mass balance was not calculated for sampling date August 26 because, due to technical difficulties, a potential denitrification rate could not be found.

On all sampling dates, the shallower depths (0-10 cm below the sediment surface), where most of the denitrification occurred, contributed the most to the sum of potential nitrate removal (Table 7). This observation corresponded with the fact that the greatest observed pore water nitrate decrease also occurred in these shallow depths (Figure 9). On July 11, the potential removal rate was 9.28 mg NO_3^- L^{-1} hr^{-1} compared to the observed nitrate loss rate of 0.15 mg NO_3^- L^{-1} hr^{-1}. On August 4, 10.07 mg NO_3^- L^{-1} hr^{-1} was potentially removed compared to the observed nitrate loss rate of 0.11 mg NO_3^- L^{-1} hr^{-1}. On October 26, 0.40 mg NO_3^- L^{-1} hr^{-1} was potentially removed compared to the observed nitrate loss rate of 0.12 mg NO_3^- L^{-1} hr^{-1}. The potential nitrate removal rate was sufficient to account for the observed nitrate loss; it was 60, 90, and 3 fold greater than the "observed" nitrate loss rate for sampling dates July 11, August 4, and October 26, respectively. The potential nitrate removal rate was lowest on October 26, 2003.

The potential nitrate removal rates for each depth increment in each single core were summed to determine the maximum amount of denitrification potential at each sampling location in the stream reach (Table 8). In most cases, there were nine sampling locations in the stream (Figure 4). For all sampling dates, this potential rate was compared to the observed nitrate loss rate along the length of the core to examine lateral patterns of

denitrification potential. Much variability existed between sampling dates considering the relationship between the stream position and high denitrification potential rates. In general, among all the sampling dates, the highest potential nitrate removal rate was found in the middle of the stream in cross section two (in line with piezometer nest 4).

Table 7: Mass balance comparing potential NO_3^--N removal rates (based on N_2O production) to the observed NO_3^--N loss rate (based on advection equation) along the length of the sediment cores.

Depth (cm)	Pot DNT Rate (nmol N_2O ml^{-1} hr^{-1})	NO_3^- Removal Rate (mg NO_3^--N L^{-1} hr^{-1})	Obs NO_3^- Loss (slope)	Obs NO_3^- Loss Rate (mg NO_3^--N L^{-1} hr^{-1})
7/11/03				
2	80.93	6.47		
10	26.95	2.16		
20	5.23	0.42		
30	2.83	0.23		
40	0.00	0.00		
50	0.00	0.00		
Total	115.94	9.28	-0.14	0.15
8/4/03				
2	62.39	4.99		
10	26.14	2.09		
20	16.49	1.32		
30	7.72	0.62		
40	5.67	0.45		
50	4.29	0.34		
60	3.21	0.26		
Total	125.91	10.07	-0.10	0.11
10/26/03				
2	2.63	0.21		
10	2.39	0.19		
20	0.00	0.00		
30	0.00	0.00		
40	0.00	0.00		
50	0.00	0.00		
60	0.00	0.00		
Total	5.02	0.40	-0.11	0.12

In these cases, the denitrification potential rate was sufficient to account for the observed nitrate loss. As shown in the vertical mass balance (Table 7), at most stream locations, the

denitrification potential rate was sufficient to account for the observed nitrate loss. There was not a general pattern between positions in the stream and incidences where the denitrification potential could not account for the observed nitrate loss rate.

Table 8: Comparison of Potential Nitrate Removal Rate and Observed Nitrate Loss Rate (gray column) (mg NO_3^--N^{-1}) for Cross section Profiles. Columns are placed on the page to correspond to sampling locations of cores in the stream (see Figure 4) in a downstream orientation starting at cross section 1. The columns on the left show cores collected on the left bank and columns on the right show cores collected on the right bank. Numbers in italics indicate stream positions where the potential nitrate removal rate was sufficient to account for the observed the nitrate loss rate.

Sampling Date	Total Potential Nitrate Removal Rate	Total Observed Nitrate Loss Rate	Total Potential Nitrate Removal Rate	Total Observed Nitrate Loss Rate	Total Potential Nitrate Removal Rate	Total Observed Nitrate Loss Rate
7/11/2003						
Cross section 3						
Cross section 2			*15.67*	0.22	*5.25*	0.28
Cross section 1			0	0.32	*6.47*	0.30
8/4/2003						
Cross section 3	5.94	n/a	0.21	0.60	11.14	n/a
Cross section 2	*6.13*	0.11	*15.29*	0.26	*13.23*	0.15
Cross section 1	*1.82*	0.03	4.89	n/a	*0.48*	0.23
10/26/2003						
Cross section 3	0.09	0.23	*0.17*	0.13	*0.62*	0.19
Cross section 2	0	0.20	*0.45*	0.14	n/a	n/a
Cross section 1	*0.21*	0.17	*0.46*	0.20	0.05	0.15
Stream Position	Left Bank		Middle		Right Bank	

DISCUSSION

Hydrological Gradients and Ground-water Nitrate Concentrations

During base flow conditions in low order streams, such as Cobb Mill Creek, when the majority of the stream flow is ground-water fed, it is expected that the stream water chemistry should correspond to its ground-water source. The application of excess fertilizers containing nitrate to some upland agricultural fields often does not to cause a comparable rise in nitrate in adjacent streams (McClain et al., 2003). This discrepancy between nitrate-rich discharging ground water and nitrate-poor stream water was observed early in the current study. In order to determine the major location and mechanism of nitrate removal along the ground water flow path, the water table profile, vertical head gradients, and nitrate concentrations were determined along the experimental hillslope and in the stream.

The water table was determined to be shallow (less than two meters below the ground surface) and it followed the ground contours from the upland agricultural field, down the hillslope to the stream, except at the bankside well closest to the stream where the water table was level with the stream despite the sloping ground. The ground water flow paths along the hillslope that deliver nitrate to the stream were determined by coupling the nitrate data and the vertical head gradients in the shallow region of the saturated zone (less than one meter deep). The local vertical head gradients of two of the bankside piezometer nests, N1 and N3, indicated upward flow during all the sampling dates. A consistent pattern of increasing nitrate concentrations with depth was found in these two piezometer nests. Alternately, vertical head gradients in the adjacent bankside

piezometers, N4, N5, and N6, located slightly downstream, showed a less consistent pattern over time but indicated that more downward flow occurred in these locations compared to N1 and N3, despite their close proximity. Nitrate concentrations in bank side piezometer nests N4, N5, and N6 were much lower compared to the other piezometers nests. The pattern of increasing nitrate concentrations with depth was found in nests N5 and N6, but in nest N4, nitrate was found to decrease with depth, although these piezometers were placed at approximately the same depth underground. Differences in the vertical head gradients and nitrate concentrations in shallow piezometer nests in close proximity to each other reflect the heterogeneity of local shallow ground water flows. Vertical head gradients at N7, located higher on the hillslope, indicated that strong downward flow occurs at this location, and therefore may be an important recharge area. Nitrate concentrations were higher at this location. On the other hand, nitrate concentrations were lower at another parallel hilltop location (about 18 meters upstream), N10. Since only one piezometer was installed, a vertical head gradient could not be established. The negative vertical head gradients in the stream piezometers suggested that there was an upward flow of deeper ground water directly into the stream. The highest nitrate concentrations were found one meter directly below the stream by pore water collected by stream piezometers (9-11 mg NO_3^- L^{-1}), while stream nitrate concentrations were low (1-2 mg NO_3^- L^{-1}).

In the Cobb Mill Creek watershed, a local ground-water flow system predominates in which the topographic high is the agricultural field and the topographic low is the stream. The hydrologic and chemical data in the Cobb Mill Creek study suggest two distinct flow paths within the local flow system, which differ in nitrate

concentration. High concentrations of nitrate leach from the upland agricultural field and flow along an oxidized deeper ground water flow path generally greater than two meters below the water table and the nitrate discharges vertically towards the stream. The pore water nitrate is removed at the ground water- surface water interface before the water reaches the open stream channel. On the other hand, the ground water in the shallow bankside piezometers was found to have lower nitrate concentrations suggesting a shallower oxidized ground water flow path in which the nitrate most likely originates from natural decomposition and deposition processes. These flow paths receive less nitrate from the agricultural fertilizers. The nitrate transported by these shallow flow paths are most likely discharged laterally into the stream at the stream bank and contribute to the open channel nitrate concentration.

It is important to keep in mind that the hillslope cross section profile is based on only four piezometer nests in one transect. More hillslope piezometers that are installed deeper into the ground water will be necessary to establish the ground water flow paths along the hillslope in a comprehensive manner. The vertical head gradients described in this work only encompass a very shallow lens of the ground water (approximately one meter deep) in the Cobb Mill Creek riparian zone. Variations in vertical head gradients in the piezometers among sampling dates are due to changes in ground water and stream elevation based on precipitation events. Further research is warranted to correlate changes in local ground water flow paths due to precipitation events. Multiple deep piezometers along the hillslope are needed to confirm the suggested deeper flow paths connecting the agricultural field and the stream and relate them to the sources and sinks of nitrate along that flow path.

Vertical Profiles in Stream Sediments

Concentration profiles of nitrate in pore water collected from intact sediment cores taken in Cobb Mill Creek matched concentrations from water collected in the stream piezometers and showed that nitrate concentrations generally increased with depth in the sediment and were higher than the stream channel. The average of all cores taken over the four sampling dates indicated a decrease of 8.27 mg NO_3^--N L^{-1} or 84.24% between a point 60 cm below the sediment surface and the open channel. The change in nitrate concentration was not uniform with depth in the sediments; the greatest nitrate loss occurred in the top 20 cm. The distinct decrease in nitrate concentration in the top 20 cm in the sediments is especially evident on sampling dates July 11, August 26, and October 26, 2003, whereas the decrease in nitrate appeared more linear August 4, which is most likely due to technical problems of collecting pore water on that date. On sampling dates August 4 and August 26, 2003, there was a slight increase of nitrate concentration between sediments 2 cm deep and the open channel. This observation supports the idea that nitrate was removed in the upwelling ground water and the additional nitrate in the stream originated from lateral flow from the bank.

Although nitrate and chloride behave similarly in aqueous solutions in that they do not sorb to particle surfaces, chloride does not undergo biological transformations and therefore concentrations are not biologically controlled. The decrease of the nitrate concentration in the shallow stream sediments did not correspond to a decrease in chloride, suggesting that the nitrate loss is a biological process. Chloride and sulfate concentrations were higher in the stream and decreased with depth in the stream sediments. These anions may originate from the downstream estuary and Atlantic Ocean

through seawater spray reaching the stream during storms. With strong upward advective ground water flow through the stream sediments, these anions most likely only enter the shallow sediment by hyporheic exchange. However, it was found that the vertical head gradients were approximately a magnitude greater than the longitudinal head gradients in the stream sediments indicating that the advective flow of the discharging ground water was stronger than the longitudinal in the streambed. Therefore, hyporheic exchange is not a significant solute transport mechanism along the experimental reach. In addition, hyporheic exchange was not shown to occur by previous tracer studies in the Cobb Mill Creek sediments.

The nitrate concentration of the samples collected with the MDPP from depths between the intact cores samples (collected at 10-cm intervals) showed some variability but generally fell along the depth profile collected with the cores. The results of this study concur with other studies, such as Duff et al. (1998), that suggest that using this technique to collect high-resolution nitrate profiles is important when looking at heterogeneity of denitrification, especially when considering microsites of biogeochemical activity close to the stream sediment surface.

Along the examined depth profile, from the sediment surface down to approximately 60 cm, it was found that the majority of the nitrate was lost in the top 20 cm. Furthermore, on all four sampling dates, the potential denitrification rates were greatest in the top 20 cm of the stream sediments. The sediment conditions in this shallow zone were conducive to stimulating denitrification; organic matter (as the electron donor) was sufficient, the upwelling pore water nitrate-rich (as the electron acceptor), and the low platinum electrode potential suggested adequate hypoxic oxygen levels. Depths

below this zone had on average less than 2% organic matter and higher platinum electrode potential. Low platinum electrode potentials were also found at various depths below 20 cm and these may represent microsites of low oxygen conditions rather than a specific pattern. The measured profiles of organic matter and platinum electrode potential were supported by physical observations of sediment color in intact cores cut lengthwise. Thick black layers of organic matter were seen near the sediment surface. Small pockets of organic matter were seen at depth; these pockets represent microsites of anaerobic microbial activity. In some cores, red sediment was observed at depth. Such coloration is associated with oxidized iron coatings in aquifer materials in the vicinity (Dobson, R.W., 1997, Knapp, et al., 2002). This observation supports the suggestion that at depth, upwelling ground water is aerobic and therefore nitrate flowing along that subsurface path is conserved. As the water enters areas with increased organic matter, anoxic conditions become more frequent promoting removal of nitrate from the water by denitrification.

There was a significant positive correlation between denitrification potential and total organic matter content for all sampling dates. Organic matter in the shallow sediments serves two purposes. It fuels not only denitrification, but also oxygen respiration. Oxygen respiration consumes oxygen and creates the hypoxic conditions necessary for denitrification to occur. There was a negative correlation between denitrification potential and PtEP on August 26, but it was not significant. This correlation may be weak since the sample size was low (5 cores) due to technical difficulties. Denitrification potential was significantly negatively correlated to pore water nitrate concentrations in two of the sampling dates, July 11 and October 26. This

relationship is expected to be negative because as denitrification occurs, the nitrate is reduced to nitrogen gas and its concentrations decrease. The lack of significance on the other two sampling dates may be due to technical difficulties associated with collecting sufficient pore water from the cores for analysis because of leaking cores and low sediment porosity. Total organic matter was also significantly negatively correlated to pore water nitrate concentrations on July 11, August 26, and October 26. This relationship is consistent with the reasoning given above. In locations with available organic matter, processes such as respiration consume oxygen and produce suitable conditions for denitrifying activity, which in turn, decreases the nitrate concentrations. The lack of significance on August 4 is likely due to low pore water sample size associated with the collection procedure.

The premise that nitrate removal from the upwelling pore water in the stream sediments is attributed to denitrification occurring mostly in the shallow sediments (top 20 cm) was further supported by the mass balance calculations. The mass balance included the comparison between the potential denitrification rate converted to a potential nitrate Removal rate versus the observed nitrate loss rate along the length of the intact sediment cores. During all sampling dates, the vertical profiles showed that the majority of the potential nitrate Removal occurred at the shallower depths (0-10 cm below the sediment surface). This finding corresponded to the observation that the greatest pore water nitrate loss rates also occurred in these shallow depths. The overall potential nitrate Removal rate was not only sufficient to account for the observed nitrate loss rate but was 30, 105, and 2.9 times greater for sampling dates July 11, August 4, and October 26, respectively. It is also important to consider not only the potential nitrate removal rate

based on the N_2O production, but also the required rate of organic matter removal. Based on the stoichiometry of the denitrification reaction (1), it would require a minimum oxidation rate for organic carbon of 1.25 mm C/ mm N given that carbon is 12 mg/mm and nitrogen is 14 mg/mm. The ratio of carbon to nitrogen is ((12*1.25)/14) = 15/14 or about 1:1. Therefore, on sampling dates July 11, August 4, and October 16, the potential denitrification rate reflected a loss of approximately 9.42, 10.07, 0.402 mg C L^{-1} hr^{-1}, respectively. This calculated loss of carbon is great but is most likely realistic when considering the short incubation times of the laboratory incubations.

The discrepancy between potential rate and the observed rate may be due to several factors derived from differences between the conditions in the incubation bottles and field conditions. The sediment slurries used to determine the denitrification potential rate were made completely anaerobic by bubbling with N_2 gas to ensure that denitrification would not be inhibited by mixing oxygenated water through the entire slurry. These conditions likely do not match those in the stream sediments where there is an upwelling of aerobic ground water and heterogenous distribution of anoxic zones due to the distribution of organic matter. In addition, the sediment samples were mixed with artificial ground water and shaken to distribute the acetylene. This action created more surface area for contact between denitrifying bacteria, that are attached to the sediment particles or suspended in solution, and organic matter, which should increase the denitrification potential. Furthermore, the denitrification potential assay was carried out at room temperature, which may be slightly higher than the *in situ* sediment temperature allowing for faster rates. Whereas, in this study the denitrification potential assay most certainly reflects an inflated rate, the linear velocity used to determine the observed

nitrate loss rate may also not reflect *in situ* conditions and may be an underestimate of the flow rate. The Darcy velocity was determined by laboratory sediment column experiments in which the flow rate was varied until the inflow and outflow nitrate concentrations reflected field observations. Oxygen levels of the pore water in the laboratory column may be a factor in controlling the change in nitrate and therefore affecting the laboratory determined flow rate. Higher oxygen conditions in the column than the *in situ* levels in the sediments would require a slower flow rate (higher residence time) than exists in the field to hypoxic create conditions necessary to reduce the pore water nitrate by denitrification.

On the other hand, the acetylene block assay has been found to underestimate denitrification in previous studies in which the acetylene was only 50-70% effective in blocking N_2O reduction to N_2 (Seitzinger, 1993). In addition, it has been found that acetylene also blocks nitrification, so that it may reduce denitrification by decreasing the supply of nitrate in systems where nitrification and denitrification are coupled (Watts, 2000). However, as with other studies, this limitation is not important in our Cobb Mill Creek study because the major source of nitrate is the upwelling ground water from the hill- slope adjacent to a fertilized agricultural field and not *in situ* nitrification of NH_4^+ released from decaying organic matter (Hill et al., 2000). Furthermore, determining nitrogen removal by denitrification does not account for uptake by benthic plants and microbes (Seitzinger et al., 2002). These are important considerations to keep in mind, although the denitrification potential rates in our study were more than sufficient to account for the observed nitrate loss rate.

Riparian zones separating agricultural fields and streams are an important control point of nitrate along its subsurface flow path from the terrestrial to the aquatic ecosystem (Hill, 1996). Up to 98% nitrate removal has been reported along this subsurface flow through a riparian forest (Hill, 1996). It is also well documented that particularly the narrow zone comprising the ground water/ stream water interface, often within a riparian wetland, is the optimal location for nitrate transformations (Lowrance et al., 1984, Peterjohn and Correll, 1984, Jacobs and Gilliam, 1985a,b, Cooper 1990, McDowell et al. 1992, Triska et al., 1993, Hedin, 1998). The results in the current study correspond to these findings, given that even in the absence of a riparian wetland along the study reach, approximately 85% of the nitrate was removed and the highest denitrification potential was found at the ground water- stream sediment interface at Cobb Mill Creek. Hedin et al. (1998) proposed that in order to understand and predict the locations of high rates of biogeochemical function (in this case, denitrification) in riparian zones, the interaction between microbes and variations in the supplies of electron donors and acceptors must be known. Hedin et al. (1998) found that denitrification was restricted to a narrow zone at 20-40 cm deep near a stream bank where a lateral flow of pore water with high DOC from organic surface sediment (electron donor) interacted with the vertical upwelling of nitrate-rich ground water (electron acceptor). The results of the Cobb Mill Creek study support a similar conclusion: that total organic matter is an important controller of the denitrification rates, given that the highest rates were found at the location of the intersection of upwelling nitrate-rich pore water with layers of organic matter near the sediment surface. The deposition and burial of organic matter from the surrounding riparian forest and shallow lateral ground water flow were important sources of organic

matter to the shallow stream sediments of Cobb Mill Creek. Using a similar acetylene block method with sediment slurries, Pfenning and McMahon (1996) also found higher rates of denitrification potential in surface stream sediments, receiving upwelling nitrate-rich ground water while stream water maintained lower nitrate concentrations. The surface sediments contained relatively high amounts of organic matter, compared to deeper sediments. In addition, these researchers found lower rates of N_2O production occurred in buried sediments with less organic matter, but higher nitrate concentrations.

The form of the available organic matter is also an important factor in determining denitrification rates. Labile organic matter availability is an important control on denitrification rates in soils and sediments (Starr & Gillham, 1989). In Cobb Mill Creek, some locations below 20 cm, especially along the right bank of the stream, were found where nitrate-rich pore water intersects pockets of deeper organic matter, yet lower potential denitrification was observed than in the shallower sediments. The conditions at these locations may not be sufficiently reducing for the denitrifiers to remove significant amounts of nitrate. Although organic matter can be transported in the flow of upwelling ground water, the organic matter may not be in a labile form to act as an electron donor either for respiration (creates reducing conditions) or for denitrification to occur. The most labile form, dissolved organic carbon, was not measured in the Cobb Mill Creek sediments. Yet, this conclusion is supported by many studies, including the following. Pfenning & McMahon (1996) found higher denitrification rates occurred with sediments amended with surface water derived fulvic acid as compared to ground water derived fulvic acid or sedimentary organic carbon. The surface derived organic matter was more labile, and more easily taken up by microbes. Hill & Sanmugadas (1985) found

the potential for nitrate removal in stream sediments at twenty-two sites in Southern Canada was positively correlated with water- soluble content of the 0 – 5 cm sediment depth (r = 0.82-89). Baker & Vervier (2004) determined through multiple linear regressions, that denitrification rates were not predicted by dissolved organic carbon content alone, but were best predicted by the concentration of low molecular weight organic acids and the percent surface water in the alluvial sediments of the Garonne River.

The denitrification rates reported in the current study at Cobb Mill Creek (range 16.91- 600 μmol N m^{-2} h^{-1}) were comparable to other studies measuring denitrification in stream and river sediments (range 0- 3214 μmol N m^{-2} h^{-1}) (Table 9). Many of the studies looking at nitrate loss by denitrification in stream sediments are based on shallow stream sediments (0- 10 cm below the sediment surface). The study at Cobb Mill is one of the few studies that has analyzed denitrification at greater depths in stream sediments. Similar denitrification potential rates were found in the sediments at Cobb Mill Creek as those found in the South Platt River, CO by Pfenning & McMahon (1996) at a depth of 60 cm below the sediment surface (Table 10). These two studies did confirm the fact that shallow stream sediments are indeed a location where significant denitrification occurs.

Lateral Profiles in Stream Sediments

Results from lateral profiles of pore water nitrate concentration, total organic matter, and potential denitrification show that in general, increased total organic matter and increased potential denitrification at depths greater than 20 cm below the stream sediment surface were only found along the right bank (facing downstream, cores 3, 6,

and 9) during all sampling dates. Allochthonous organic matter deposited into the stream from the surrounding riparian forest may be consolidated and buried specifically along the right bank of the stream due to the curvature of the stream at the sampling reach. High nitrate concentrations at depths below 20 cm in some of these cores along the right bank of the stream indicate that while high amounts of organic matter are present and some potential denitrification was observed, the conditions may not be sufficiently reducing for the denitrifiers to remove significant amounts of nitrate. The denitrification may occur only in hot spots.

Tremendous spatial variability of potential nitrate Removal was shown by the mass balance analysis for cores distributed laterally across the stream (Table 6). In general, the highest potential nitrate Removal rate was found in the middle of the stream in cross section two (in line with piezometer nest 4). Although the vertical profiles of denitrification potential show more denitrification occurring at greater depths along the right bank of the stream, there was not more total denitrification occurring at these locations. Similarly shown in the vertical mass balance profiles, in most cases the denitrification potential rate was sufficient to remove the observed nitrate loss at each lateral location in the stream.

Similar areal variation in denitrification has been shown in other studies. In a study of *in situ* denitrification activity (IDA) in sediments of the River Dorn, England, there was no significant difference in IDA due to position in the cross-section, but it was noted that high IDAs were found in areas of fine-grained sediment accumulation in stream margins, especially on the outside of meander bends at points where there was no distinct stream bank (Cooke and White, 1987).

Temporal Variation

The measured ground water nitrate concentrations in the stream piezometers were generally half the concentration in the Fall 2002 of those samples collected in the Summer-Winter of 2003. Nitrate concentrations might be expected to be higher in the fall and winter since biotic uptake and microbial transformations decrease with lower temperatures. The lower nitrate concentrations found in 2002 could be due to the drought conditions of that Summer when slow discharge delivered less nitrate to the ground water. It is also possible that the discrepancy may be attributed to the difference in techniques of the colorimetric cadmium reduction method and ion chromatography. The upper concentration limit may be incorrect in the colorimetric method since it was discovered after testing that the color production was saturated and was not reflecting the true nitrate concentration of the samples. Nitrate concentration was not linear with absorbance at higher concentrations.

The potential denitrification rates were highest in the July sampling event, lower in August, and an order of magnitude lower in October. This temporal variation may be due to lower temperatures; denitrifiers are temperature sensitive although direct evidence of temporal variation was not collected in this study. Pfenning, & McMahon (1996) found that lowering incubation temperatures from 22 to 4^{o}C in the laboratory sediment slurries resulted in a 77% decrease in the N_2O production rates.

Conceptual Model

Synthesis of the hydrological and chemical ground water and stream data led to the development of a conceptual model to explain the discrepancy between high

concentrations of nitrate in the deeper ground water flow paths that discharge into the stream, and the low nitrate concentrations found in open channel of Cobb Mill Creek. As described above, it is proposed that a local oxygenated ground flow path determines the nitrate concentration in the stream. Within this local system there is a deep and shallow ground water flow path with differing nitrate concentrations. The shallow local flow path is less than two meters deep and contains low nitrate concentrations (1-5 mg NO_3^- L^{-1}) originating most likely from natural decomposition or deposition processes. This shallow local flow path discharges into the stream laterally through the stream bank and combines with the upstream flow contributing to the stream nitrate concentration at approximately 1-2 mg NO_3^- L^{-1}. The deeper flow path is greater than two meters deep and contained higher nitrate concentrations (9- 12 mg NO_3^- L^{-1}) originating from the agricultural field. As pore water that contains nitrates leached from the agricultural field flows along the deeper oxygenated ground water flow path, it undergoes little alteration in nitrate concentration. The ground water discharges vertically upward into the stream sediment, and the nitrate is not removed until it reaches the shallow stream sediments approximately 20 cm below the sediment surface. In those 20 centimeters, the high denitrification potential, high organic matter content, low redox potential, and decreasing nitrate to chloride ratio lead to the conclusion that conditions at this depth in the stream sediments are optimal for denitrifiers to reduce NO_3^- to N_2. Our results indicate that, while denitrification rates in Cobb Mill Creek sediments are spatially and temporally variable, denitrification is a significant nitrate sink during transport from the nitrate contaminated hillslope to the stream. Organic matter availability and reducing conditions are critical factors influencing the observed spatial and temporal patterns.

CONCLUSION

Forested riparian buffers surrounding streams provide vital functions such as assimilation of nutrients; provide habitat and shade to terrestrial and aquatic species; and input organic matter. This input of organic matter to stream sediments fuels denitrifying bacteria. The organic matter can be deposited both directly into the stream and to shallow ground water, and can be subsequently laterally transferred to shallow sediments and buried. The results of this research support several studies in the current literature that conclude that organic carbon is of greatest significance in determining the ability of ground water- surface water interface to remove nitrate by denitrification. In an agricultural watershed, increasing denitrification rates in riparian zones such as those encompassing Cobb Mill Creek on the Eastern Shore of Virginia is an important management strategy to controlling aqueous nitrate concentrations. Enhancing nitrate removal by directly supplying organic matter to stream sediments may cause problems to downstream environments (Hedin, 1998). However, the maintenance of riparian buffers with organic-rich soils that separate agricultural fields and streams is essential for natural remediation of nitrate concentrations in streams in order to prevent nutrient enrichment of downstream environments.

REFERENCES

Baker, M.A., Vervier P. (2004) Hydrological variability, organic matter supply and denitrification in the Garonne River ecosystem. *Freshwater Biology*. 49 (2): 181.

Bragan, R.J., Starr, J.L., and Parkin, T.B. (1997) Shallow Ground water Denitrification Rate Measurement by Acetylene Block. *Journal of Environmental Quality*. 26: 1531-1538.

Bohlke. J.K., Wanty, R., Tuttle, M., Delin, G., and Landon, M. (2002) Denitrification in the recharge area and discharge area of a transient agricultural nitrate plume in a glacial outwash sand aquifer, Minnesota. *Water Resources Research*. 38 (7): 10-26.

Brady, N.C., and Weil, R.R. (1999) The Nature and Properties of Soils. Twelfth Edition. Prentice Hall, Inc., Upper Saddle River, New Jersey.

Chauhan, M.J., and Mills, A.M. (2002) Modeling baseflow nitrate loading on the Eastern Shore of Virginia. In: Atlantic Estuarine Research Federation Spring Meeting, Lewes, DE.

Christensen, P.B., Sorensen, J. (1988) Denitrification in sediment of lowland streams: Regional and seasonal variation in Gelaek and Rabis Baek, Denmark. *FEMS Microbiology Ecol*ogy. 53: 335- 344.

Cirmo, C.P., McDonnell, J.J. (1997) Linking the hydrologic and biogeochemical controls on nitrogen transport in near-stream zones of temperate-forested catchments: a review. *Journal of Hydrology*. 199: 88-120.

Cobb, P.R.& Smith, D.W. (1989) Soil Survey of Northhampton County, Virginia. U.S.D.A., Soil Conservation Service, Virginia Polytechnic Institute and State University.

Cooke, J.G. and White, R.E. (1987) Spatial distribution of denitrifying activity in a stream draining an agricultural catchment. *Freshwater Biology*. 18: 509- 519.

Cooper, A.B. (1990) Nitrate depletion in the riparian zone and stream channel of a small headwater catchment. *Hydrobiologia*. 202: 13- 26.

Cooper, A.B., Cooke, J.G. (1984) Nitrate loss and transformation in two vegetated headwater stream. *New Zealand Journal of Marine and Freshwater Research*. 19: 441-450.

Delwiche, C.C. and Bryan, B.A. (1976) Denitrification. *Annual Review of Microbiology*. 30: 241-262.

Dobson, R.W. (1997) Sulfate sorption in a shallow sandy aquifer. MS Thesis. University of Virginia.

Duff, J.H., Triska, F.J., and OremLand, R.S. (1984) Denitrification associated with stream periphyton: Chamber estimates from undisturbed communities. *Journal of Environmental Quality*. 13: 514- 518.

Duff, J.H., Murphy, F., Fuller, C.C., Triska, F.J., Harvey, J.W., and Jackman, A.P. (1998) A mini drivepoint sampler for measuring porewater solute concentrations in the hyporheic zone of sand-bottom streams. *Limnology and Oceanography*. 43: 1378-1383.

Fraser, B.G. and Williams, D.D. (1998) Seasonal Boundary Dynamics of a Ground water- surface-Water Ecotone. *Ecology*, 79 (6): 2019- 2031.

Freeze, R.A., and Cherry, J.A. (1979) Ground Water. Prentice-Hall, Inc. Englewood Cliffs, New Jersey. p.415.

Hedin, L.O., von Fisher, J.C., Ostrom, J.C., Kennedy, B.P., Brown, M.G., and Robertson, G.P. (1998) Thermodynamic Constraints on Nitrogen Transformations and other biogeochemical processes at soil-stream interfaces. *Ecology*. 79 (2): 684-703.

Hill, A.R. (1990) Ground water flow paths in relation to nitrogen chemistry in the near-stream zone. *Hydrobiologia*. 206: 39- 52.

Hill, A.R. (1996) Nitrate removal in stream riparian zones. *Journal of Environmental Quality*. 25: 743-754.

Hill, A.R., Sanmugadas, K. (1985) Denitrification rates in relation to stream sediment characteristics. *Water Research*. 19: 1579- 1586.

Hill, A.R., Devito, K.J., Campangnolo, S., Sanmugadas, K. (2000) Subsurface denitrification in a forest riparian zone: Interactions between hydrology and supplies of nitrate and organic carbon. *Biogeochemistry*. 51: 193- 223.

Hinkle, S.R., Duff, J.H, Triska, F.J., Laenan, A., Gates, E.B., Bencala, K.E., Wentz, D.A, & Silva, S.R. (2001) Linking hyporheic flow and nitrogen cycling near the Williamette River- a large river in Oregon, USA. *Journal of Hydrology*. 244: 157-180.

Hubbert, M.K. (1940) The theory of ground water motion. *Journal of Geology*. 48 (8) pt. 1. 78-944.

Jacobs, T.C. & Gilliam, J.W. (1985a) Headwater stream losses of nitrogen from two coastal plain watersheds. *Journal of Environmental Quality*, 14: 467-472.

Jacobs, T.C. & Gilliam, J.W. (1985b) Riparian losses of nitrate from agricultural drainage water. *Journal of Environmental Quality*, 14: 472-478.

Jones, M.N. (1984) Nitrate reduction by shaking with Cadmium: Alternative to Cadmium Columns. *Water Resources*. 18 (5): 643-646.

Knapp, E.W., Herman, J.S. Mills, A.L., and Hornberger, G.M. (2002) Changes in the sorption capacity of Coastal Plain sediments due to redox alterations of mineral surfaces. *Applied Geochemistry.* 17: 387-398.

Lamontagne, M.G., Valiela, I. (1995) Denitrification Measured by a Direct N2 Flux method in Sediments of Waquoit, MA. *Biogeochemistry*. 31: 63-83.

Lowrance, R.R., Todd R.L., & Asmussen, L.E. (1984) Nutrient Cycling in an agricultural watershed: I. Phreatic movement. *Journal of Environmental Quality*. 13: 22-27.

Lowrance, R. (1992) Ground water Nitrate and Denitrification in a Coastal Plain Riparian Forest. *Journal of Environmental Quality*. 21: 401-405.

McClain, M.E., Boyer, E.W., Dent, C.L., Gergel, S.E., Grimm, N.B., Groffman, P.M., Hart, S.C., Harvey, J.W., Johnston, C.A., Mayorga, E., McDowell, W.H., Pinay, G. (2003) Biogeochemical Hot Spots and Hot Moments at the Interface of Terrestrial and Aquatic Ecosystems. *Ecosystems*. 6: 301-312.

McDowell, W.H., Bowden, W.B., Asbury, C.E. (1992) Riparian nitrogen dynamics in two geomorphologically distinct tropical rain forest watersheds: subsurface solute patterns. *Biogeochemistry*. 18: 53- 75.

Mills, A.L., Hornberger, G.M., Herman, J.S, Chauhan, M.J., Galavotti, H.S. (2002) Hyporheic Zones in Coastal Streams: Filters for Removal of Agricultural Nitrate. In: Fall Meeting of the American Geophysical Union San Francisco, CA.

Mills, A.L., Hornberger, G.M., Herman, J.S. NSF Proposal.

Montgomery, H.A.C. & Dymock, J.F. (1961) *Analyst* 86: 414-416.

Nolan, B.T. (1999) Nitrate Behavior in Ground Waters of the Southeastern United States. *Journal of Environmental Quality*. 28 (5): 1518-1527.

Pattinson, S.N., Garcia-Ruiz, R., Whitton, B.A. (1998) Spatial and Seasonal Variation in Denitrification in the Swale-Ouse System, a River Continuum. *The Science of the Total Environment*. 210/211: 289-305.

Peterjohn, W.T. & Correll, D.L. (1984) Nutrient Dynamics in an agricultural watershed: observations on the role of a riparian forest. *Ecology*. 65: 1466-1475.

Pfenning, K.S., McMahon, P.B. (1996) Effect of nitrate, organic carbon, and temperature on potential denitrification rates in nitrate-rich riverbed sediments. *Journal of Hydrology*. 187: 283-295.

Pinay, G., Roques, L., & Fabre, A. (1993) Spatial and temporal patterns of denitrification in a riparian forest. *Journal of Applied Ecology*. 30: 581-591.

Reay, W.G., Robinson, M.A., Lunsford, C.A. (2001) Ground Water Nitrogen Contributions to Coastal Waters of Virginia's Eastern Shore: Indentification of High-Risk Discharge Regions and Remediation Strategies. http://www.epa.gov/OWOW/watershed/Proceed/reay.htmL.

Rice, W.R. (1989) Analyzing Tables of Statistical Tests. *Evolution*. 43: 223- 225.

Richardson, D. (1992) Hydrogeology and analysis of the ground water flow system of the Eastern Shore, Virginia. U.S. Geological Survey. Open File Report. 91-190.

Robinson J.B., Whiteley, H.R. Stammers, W. Kaushik, N.K., Sain, P. (1979) The fate of nitrate in small streams and its management implications. *In* Proc 10th Annual Agric. Waste Manage. Conf. Cornell University. p. 247 259.

Seitzinger, S.P. (1987) The effect of pH on the release of phosphorus from Potomac River Sediments. CBP/TRS 15. U.S. EPA, Chesapeake Bay Program. Annapolis. p. 54.

Seitzinger, S.P. (1988) Denitrification in freshwater and coastal marine ecosystems: Ecological and geochemical significance. *Limnology and Oceanography*. 33 (4, part 2): 702-724.

Seitzinger, S.P. (1993) Denitrification measurements in aquatic sediments: A comparison of three methods. *Biogeochemistry.* 23: 147- 167.

Seitzinger, S.P. (in press) Benthic nutrient cycling and oxygen consumption in the Delaware estuary. *In* S.K. Majumdar et al. [eds.], Ecology and Restoration of the Delaware River Basin. Penn. Acad. Sci.

Seitzinger, S.P. Styles, R.V., Boyer, E.W., Alexander, R.B., Billen, G., Howarth, R.W., Mayer, B., Breemen, N.V. (2002) Nitrogen retention in rivers: model development and application to watersheds in the northeastern U.S.A. *Biogeochemistry*. 57/58: 199-237.

Simmons, R.C., Gold, A.J., Groffman, P.M. (1992) Nitrate Dynamics in Riparian Forests: Ground water Studies. *Journal of Environmental Quality*. 21: 659-665.

Starr, R.C., Gillham, R.W. (1989) Controls on denitrification in shallow unconfined aquifers. In: Contaminant Transport in Ground water. Kobus & Kinzelback (eds). p. 51-56.

Starr, R.C., Gillham R.W. (1993) Denitrification and Organic Carbon Availability in two Aquifers. *Ground Water*. 31 (6): 934- 947.

Steinhart, G.S., Likens, G.E., Groffman, P.M. (2000) Denitrification in stream sediments in five northeastern (USA) streams. *Verh. Internat. Verein. Limnol*. 27: 1331-1336.

Tesoriero, A.J., Liebscher, H., Cox, S.E. (2000) Mechanism and rate of denitrification in an agricultural watershed: Electron and mass balance along ground water flow paths. *Water Resource Research*. 36 (6): 1545- 1559.

Tiedje, J. M. (1982) Denitrification. In: A. L. Page (Ed.), Methods of Soil Analysis. Madison, WI: ASA-SSSA. Part 2. pp.1011-1026.

Triska, F.J. Duff, J.H., & Avanzino, R.J. (1993) The role of water exchange between a stream channel and its hyporheic zone in nitrogen cycling at the terrestrial-aquatic interface. *Hydrolobiologia*. 251: 167-184.

U.S. EPA, Federal Register: (April 9, 1997) Sole Source Aquifer Designation for the Columbia and Yorktown-Eastover Multiaquifer System. 62 (68).

U.S. EPA (1983) Methods for Chemical Analysis of Water and Wastes, Method 353.2 EPA-600/4-79-020. U.S.E.P.A., Cincinnati, Ohio, USA.

Wagner-Riddle, C., Thurtell, G.W., King, K.M., Kidd, G.E., & Beauchamp, E.G. (1996) Nitrous Oxide and Carbon Dioxide Fluxes from a Bare Soil Using a Micrometerological Approach. *Journal of Environmental Quality*. 25: 898-907.

Watts, S.H., Seitzinger, S.P. (2000) Denitrification rates in organic and mineral soils from riparian sites: a comparison of N_2 flux and acetylene inhibition methods. *Soil Biology and Biochemistry*. 32: 1383-1392.

Williams, D.D. (1993) Nutrient and flow vector dynamics at the hyporheic-ground water interface and their effects on the interstitial fauna. *Hydrobiologia*. 251: 185-198. in (Fraser, B.G. & Williams, D.D. (1998) Seasonal Boundary Dynamics of a Ground water-surface-Water Ecotone. *Ecology*. 79 (6): 2019- 2031.

Winter, T.C., Harvey, J.D, Franke, O.L., Alley, W.M. (1998) Ground water and Surface Water: A Single Resource. U.S. Geological Survey Circular 1139. Denver, Colorado.

Appendix A: Piezometer and Well Locations

Table A-1: Locations of Piezometers (A,B,& C) and Wells (W) by Total Station referenced to permanent monuments located by Global Positioning System. Elevation measured at the ground surface adjacent to each nest (N#) and at the top of the riser of each piezometer and well.

Point	Easting (X)	Northing (Y)	Long (X)	Lat (Y)	Elevation (ASL)
MLSW	417722.970	4127572.070	-75.9282	37.2911	7.782
MLSE	417740.260	4127554.310	-75.9281	37.291	7.843
HT Well	417698.340	4127551.770	-75.9285	37.2909	7.671
Hill Mon	417652.090	4127552.510	-75.929	37.2909	4.480
N9	417648.880	4127563.300	-75.9291	37.291	3.949
N9W					4.603
Still W	417635.340	4127565.830	-75.9292	37.2911	1.335
N3	417638.890	4127556.130	-75.9292	37.291	2.033
N3A					2.441
N3B					2.269
N3C					2.101
N3W					1.960
N1	417637.940	4127555.980	-75.9292	37.291	1.690
N1A					2.411
N1B					2.122
N1C					1.776
N1W					2.003
N4	417638.830	4127553.650	-75.9292	37.2909	1.988
N4A					2.458
N4B					2.268
N4C					2.081
N4W					2.156
N5	417638.460	4127547.820	-75.9292	37.2909	1.645
N5A					2.269
N5B					2.114
N5C					1.888
N5W					1.857

Appendix A: Piezometer and Well Locations

Table A-1: continued.

N6	417636.710	4127544.650	-75.9292	37.2909	1.423
N6A					2.134
N6B					1.953
N6C					1.779
N6W					1.772
N7	417644.235	4127556.036	-75.9291	37.291	3.121
N7A					3.800
N7B					3.807
N7W					3.793
N8	417643.910	4127544.890	-75.9291	37.2909	2.888
N8W					3.418
N10	417650.090	4127536.800	-75.9291	37.2908	3.944
N10A					4.570
N10B					4.565
S2	417633.880	4127547.400	-75.9293	37.2909	0.987
S2A					1.925
S2B					1.755
S1	417636.400	4127555.810	-75.9292	37.291	0.878
S1A					1.811
S1B					1.550

Appendix A: Piezometer and Well Locations

Table A-2: Elevations of Piezometer and Well Openings above Sea Level

Piezometer number	Length from top of riser to hole (m)	Depth of riser above ground (m)	Depth below ground (m)	Elevation above sea level (m)	Height of hole ASL
N1A	1.508	0.608	0.900	2.411	0.903
N1B	1.509	0.500	1.009	2.122	0.613
N1C	1.510	0.103	1.407	1.776	0.266
N1W	1.508	0.301	1.207	2.003	0.495
N3A	1.470	0.400	1.070	2.441	0.971
N3B	1.475	0.255	1.220	2.269	0.794
N3C	1.475	0.075	1.400	2.101	0.626
N3W	1.470	0.070	1.400	1.960	0.490
N4A	1.470	0.475	0.995	2.458	0.988
N4B	1.470	0.295	1.175	2.268	0.798
N4C	1.470	0.100	1.370	2.081	0.611
N4W	1.470	0.160	1.310	2.156	0.686
N5A	1.475	0.630	0.845	2.269	0.794
N5B	1.470	0.470	1.000	2.114	0.644
N5C	1.475	0.260	1.215	1.888	0.413
N5W	1.470	0.230	1.240	1.857	0.387
N6A	1.475	0.720	0.755	2.134	0.659
N6B	1.470	0.550	0.920	1.953	0.483
N6C	1.470	0.350	1.120	1.779	0.309
N6W	1.470	0.345	1.125	1.772	0.302
S1A	1.520	0.920	0.600	1.811	0.291
S1B	1.520	0.640	0.880	1.550	0.030
S2A	1.500	1.100	0.400	1.925	0.425
S2B	1.500	0.880	0.620	1.755	0.255
N7A	2.699	0.668	2.031	3.800	1.101
N7B	3.004	0.672	2.332	3.807	0.803
N7W	3.010	0.660	2.350	3.793	0.783
N8W	3.010	0.658	2.352	3.418	0.408
N9W	3.010	0.646	2.364	4.603	1.593
N10A	2.997	0.669	2.329	4.570	1.573
N10W	3.010	0.663	2.347	4.565	1.555
still (stage)				1.335	

Appendix B: Ground Water Solute Concentration

Table B-1: Chloride concentration (mg $Cl^- L^{-1}$) of Ground Water collected from Piezometer Nests for all sampling dates. Depth below ground surface is generally shown by piezometer letter: A: Shallowest, B: Mid and C: Deepest Depth.

Piezometer	7/11/03				11/30/03		12/19/03	
ID	07/11/03	SEM	10/26/03	10/26/03SEM	11/30/03	SEM	12/19/03	SEM
N1A	n/a	n/a	32.24	0.00	31.2	0.4	57.9	1.8
N1B	n/a	n/a	26.90	2.81	19.0	0.0	31.1	1.1
N1C	n/a	n/a	17.81	1.24	16.4	0.0	25.2	0.2
N3A	n/a	n/a	32.24	0	ns	ns	52.8	0.3
N3B	n/a	n/a	31.23	1.01	22.2	0.9	30.0	0.5
N3C	n/a	n/a	20.00	1.73	17.3	0.1	26.5	0.0
N4A	n/a	n/a	28.53	0.03	25.4	0.2	35.1	0.7
N4B	n/a	n/a	26.98	0.14	25.7	0.1	35.9	0.2
N4C	n/a	n/a	31.38	0.86	26.8	0.1	33.9	0.1
N5A	n/a	n/a	32.24	0.00	36.9	0.9	47.8	0.0
N5B	n/a	n/a	32.24	0.00	31.2	0.2	36.4	0.7
N5C	n/a	n/a	46.30	7.10	25.8	0.1	28.3	0.0
N6A	36	0	127.78	5.56	18.8	0.0	26.6	0.1
N6B	29.8	0.46	69.44	16.92	17.3	0.1	27.0	0.1
N6C	30.73	0.18	83.06	5.70	19.1	0.4	26.3	0.2
N7A	19	0.4	16.98	0.29	17.3	0.1	29.2	0.3
N7B	13.07	0.29	16.72	0.15	16.0	0.1	23.9	0.1
N10A	14.07	0.97	20.50	2.99	16.1	0.1	24.4	0.2
S1A	13.53	0.07	12.24	0.06	11.4	0.0	18.7	0.8
S1B	13.87	0.13	12.72	0.08	11.3	0.0	17.5	0.0
S2A	12.33	0.64	136.67	5.36	12.5	0.0	16.8	0.0
S2B	12	0.12	195.28	0.73	14.2	0.0	17.4	0.0
Stream at Exp Hillslope	23.6	0.12	30.47	0.00	23.4	0.0	27.0	0.1
Stream at Culvert	n/a	n/a	22.24	5.90	n/a	n/a	n/a	n/a

Appendix B: Ground Water Solute Concentration

Table B-2: Sulfate concentration (mg SO_4^{2-} L^{-1}) of Ground Water collected from Piezometer Nests for all sampling dates. Depth below ground surface is generally shown by piezometer letter: A: Shallowest, B: Mid and C: Deepest Depth.

Piezometer	7/11/03				11/30/03		12/19/03	
ID	07/11/03	SEM	10/26/03	10/26/03SEM	11/30/03	SEM	12/19/03	SEM
N1A	n/a	n/a	29.28	0.47	32.4	0.7	42.6	1.2
N1B	n/a	n/a	24.62	1.53	19.1	0.0	22.6	0.5
N1C	n/a	n/a	18.54	1.06	16.9	0.0	19.3	0.3
N3A	n/a	n/a	33.81	0	ns	ns	36.7	0.3
N3B	n/a	n/a	32.26	4.36	23.9	0.9	21.8	0.4
N3C	n/a	n/a	23.07	1.44	19.5	0.3	20.3	0.2
N4A	n/a	n/a	25.40	0.26	29.7	3.2	28.1	0.6
N4B	n/a	n/a	27.34	0.26	32.9	0.2	32.2	0.3
N4C	n/a	n/a	27.47	0.26	32.1	0.2	32.2	0.0
N5A	n/a	n/a	22.29	0.93	24.9	0.0	26.9	0.0
N5B	n/a	n/a	44.04	23.04	24.6	0.3	23.7	0.0
N5C	n/a	n/a	31.05	6.05	22.7	0.2	22.5	0.2
N6A	26.56	0.3	28.91	1.56	24.7	0.0	21.6	0.0
N6B	27.16	0	25.17	1.23	24.1	0.6	21.9	0.2
N6C	25.96	0.3	30.03	2.16	22.2	0.2	20.7	0.2
N7A	24.76	1.49	18.31	0.43	16.9	0.0	19.3	0.2
N7B	21.18	0.3	16.81	0.43	16.5	0.0	18.9	0.0
N10A	26.26	0.52	17.93	0.92	18.2	0.0	22.5	0.2
S1A	20.28	0.3	21.30	0.00	22.2	0.1	25.3	0.6
S1B	20.88	0	21.30	0.00	22.2	0.1	26.5	0.2
S2A	17.29	0	240.00	25.17	20.3	0.0	22.1	0.0
S2B	17.59	0.3	127.21	3.06	21.5	0.1	23.2	0.0
Stream at Exp Hillslope	56.45	0.3	45.38	0.12	50.7	0.2	35.0	0.2
Stream at Culvert	n/a	n/a	34.53	9.61	n/a	n/a	n/a	n/a

Appendix C: Denitrification Potential Assay

Table C-1: Denitrification Assay on July 11, 2003. Bold indicates data used for analysis.

Core	Depth (cm)	Time (hr)	Peak Area (mvolt*sec)	Convert peak area to mass (nmol)	Convert mass to Conc. (nmol/0.5 mL)	Total N_2O using Bunsen Absorpion Coefficient (nmol)	Volume of sample (mL)	nmol N_2O/ ml/hr
1	2	1.42	44.00	5.49	10.98	550.52	7	55.52
	2	**2.58**	**98.50**	**12.29**	**24.58**	**1232.42**	**7**	**68.15**
	2	17.63	293.00	36.55	73.11	3665.99	7	29.70
1	10	1.80	4.74	0.59	1.18	59.31	8.4	3.92
	10	**2.83**	**5.52**	**0.69**	**1.38**	**69.07**	**8.4**	**2.90**
	10	17.98	0.00	0.00	0.00	0.00	8.4	0.00
1	20	1.73	7.89	0.98	1.97	98.72	10	5.70
	20	**2.78**	**21.80**	**2.72**	**5.44**	**272.76**	**10**	**9.80**
	20	17.93	126.00	15.72	31.44	1576.50	10	8.79
1	30	1.25	0.00	0.00	0.00	0.00	11	0.00
	30	**2.45**	**0.00**	**0.00**	**0.00**	**0.00**	**11**	**0.00**
	30	17.53	5.81	0.72	1.45	72.69	11	0.38
2	10	1.85	0.00	0.00	0.00	0.00	8.8	0.00
	10	**2.88**	**0.00**	**0.00**	**0.00**	**0.00**	**8.8**	**0.00**
	10	18.02	17.20	2.15	4.29	215.20	8.8	1.36
2	20	1.08	0.00	0.00	0.00	0.00	10	0.00
	20	**2.32**	**0.00**	**0.00**	**0.00**	**0.00**	**10**	**0.00**
	20	17.42	0.00	0.00	0.00	0.00	10	0.00
2	30	1.32	0.00	0.00	0.00	0.00	8.6	0.00
	30	**2.52**	**0.00**	**0.00**	**0.00**	**0.00**	**8.6**	**0.00**
	30	17.60	0.00	0.00	0.00	0.00	8.6	0.00
3	2	0.40	28.50	3.56	7.11	356.59	9	99.05
	2	0.80	120.00	14.97	29.94	1501.43	9	208.53
	2	2.22	187.00	23.33	46.66	2339.73	9	117.28
	2	**3.20**	**270.00**	**33.69**	**67.37**	**3378.22**	**9**	**117.30**
	2	18.33	668.00	83.34	166.68	8357.96	9	50.65
3	10	1.97	101.00	12.60	25.20	1263.70	10	64.26
	10	**3.00**	**180.00**	**22.46**	**44.91**	**2252.14**	**10**	**75.07**
	10	18.13	681.00	84.96	169.92	8520.61	10	46.99
3	20	0.50	0.00	0.00	0.00	0.00	10	0.00
	20	1.92	0.00	0.00	0.00	0.00	10	0.00
	20	**2.95**	**1.54**	**0.19**	**0.38**	**19.27**	**10**	**0.65**
	20	18.07	0.00	0.00	0.00	0.00	10	0.00

Table C-1: continued.

Core	Depth (cm)	Time (hr)	Peak Area (mvolt*sec)	Convert peak area to mass (nmol)	Convert mass to Conc. (nmol/0.5 mL)	Total N_2O using Bunsen Absorpion Coefficient (nmol)	Volume of sample-mL	nmol N_2O/ ml/hr
3	30	0.75	0.00	0.00	0.00	0.00	10.5	0.00
	30	2.08	0.00	0.00	0.00	0.00	10.5	0.00
	30	**3.10**	**7.37**	**0.92**	**1.84**	**92.21**	**10.5**	**2.83**
	30	18.23	0.00	0.00	0.00	0.00	10.5	0.00
4	2	1.62	68.90	8.60	17.19	862.07	10	53.32
	2	**2.68**	**123.00**	**15.35**	**30.69**	**1538.97**	**10**	**57.35**
	2	17.82	348.00	43.42	86.83	4354.15	10	24.44
4	10	1.47	2.17	0.27	0.54	27.15	10	1.85
	10	1.50	1.82	0.23	0.45	22.77	10	1.52
	10	**2.65**	**6.09**	**0.76**	**1.52**	**76.20**	**10**	**2.88**
	10	17.70	117.00	14.60	29.19	1463.89	10	8.27
4	20	0.58	0.00	0.00	0.00	0.00	9.6	0.00
	20	0.92	0.00	0.00	0.00	0.00	9.6	0.00
	20	1.55	0.00	0.00	0.00	0.00	9.6	0.00
	20	2.02	0.00	0.00	0.00	0.00	9.6	0.00
	20	**3.05**	**0.00**	**0.00**	**0.00**	**0.00**	**9.6**	**0.00**
	20	18.18	0.00	0.00	0.00	0.00	9.6	0.00
4	30	1.18	0.00	0.00	0.00	0.00	10.2	0.00
	30	**2.38**	**0.00**	**0.00**	**0.00**	**0.00**	**10.2**	**0.00**
	30	17.47	0.00	0.00	0.00	0.00	10.2	0.00
4	40	1.55	0.00	0.00	0.00	0.00	9.4	0.00
	40	**2.67**	**0.00**	**0.00**	**0.00**	**0.00**	**9.4**	**0.00**
	40	17.75	0.00	0.00	0.00	0.00	9.4	0.00
4	50	1.08	0.00	0.00	0.00	0.00	10.5	0.00
	50	**2.27**	**0.00**	**0.00**	**0.00**	**0.00**	**10.5**	**0.00**
	50	17.38	0.00	0.00	0.00	0.00	10.5	0.00

Appendix C: Denitrification Potential Assay

Table C-2: Denitrification Assay on August 4, 2003. Bold indicates data used in analysis

Core	Depth (cm)	Time (hr)	Peak Area (mvolt*sec)	Convert peak area to mass (nmol)	Convert Mass to Conc. (nmol/0.5ml)	Total N_2O using Bunsen Absorpion coefficient (nmol)	Dry weight (grams)	nmol N_2O/(g) dry weight/hr	nmol N_2O/ml/ hr
1	4	1.87	16.9	2.11	4.22	211.45	16.47	6.88	11.33
		3.00	47.5	5.93	11.85	594.32	16.47	12.03	19.81
		3.30	**59.9**	**7.47**	**14.95**	**749.46**	**16.47**	**13.79**	**22.71**
		4.12	65.2	8.13	16.27	815.78	16.47	12.03	19.82
		24.07	148	18.46	36.93	1851.76	16.47	4.67	7.69
		56.20	265	33.06	66.12	3315.66	16.47	3.58	5.90
		92.48	227	28.32	56.64	2840.20	16.47	1.86	3.07
1	11	0.92	0	0.00	0.00	0.00	17.33	0.00	0.00
		2.05	0	0.00	0.00	0.00	17.33	0.00	0.00
		3.10	0	0.00	0.00	0.00	17.33	0.00	0.00
		3.85	**0**	**0.00**	**0.00**	**0.00**	**17.33**	**0.00**	**0.00**
		23.90	19.3	2.41	4.82	241.48	17.33	0.58	1.01
		92.62	110	13.72	27.45	1376.31	17.33	0.86	1.49
1	21	1.70	0	0.00	0.00	0.00	15.05	0.00	0.00
		3.13	0	0.00	0.00	0.00	15.05	0.00	0.00
		3.90	**0**	**0.00**	**0.00**	**0.00**	**15.05**	**0.00**	**0.00**
		23.95	0	0.00	0.00	0.00	15.05	0.00	0.00
1	31	1.75	0	0.00	0.00	0.00	15.44	0.00	0.00
		3.05	0	0.00	0.00	0.00	15.44	0.00	0.00
		3.78	**0**	**0.00**	**0.00**	**0.00**	**15.44**	**0.00**	**0.00**
		23.87	0	0.00	0.00	0.00	15.44	0.00	0.00
		92.58	0	0.00	0.00	0.00	15.44	0.00	0.00
1	41	1.78	0	0.00	0.00	0.00	11.08	0.00	0.00
		3.23	**0**	**0.00**	**0.00**	**0.00**	**11.08**	**0.00**	**0.00**
		4.07	0	0.00	0.00	0.00	11.08	0.00	0.00
		24.03	0	0.00	0.00	0.00	11.08	0.00	0.00
1	51	2.25	0	0.00	0.00	0.00	18.19	0.00	0.00
		3.18	**0**	**0.00**	**0.00**	**0.00**	**18.19**	**0.00**	**0.00**
		4.02	0	0.00	0.00	0.00	18.19	0.00	0.00
		24.00	0	0.00	0.00	0.00	18.19	0.00	0.00
2	2	**4.05**	**190**	**23.70**	**47.41**	**2377.26**	**13.87**	**42.32**	**58.70**
		5.12	250	31.19	62.38	3127.98	13.87	44.08	61.13
		22.97	324	40.42	80.84	4053.86	13.87	12.73	17.65

Table C-2 continued

Core	Depth	Time	Area	mass (nmol)	Concentration (nmol/ml)	Total N_2O (nmol)	Dry wt. (grams)	nmol N_2O/(g)/hr	nmol N_2O/ml/ hr
2	22	**4.15**	**1.22**	**0.15**	**0.30**	**15.26**	**14.94**	**0.25**	**0.37**
		23.05	0	0.00	0.00	0.00	14.94	0.00	0.00
2	32	**4.20**	**0**	**0.00**	**0.00**	**0.00**	**16.25**	**0.00**	**0.00**
		23.13	1.4	0.17	0.35	17.52	16.25	0.05	0.08
2	42	**4.25**	**0**	**0.00**	**0.00**	**0.00**	**15.86**	**0.00**	**0.00**
		23.10	0	0.00	0.00	0.00	15.86	0.00	0.00
2	52	**4.30**	**0**	**0.00**	**0.00**	**0.00**	**10.99**	**0.00**	**0.00**
		23.18	0	0.00	0.00	0.00	10.99	0.00	0.00
3	10	1.00	0	0.00	0.00	0.00	13.18	0.00	0.00
		2.10	0	0.00	0.00	0.00	13.18	0.00	0.00
		2.70	0	0.00	0.00	0.00	13.18	0.00	0.00
		3.53	**0**	**0.00**	**0.00**	**0.00**	**13.18**	**0.00**	**0.00**
		23.62	0	0.00	0.00	0.00	13.18	0.00	0.00
3	20	1.67	0	0.00	0.00	0.00	8.28	0.00	0.00
		2.77	0	0.00	0.00	0.00	8.28	0.00	0.00
		3.57	**0**	**0.00**	**0.00**	**0.00**	**8.28**	**0.00**	**0.00**
		23.67	0	0.00	0.00	0.00	8.28	0.00	0.00
3	30	1.60	0	0.00	0.00	0.00	7.95	0.00	0.00
		2.78	0	0.00	0.00	0.00	7.95	0.00	0.00
		3.62	**0**	**0.00**	**0.00**	**0.00**	**7.95**	**0.00**	**0.00**
		23.72	0	0.00	0.00	0.00	7.95	0.00	0.00
3	40	1.92	0	0.00	0.00	0.00	8.73	0.00	0.00
		2.83	**7.85**	**0.98**	**1.96**	**98.22**	**8.73**	**3.97**	**3.47**
		3.67	0	0.00	0.00	0.00	8.73	0.00	0.00
		23.77	0	0.00	0.00	0.00	8.73	0.00	0.00
		92.52	1.54	0.19	0.38	19.27	8.73	0.02	0.02
3	60	2.15	3.42	0.43	0.85	42.79	7.30	2.73	1.99
		2.93	**5.89**	**0.73**	**1.47**	**73.70**	**7.30**	**3.44**	**2.51**
		3.72	5.77	0.72	1.44	72.19	7.30	2.66	1.94
		23.82	66.8	8.33	16.67	835.80	7.30	4.81	3.51
		92.45	92.3	11.52	23.03	1154.85	7.30	1.71	1.25
4	4	**4.35**	**261**	**32.56**	**65.12**	**3265.61**	**12.97**	**57.88**	**75.07**
		23.23	502	62.63	125.26	6280.98	12.97	20.84	27.03
4	10	**4.40**	**0**	**0.00**	**0.00**	**0.00**	**14.31**	**0.00**	**0.00**
		23.28	0	0.00	0.00	0.00	14.31	0.00	0.00
4	18	**4.58**	**0**	**0.00**	**0.00**	**0.00**	**13.63**	**0.00**	**0.00**
		23.52	3.9	0.49	0.97	48.80	13.63	0.15	0.21
4	26	**4.43**	**5.27**	**0.66**	**1.31**	**65.94**	**19.56**	**0.76**	**1.49**
		23.32	22.9	2.86	5.71	286.52	19.56	0.63	1.23

Table C-2 continued

Core	Depth	Time	Area	mass (nmol)	Concentration(nmol/ml)	Total N_2O (nmol)	Dry wt. (grams)	nmol N_2O/(g)/hr	nmol N_2O/ml/ hr
4	36	**4.48**	**0**	**0.00**	**0.00**	**0.00**	**11.68**	**0.00**	**0.00**
		23.38	2.74	0.34	0.68	34.28	11.68	0.13	0.15
4	46	**5.07**	**0**	**0.00**	**0.00**	**0.00**	**13.73**	**0.00**	**0.00**
		22.33	0	0.00	0.00	0.00	13.73	0.00	0.00
4	56	**4.53**	**0**	**0.00**	**0.00**	**0.00**	**18.92**	**0.00**	**0.00**
		23.42	0	0.00	0.00	0.00	18.92	0.00	0.00
5	2	**3.80**	**488**	**60.88**	**121.77**	**6105.81**	**14.54**	**110.51**	**160.68**
		22.70	408	50.90	101.80	5104.86	14.54	15.47	22.49
5	9	**3.85**	**90.7**	**11.32**	**22.63**	**1134.83**	**13.20**	**22.33**	**29.48**
		22.75	238	29.69	59.39	2977.84	13.20	9.92	13.09
5	18	**3.90**	**2.97**	**0.37**	**0.74**	**37.16**	**11.42**	**0.83**	**0.95**
		22.78	42.4	5.29	10.58	530.51	11.42	2.04	2.33
5	29	**3.95**	**0**	**0.00**	**0.00**	**0.00**	**15.41**	**0.00**	**0.00**
		22.90	24.6	3.07	6.14	307.79	15.41	0.87	1.34
5	39	**4.02**	**0**	**0.00**	**0.00**	**0.00**	**14.97**	**0.00**	**0.00**
		22.95	4.58	0.57	1.14	57.30	14.97	0.17	0.25
5	49	**4.07**	**0**	**0.00**	**0.00**	**0.00**	**17.60**	**0.00**	**0.00**
		23.00	1.13	0.14	0.28	14.14	17.60	0.03	0.06
5	59	**4.10**	**0**	**0.00**	**0.00**	**0.00**	**14.79**	**0.00**	**0.00**
		23.05	0	0.00	0.00	0.00	14.79	0.00	0.00
5	69	**4.15**	**0**	**0.00**	**0.00**	**0.00**	**15.05**	**0.00**	**0.00**
		23.08	0	0.00	0.00	0.00	15.05	0.00	0.00
5	79	**4.20**	**0**	**0.00**	**0.00**	**0.00**	**17.36**	**0.00**	**0.00**
		23.13	0	0.00	0.00	0.00	17.36	0.00	0.00
6	2	1.60	148	18.46	36.93	1851.76	17.25	67.09	115.74
		2.77	**251**	**31.31**	**62.63**	**3140.49**	**17.25**	**65.80**	**113.51**
		34.23	699	87.21	174.41	8745.83	17.25	14.81	25.55
		70.90	492	61.38	122.76	6155.86	17.25	5.03	8.68
6	12	1.65	20.8	2.60	5.19	260.25	15.34	10.28	15.77
		2.67	**29**	**3.62**	**7.24**	**362.85**	**15.34**	**8.87**	**13.61**
		34.15	45.7	5.70	11.40	571.79	15.34	1.09	1.67
6	22	1.70	12	1.50	2.99	150.14	14.77	5.98	8.83
		2.83	**22**	**2.74**	**5.49**	**275.26**	**14.77**	**6.58**	**9.72**
		34.38	24.9	3.11	6.21	311.55	14.77	0.61	0.91
6	32	1.82	16.2	2.02	4.04	202.69	12.50	8.93	11.16
		2.88	**22.5**	**2.81**	**5.61**	**281.52**	**12.50**	**7.81**	**9.76**
		34.42	268	33.44	66.87	3353.19	12.50	7.79	9.74
6	42	1.87	14.5	1.81	3.62	181.42	17.19	5.65	9.72
		2.93	**29.7**	**3.71**	**7.41**	**371.60**	**17.19**	**7.37**	**12.67**
		34.48	303	37.80	75.60	3791.11	17.19	6.40	10.99

Table C-2 continued

Core	Depth	Time	Area	mass (nmol)	Concentration(nmol/ml)	Total N_2O (nmol)	Dry wt. (grams)	nmol N_2O/(g)/hr	nmol N_2O/ml/ hr
6	52	1.55	5.56	0.69	1.39	69.57	13.67	3.28	4.49
		2.72	**13.2**	**1.65**	**3.29**	**165.16**	**13.67**	**4.45**	**6.08**
		34.18	347	43.29	86.58	4341.63	13.67	9.29	12.70
7	2	**3.73**	**14.4**	**1.80**	**3.59**	**180.17**	**5.58**	**8.65**	**4.83**
		22.45	0	0.00	0.00	0.00	5.58	0.00	0.00
7	10	**3.82**	**50.7**	**6.33**	**12.65**	**634.35**	**11.15**	**14.91**	**16.62**
		22.48	242	30.19	60.38	3027.88	11.15	12.08	13.47
7	20	**3.90**	**127**	**15.84**	**31.69**	**1589.01**	**10.00**	**40.74**	**40.74**
		22.53	374	46.66	93.32	4679.46	10.00	20.77	20.77
7	30	**4.00**	**15.1**	**1.88**	**3.77**	**188.93**	**14.93**	**3.16**	**4.72**
		22.58	58.3	7.27	14.55	729.44	14.93	2.16	3.23
7	40	**4.07**	**2.84**	**0.35**	**0.71**	**35.53**	**16.88**	**0.52**	**0.87**
		22.65	10.4	1.30	2.60	130.12	16.88	0.34	0.57
7	50	**4.12**	**8.2**	**1.02**	**2.05**	**102.60**	**13.85**	**1.80**	**2.49**
		22.68	33.4	4.17	8.33	417.90	13.85	1.33	1.84
7	60	**4.17**	**13**	**1.62**	**3.24**	**162.65**	**14.05**	**2.78**	**3.90**
		22.73	79	9.86	19.71	988.44	14.05	3.09	4.35
8	2	**4.20**	**4.19**	**0.52**	**1.05**	**52.42**	**16.80**	**0.74**	**1.25**
		22.78	5.19	0.65	1.30	64.94	16.80	0.17	0.29
8	12	**4.27**	**4.85**	**0.61**	**1.21**	**60.68**	**13.89**	**1.02**	**1.42**
		22.87	7.07	0.88	1.76	88.46	13.89	0.28	0.39
8	22	**4.30**	**0**	**0.00**	**0.00**	**0.00**	**12.35**	**0.00**	**0.00**
		22.90	275	34.31	68.62	3440.78	12.35	12.17	15.03
8	32	**4.32**	**0**	**0.00**	**0.00**	**0.00**	**14.48**	**0.00**	**0.00**
		22.97	0	0.00	0.00	0.00	14.48	0.00	0.00
8	42	**4.37**	**0**	**0.00**	**0.00**	**0.00**	**15.45**	**0.00**	**0.00**
		23.05	0	0.00	0.00	0.00	15.45	0.00	0.00
8	52	**4.40**	**0**	**0.00**	**0.00**	**0.00**	**15.92**	**0.00**	**0.00**
		23.12	3.8	0.47	0.95	47.55	15.92	0.13	0.21
8	62	**4.47**	**0**	**0.00**	**0.00**	**0.00**	**16.29**	**0.00**	**0.00**
		23.17	12.8	1.60	3.19	160.15	16.29	0.42	0.69
9	8	1.28	86.4	10.78	21.56	1081.03	11.61	72.55	84.24
		2.48	**186**	**23.21**	**46.41**	**2327.22**	**11.61**	**80.72**	**93.71**
		3.00	172	21.46	42.92	2152.05	11.61	61.79	71.73
		33.93	120	14.97	29.94	1501.43	11.61	3.81	4.42
		92.72	85.5	10.67	21.33	1069.77	11.61	0.99	1.15
9	18	1.37	32.1	4.00	8.01	401.63	15.86	18.53	29.39
		2.63	**64.5**	**8.05**	**16.09**	**807.02**	**15.86**	**19.32**	**30.65**
		34.12	230	28.69	57.39	2877.74	15.86	5.32	8.43

Table C-2 continued

Core	Depth	Time	Area	mass (nmol)	Concentration(nmol/ml)	Total N_2O (nmol)	Dry wt. (grams)	nmol N_2O/(g)/hr	nmol N_2O/ml/ hr
9	28	1.40	16.6	2.07	4.14	207.70	17.87	8.30	14.84
		2.58	**30.8**	**3.84**	**7.69**	**385.37**	**17.87**	**8.35**	**14.92**
		34.05	257	32.06	64.13	3215.56	17.87	5.28	9.44
9	38	1.45	0	0.00	0.00	0.00	15.28	0.00	0.00
		2.53	**0**	**0.00**	**0.00**	**0.00**	**15.28**	**0.00**	**0.00**
		33.97	220	27.45	54.89	2752.62	15.28	5.30	8.10
		34.02	221	27.57	55.14	2765.13	15.28	5.32	8.13
9	48	1.50	0	0.00	0.00	0.00	17.10	0.00	0.00
		2.80	**0**	**0.00**	**0.00**	**0.00**	**17.10**	**0.00**	**0.00**
		34.28	2.44	0.30	0.61	30.53	17.10	0.05	0.09

Appendix C: Denitrification Potential Assay

Table C-3: Denitrification Assay on August 26, 2003. Rates not determined on this date

Core	Depth	Peak Area (mvolt*sec)	Convert peak area to mass (nmol)	Convert mass to concen. Divide by 0.5ml (nmol/ml)	Total N_2O using Bunsen Absorpion coefficient (nmol)	Dry weight (grams)	nmol N_2O/gram of dry sediment	nmol Total N_2O/ml
1	2	31.4	3.92	7.83	392.87	8.23	47.74	39.29
	6	0	0.00	0.00	0.00	13.94	0.00	0.00
	16	0	0.00	0.00	0.00	15.36	0.00	0.00
	26	1.4	0.17	0.35	17.52	15.27	1.15	1.75
	36	0	0.00	0.00	0.00	16.36	0.00	0.00
	46	1.38	0.17	0.34	17.27	11.42	1.51	1.73
	56	7.11	0.89	1.77	88.96	15.32	5.81	8.90
	66	5.55	0.69	1.38	69.44	15.54	4.47	6.94
2	2	26	3.24	6.49	325.31	14.75	22.05	32.53
	12	7.8	0.97	1.95	97.59	14.75	6.62	9.76
	22	3.45	0.43	0.86	43.17	14.75	2.93	4.32
	32	0	0.00	0.00	0.00	14.75	0.00	0.00
	42	1.03	0.13	0.26	12.89	14.75	0.87	1.29
	52	0	0.00	0.00	0.00	14.75	0.00	0.00
	62	0	0.00	0.00	0.00	14.75	0.00	0.00
3	2	13.3	1.66	3.32	166.41	14.75	11.28	16.64
	10	0	0.00	0.00	0.00	14.75	0.00	0.00
	20	0	0.00	0.00	0.00	14.75	0.00	0.00
	30	15.2	1.90	3.79	190.18	14.75	12.89	19.02
	40	12.7	1.58	3.17	158.90	14.75	10.77	15.89
	50	4.05	0.51	1.01	50.67	14.75	3.44	5.07
4	1	395	49.28	98.56	4942.21	14.23	347.41	494.22
	10	0	0.00	0.00	0.00	14.87	0.00	0.00
	20	17.4	2.17	4.34	217.71	13.81	15.77	21.77
	30	3.2	0.40	0.80	40.04	13.42	2.98	4.00
	40	0	0.00	0.00	0.00	16.31	0.00	0.00
	50	1.6	0.20	0.40	20.02	16.98	1.18	2.00
	60	6.45	0.80	1.61	80.70	13.93	5.80	8.07
5	1	39.8	4.97	9.93	497.97	15.14	32.89	49.80
	10	9.71	1.21	2.42	121.49	11.51	10.56	12.15
	20	10.2	1.27	2.55	127.62	12.83	9.95	12.76
	30	3.46	0.43	0.86	43.29	16.13	2.68	4.33
	40	0	0.00	0.00	0.00	13.60	0.00	0.00
	50	7.98	1.00	1.99	99.85	16.14	6.19	9.98
	60	0	0.00	0.00	0.00	15.58	0.00	0.00
	70	4.15	0.52	1.04	51.92	15.24	3.41	5.19

Table C-3 continued

Core	Depth	Area	Mass (nmol)	Concentration (nmol/ml)	Total N_2O (nmol)	Dry weight (grams)	nmol N_2O/gram	nmol Total N_2O/ml
6	8	10.9	1.36	2.72	136.38	12.75	10.70	13.64
	18	68.8	8.58	17.17	860.82	14.17	60.75	86.08
	28	28	3.49	6.99	350.33	10.57	33.16	35.03
	38	53.1	6.62	13.25	664.38	13.21	50.30	66.44
	48	0	0.00	0.00	0.00	14.83	0.00	0.00
	58	5.56	0.69	1.39	69.57	17.42	3.99	6.96
7	1	63.7	7.95	15.89	797.01	14.70	54.21	79.70
	11	41.8	5.21	10.43	523.00	17.16	30.48	52.30
	21	0	0.00	0.00	0.00	15.93	0.00	0.00
	31	0	0.00	0.00	0.00	16.93	0.00	0.00
	41	0	0.00	0.00	0.00	13.33	0.00	0.00
	51	1.31	0.16	0.33	16.39	19.52	0.84	1.64
	61	1.82	0.23	0.45	22.77	15.83	1.44	2.28
	71	1.05	0.13	0.26	13.14	18.11	0.73	1.31
8	2	35.9	4.48	8.96	449.18	14.75	30.45	44.92
	8	33.7	4.20	8.41	421.65	14.75	28.58	42.17
	18	1.31	0.16	0.33	16.39	14.75	1.11	1.64
	28	9.28	1.16	2.32	116.11	14.75	7.87	11.61
	38	0	0.00	0.00	0.00	14.75	0.00	0.00
	48	0	0.00	0.00	0.00	14.75	0.00	0.00
	58	0	0.00	0.00	0.00	14.75	0.00	0.00
	68	0	0.00	0.00	0.00	14.75	0.00	0.00
9	1	0	0.00	0.00	0.00	12.07	0.00	0.00
	10	0	0.00	0.00	0.00	12.51	0.00	0.00
	20	14.7	1.83	3.67	183.93	11.93	15.42	18.39
	30	45	5.61	11.23	563.04	15.53	36.26	56.30
	40	9.25	1.15	2.31	115.74	15.38	7.52	11.57
	50	0	0.00	0.00	0.00	16.14	0.00	0.00
	60	7.87	0.98	1.96	98.47	17.07	5.77	9.85

Appendix C: Denitrification Potential Assay

Table C-4: Denitrification Assay on October 26, 2003. Bold indicates data in analysis

Core	Depth	Time (hrs)	Peak Area (mvolt*sec)	Convert peak area to mass (nmol)	Convert mass to concen. Divide by 0.5ml (nmol/ml)	Total N_2O using Bunsen Absorpion coefficient (nmol)	Total N_2O/10ml of sat sed/hr
1	2	**4**	**8.57**	**1.07**	**2.14**	**107.23**	**2.68**
		6.5	8.67	1.08	2.16	108.48	1.67
		22	28.8	3.59	7.19	360.34	1.64
		68	126	15.72	31.44	1576.50	2.32
1	9	**4**	**0**	**0.00**	**0.00**	**0.00**	**0.00**
		22	0	0.00	0.00	0.00	0.00
1	19	**4**	**0**	**0.00**	**0.00**	**0.00**	**0.00**
		22	0	0.00	0.00	0.00	0.00
1	29	**4**	**0**	**0.00**	**0.00**	**0.00**	**0.00**
		22	0	0.00	0.00	0.00	0.00
1	39	**4**	**0**	**0.00**	**0.00**	**0.00**	**0.00**
		22	0	0.00	0.00	0.00	0.00
1	49	**4**	**0**	**0.00**	**0.00**	**0.00**	**0.00**
		22	0	0.00	0.00	0.00	0.00
1	59	**4**	**0**	**0.00**	**0.00**	**0.00**	**0.00**
		22	0	0.00	0.00	0.00	0.00
2	2	**4**	**17**	**2.12**	**4.24**	**212.70**	**5.32**
		6.5	27.1	3.38	6.76	339.07	5.22
		22	67.1	8.37	16.74	839.55	3.82
		68	92.4	11.53	23.06	1156.10	1.70
2	12	**4**	**1.44**	**0.18**	**0.36**	**18.02**	**0.45**
		6.5	2.6	0.32	0.65	32.53	0.50
		23	11.2	1.40	2.79	140.13	0.61
		68	35.2	4.39	8.78	440.42	0.65
2	22	**4**	**0**	**0.00**	**0.00**	**0.00**	**0.00**
		22	0	0.00	0.00	0.00	0.00
2	32	**4**	**0**	**0.00**	**0.00**	**0.00**	**0.00**
		22	0	0.00	0.00	0.00	0.00
2	42	**4**	**0**	**0.00**	**0.00**	**0.00**	**0.00**
		22	0	0.00	0.00	0.00	0.00
2	52	**4**	**0**	**0.00**	**0.00**	**0.00**	**0.00**
		22	0	0.00	0.00	0.00	0.00

Table C-4 continued

Core	Depth	Time	Area	mass (nmol)	Concentration (nmol/ml)	Total N_2O (nmol)	nmol N_2O/ml/hr
3	2	**4**	**1.92**	**0.24**	**0.48**	**24.02**	**0.60**
		6.5	1.26	0.16	0.31	15.77	0.24
		23	1.03	0.13	0.26	12.89	0.06
		68	0	0.00	0.00	0.00	0.00
3	8	**4**	**0**	**0.00**	**0.00**	**0.00**	**0.00**
		22	0	0.00	0.00	0.00	0.00
		68	0	0.00	0.00	0.00	0.00
3	18	**4**	**0**	**0.00**	**0.00**	**0.00**	**0.00**
		22	0	0.00	0.00	0.00	0.00
3	28	**4**	**0**	**0.00**	**0.00**	**0.00**	**0.00**
		22	7.89	0.98	1.97	98.72	0.45
3	38	**4**	**0**	**0.00**	**0.00**	**0.00**	**0.00**
		22	0	0.00	0.00	0.00	0.00
3	48	**4**	**0**	**0.00**	**0.00**	**0.00**	**0.00**
		22	0	0.00	0.00	0.00	0.00
4	2	**4**		**0.00**	**0.00**	**0.00**	**0.00**
4	5	**4**	**0**	**0.00**	**0.00**	**0.00**	**0.00**
		22	0	0.00	0.00	0.00	0.00
4	15	**4**	**0**	**0.00**	**0.00**	**0.00**	**0.00**
		22	0	0.00	0.00	0.00	0.00
4	25	**4**	**0**	**0.00**	**0.00**	**0.00**	**0.00**
		22	0	0.00	0.00	0.00	0.00
4	35	**4**	**0**	**0.00**	**0.00**	**0.00**	**0.00**
		22	0	0.00	0.00	0.00	0.00
4	45	**4**	**0**	**0.00**	**0.00**	**0.00**	**0.00**
		22	0	0.00	0.00	0.00	0.00
5	2	**4**	**14.4**	**1.80**	**3.59**	**180.17**	**4.50**
		6.5	17.1	2.13	4.27	213.95	3.29
		22	36	4.49	8.98	450.43	2.05
		68	40.3	5.03	10.06	504.23	0.74
5	12	**4**	**3.37**	**0.42**	**0.84**	**42.17**	**1.05**
		6.5	8.36	1.04	2.09	104.60	1.61
		22	35.1	4.38	8.76	439.17	2.00
5	22	**4**	**0**	**0.00**	**0.00**	**0.00**	**0.00**
		22	1.5	0.19	0.37	18.77	0.09
5	42	**4**	**0**	**0.00**	**0.00**	**0.00**	**0.00**
		22	0	0.00	0.00	0.00	0.00
5	52	**4**	**0**	**0.00**	**0.00**	**0.00**	**0.00**
		22	0	0.00	0.00	0.00	0.00
7	2	**4**	**3.76**	**0.47**	**0.94**	**47.04**	**1.18**
		6.5	8.61	1.07	2.15	107.73	1.66
		22	24.4	3.04	6.09	305.29	1.39

Table C-4 continued

Core	Depth	Time	Area	mass (nmol)	Concentration (nmol/ml)	Total N_2O (nmol)	nmol N_2O/ml/hr
7	32	**4**	**0**	**0.00**	**0.00**	**0.00**	**0.00**
		22	0	0.00	0.00	0.00	0.00
7	42	**4**	**0**	**0.00**	**0.00**	**0.00**	**0.00**
		22	0	0.00	0.00	0.00	0.00
7	52	**4**	**0**	**0.00**	**0.00**	**0.00**	**0.00**
		22	0	0.00	0.00	0.00	0.00
8	5	**4**	**6.72**	**0.84**	**1.68**	**84.08**	**2.10**
		6.5	8.23	1.03	2.05	102.97	1.58
		22	21.8	2.72	5.44	272.76	1.24
		68	40.3	5.03	10.06	504.23	0.74
8	15	**4**	**0**	**0.00**	**0.00**	**0.00**	**0.00**
		22	13.1	1.63	3.27	163.91	0.75
8	25	**4**	**0**	**0.00**	**0.00**	**0.00**	**0.00**
		22	0	0.00	0.00	0.00	0.00
8	35	**4**	**0**	**0.00**	**0.00**	**0.00**	**0.00**
		22	0	0.00	0.00	0.00	0.00
8	45	**4**	**0**	**0.00**	**0.00**	**0.00**	**0.00**
		22	0	0.00	0.00	0.00	0.00
8	55	**4**	**0**	**0.00**	**0.00**	**0.00**	**0.00**
		22	0	0.00	0.00	0.00	0.00
9	2	**4**	**6.5**	**0.81**	**1.62**	**81.33**	**2.03**
		6.5	9.03	1.13	2.25	112.98	1.74
		23	14.6	1.82	3.64	182.67	0.79
		68	23.5	2.93	5.86	294.03	0.43
9	12	**4**	**18.1**	**2.26**	**4.52**	**226.47**	**5.66**
		6.5	28.2	3.52	7.04	352.84	5.43
		22	36.2	4.52	9.03	452.93	2.06
9	22	**4**	**0**	**0.00**	**0.00**	**0.00**	**0.00**
		22	2.62	0.33	0.65	32.78	0.15
9	32	**4**	**0**	**0.00**	**0.00**	**0.00**	**0.00**
		22	0	0.00	0.00	0.00	0.00
9	42	**4**	**0**	**0.00**	**0.00**	**0.00**	**0.00**
		22	0	0.00	0.00	0.00	0.00
9	52	**4**	**0**	**0.00**	**0.00**	**0.00**	**0.00**
		22	0	0.00	0.00	0.00	0.00